Detecting Changes in Alternative mRNA Processing From Microarray Expression Data

by

Timothy J. Robinson

Department of Molecular Cancer Biology
Duke University

Date:_______________________
Approved:

____
Mariano Garcia-Blanco, Co-Advisor

____
Mark Dewhirst, Co-Advisor

____
Michael Datto

____
Joseph Lucas

____
Joseph Nevins, Chair

Dissertation submitted in partial fulfillment of
the requirements for the degree of Doctor of Philosophy in the Department of
Molecular Cancer Biology in the Graduate School
of Duke University

2010

ABSTRACT

Detecting Changes in Alternative mRNA Processing From Microarray Expression Data

by

Timothy J. Robinson

Department of Molecular Cancer Biology
Duke University

Date:_______________________
Approved:

____
Mariano Garcia-Blanco, Co-Advisor

____
Mark Dewhirst, Co-Advisor

____
Michael Datto

____
Joseph Lucas

____
Joseph Nevins, Chair

An abstract of a dissertation submitted in partial
fulfillment of the requirements for the degree
of Doctor of Philosophy in the Department of
Molecular Cancer Biology in the Graduate School
of Duke University

2010

Abstract

Alternative mRNA processing can result in the generation of multiple, qualitatively different RNA transcripts from the same gene and is a powerful engine of complexity in higher organisms. Recent deep sequencing studies have indicated that essentially all human genes containing more than a single exon generate multiple RNA transcripts. Functional roles of alternative processing have been established in virtually all areas of biological regulation, particularly in development and cancer. Changes in alternative mRNA processing can now be detected from over a billion dollars' worth of conventional gene expression microarray data archived over the past 20 years using a program we created called SplicerAV. Application of SplicerAV to publicly available microarray data has granted new insights into previously existing studies of oncogene over-expression and clinical cancer prognosis.

Adaptation of SplicerAV to the new Affymetrix Human Exon arrays has resulted in the creation of SplicerEX, the first program that can automatically categorize microarray detected changes in alternative processing into biologically pertinent categories. We use SplicerEX's automatic event categorization to identify changes in global mRNA processing and demonstrate the ability of the conventional U133 platform to detect five times as many 3' terminal mRNA isoform changes as the Human Exon array during B cell transformation.

Dedication

In memory of John J. Dinan.

Contents

List of Tables

Chapter 2

Chapter 3

Appendix D

List of Figures

Chapter 1

Chapter 2

Chapter 3

Chapter 4

Appendix D

Appendix E

Acknowledgements

I thank my thesis advisors, Dr. Mariano Garcia-Blanco and Dr. Mark Dewhirst, for their mentorship and advice during my graduate studies. In addition, I would like to thank James Pearson, Micah Luftig, Caroline Le Sommer, Sebastian Oltean, and Eleonora Forte for their contributions to my work. I would also like to extend my thanks to Uwe Ohler, Ashley Chi, Alexander Hartemink, Sayan Mukherjee for their valued teaching and insight, without which I would not have been able to enter the field of genomics.

My thesis committee has been instrumental in forming my projects and helping direct my research: Michael Datto, Joseph Lucas, Joseph Nevins.

I cannot thank my parents enough for their unwavering support and my brother Davin for imparting his creativity. Finally, I thank my wife, Michaela, for her loyal support, complementary perspective, drive, and uncanny ability to do back flips in heels.

1. Alternative mRNA processing

1.1 Alternative mRNA processing as an engine of diversity in Eukaryotes

The key postulate that one gene encodes one polypeptide chain (one enzyme) has been overhauled with the discovery that one gene can generate multiple RNA transcripts (and indirectly many different polypeptide chains) through a process referred to as alternative mRNA processing (Blencowe 2006). Alternative processing defines a range of events, including alternative splicing (AS) and alternative polyadenylation (APA), which result in distinct mRNA species. Recent deep sequencing studies indicate that 94% of all protein coding genes generate multiple mRNA transcripts (Wang et al. 2008) and mutations affecting mRNA splicing are responsible for an estimated 15-60% of human genetic diseases (Krawczak et al. 1992; Lopez-Bigas et al. 2005). Functional consequences of alternative processing have been shown across a wide variety of biological processes (reviewed by (Garcia-Blanco et al. 2004; Venables 2006; Cooper et al. 2009)) including drug metabolism, stem cell renewal, neurologic disease, autoimmune disease, and especially cancer.

All multiple exon genes, by definition, contain tracks of intronic sequences that are spliced, or removed, from pre-mRNA transcripts to yield mature, protein coding transcripts. When more than one mature mRNA transcript is created from a single pre-mRNA transcript, that gene is said to be alternatively processed.

There are several common mechanisms by which alternative mRNA transcripts can be generated from the same gene (Black 2003; Wang et al. 2008)(Figure 1).

Alternative promoter use describes differential use of alternative 5’ pre-mRNA transcript initiation sites. Alternative mRNA processing can occur through alternative mRNA splicing or polyadenylation. Alternative mRNA splicing describes removal or retention of internal pre-mRNA transcript content, including single cassette exons, mutually exclusive cassette exons, introns, and alternative 5’ or 3’ definition of exon boundaries (alternative 3’ or 5’ splice site (SS) use, respectively). Alternative splicing that results in differential open reading frame (ORF) content can result in the production of proteins with altered structure and function. Polyadenylation describes the addition of multiple adenine (A) nucleotides to mature messenger RNAs, required for mature mRNA stability. Alternative polyadenylation (APA) occurs when there are multiple locations within a pre-mRNA that can signal for polyadenylation to occur, resulting in differential length or selection of 3’ terminal exons.

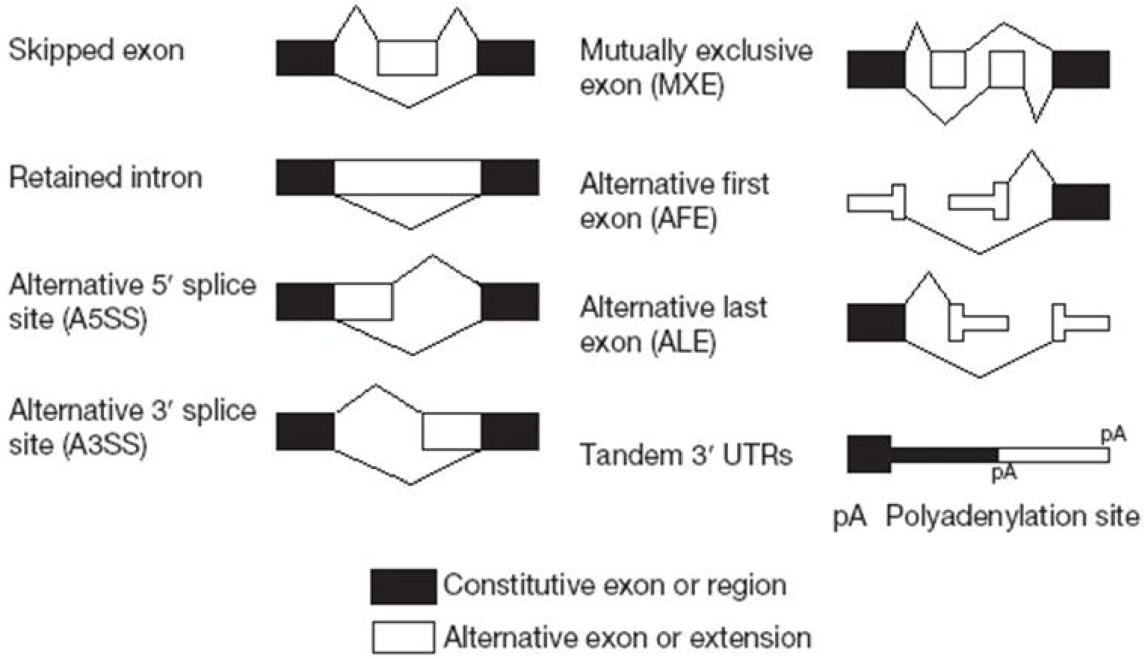
Skipped exon
Mutually exclusive exon (MXE)
Retained intron
Alternative first exon (AFE)
Alternative 5′ splice site (A5SS)
Alternative last exon (ALE)
Alternative 3′ splice site (A3SS)
Tandem 3′ UTRs
pA
pA
pA Polyadenylation site
Constitutive exon or region
Alternative exon or extension

Figure 1: Mechanisms of alternative mRNA isoform generation. Adapted from (Wang et al. 2008).

Databases of alternative mRNA processing events have emerged in recent years. These databases contain sets of observed, predicted, or curated alternative mRNA isoforms and associated regulatory sequence motifs (Koscielny et al. 2009) (Lee et al. 2003; de la Grange et al. 2005; Zheng et al. 2005; Bhasi et al. 2007; de la Grange et al. 2007; Foissac and Sammeth 2007; Kim et al. 2007; Castrignano et al. 2008). Fast DB, developed by Auboeuf and colleagues, is one such resource that has become popular among biologists (http://www.fast-db.com) by providing tools for visualizing known alternative mRNA transcript structure and performing preliminary in silico analyses of isform function, and regulation.

1.2 High throughput methods available for the study of mRNA processing

Despite the importance of alternative processing in cancer, current understanding of its global regulation remains sparse (Takeda et al. 2006) and limits the ability to fully harness alternative processing as a tool in cancer prognosis, diagnosis, and treatment. Attempts to obtain a genome scale understanding of alternative processing in cancer have focused on large-scale characterizations of changes between normal tissue and cancer.

Initial attempts to elucidate alternative mRNA transcript structure on a genomic level began shortly after the sequencing of the human genome. Using the genome as a reference point, researchers have been able to align partially sequenced mRNA transcripts, or expressed sequence tags (ESTs), to detect alternative mRNA transcript structures within thousands of genes(Kan et al. 2001). EST-based methods have been used to compare EST databases of normal tissue vs. human cancer to detect enrichment of cancer-specific splice variants(Xu and Lee 2003; He et al. 2009). EST-based methods use databases pooled from numerous samples, and do not provide an indication of how commonly any specific observed variant might be expected to appear within an individual cancer. The inability of EST-based methods to infer changes in mRNA structure at the individual level have largely prevented their use in profiling individual cancer patients.

Quantification of changes in alternative processing between individual samples became feasible with the advent of splicing sensitive microarrays (reviewed in (Blencowe 2006)). Splicing sensitive microarrays infer changes in alternative mRNA processing by assaying the expression of individual exons and/or exon-junctions using complimentary oligonucleotide probes printed as a small array on a chip. Splicing sensitive microarrays differ from gene expression arrays primarily through the location and number of features detected (Figure 22). One of the first commercially available human splicing arrays, the Affymetrix Human Exon 1.0 ST, detects roughly 1.4 million features, 30 times more than the current most commonly used gene expression array (HG-U133 2.0 plus). Exon arrays have been used to detect changes in alternative processing between normal human tissues and in breast, brain, colon, prostate, and bladder carcinomas(Gardina et al. 2006; Cheung et al. 2008; Thorsen et al. 2008; Xi et al. 2008; Andre et al. 2009).

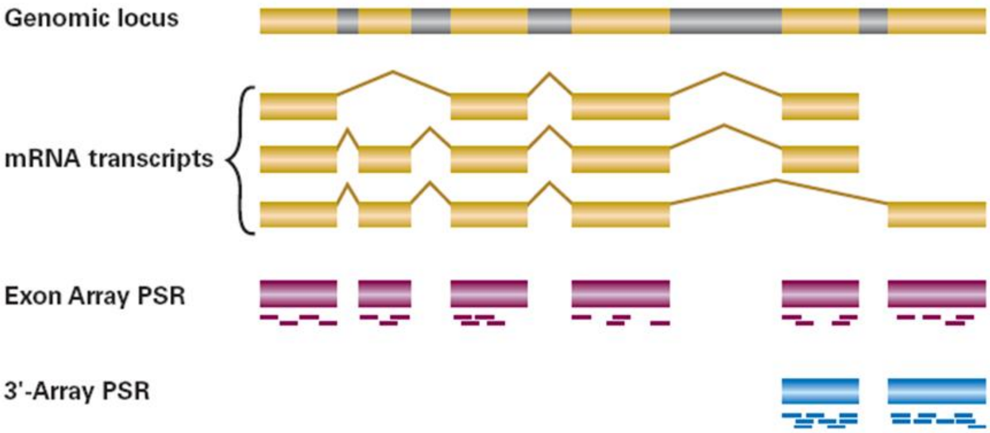

Figure 2: Comparison of exon array and 3' gene expression array probeset features. Probesets are chosen from probeset selection regions (PSR) that target selected mRNA transcript exon features. Exon array probesets target exons throughout the entire length of known mRNA transcripts. 3' gene expression array probesets preferentially target 3' ends of known mRNA transcripts. Each probeset is composed of 4 probes on the exon arrays and 11 probes on the 3' arrays.

Non array-based technologies capable of interrogating genome-wide changes in alternative mRNA processing have recently emerged and include high throughput RT-

PCR and deep sequencing. Venables et al. have used a custom, high-throughput RT-PCR technology to identify changes in mRNA splicing in both breast and ovarian cancer samples compared to normal tissue and have used them to identify a role of FOX2 in a large number of splicing events associated with these cancers (Venables et al. 2009). High-throughput RT-PCR in its present form is not widely available to the research community and can only examine internal cassette type splicing events. High-throughput deep sequencing has been recently been used to perform extensive analysis of alternative mRNA transcripts in normal human tissue, selected cell lines (Wang et al. 2008), and lymphoblastoid cell lines(Pickrell et al.). At present, current costs and complex data analysis make deep sequencing largely unavailable within the general research community.

1.3 Computational Analysis of mRNA Processing

Genome-wide analysis of alternative mRNA transcript generation, compared to conventional gene expression analysis, is inherently complex. Recent analyses of the human genome place the number of known exons at 380,000, roughly an order of magnitude greater than the number of known genes (Zhu et al. 2009). Traditional gene expression analyses typically ignore details of transcript structure, while analyses of mRNA processing, by definition, must describe changes in this structure.

Several algorithms have been developed to detect changes in mRNA processing using exon array data, recently reviewed in [(Laajala et al. 2009)]. Although these programs vary in their specific approach, common concepts have emerged in the field to describe analyses of changes in alternative mRNA processing.

The statistic that is most commonly used to describe an isoform-specific change between two groups is the splicing index (SI) (Srinivasan et al. 2005; Li et al. 2006; Clark et al. 2007). The splicing index is analogous to the gene expression concept of "fold change", and is defined as the gene-level normalized change in expression of an isoform between two comparison groups. In most analyses, minor isoforms are often represented by a single exon or probeset. For single exon events, the splicing index is calculated as follows:

$$SI = (Exon_{Treat} / Gene_{Treat}) / (Exon_{Control} / Gene_{Control})$$

Where:

$Exon_{Treat}$ = *mean expression level of the AS exon in the treatment group*

$Gene_{Treat}$ = *mean expression level of the overall gene in the treatment group*

$Exon_{Control}$ = *mean expression level of the AS exon in the control group*

$Gene_{Control}$ = *mean expression level of the overall gene in the treatment group*

[1]

Analyses of microarray expression data are typically conducted in log space, in which case equation 1 becomes the following:

$$SI = (Exon_{Treat} - Gene_{Treat}) - (Exon_{Control} - Gene_{Control})$$

[2]

The basic statistical foundation of algorithms used to evaluate changes in alternative mRNA processing is the null hypothesis that all features within a gene came from the same distribution. The MIDAS (Microarray Detection of Alternative Splicing) and ANOSVA methods both employ an analysis of variance (ANOVA) test for non-zero interactions between treatment groups and exon (Affymetrix 2005) (Cline et al. 2005). For ANOVA-based methods, the estimated interaction coefficient between exon and treatment group provides an error bounded estimate of the splice index. PLATA (Probe-Level Alternative Transcript Analysis) (Sandberg et al. 2008), MADS(Microarray Analysis of Differential Splicing)(Xing et al. 2008), and PECA-SI (Probe-level Expression Change Averaging - Splice Index) all use individual probes to test for mean probe differences or non-zero splice indicies. FIRMA (Finding Isoforms using Robust Multichip Analysis) frames detection of alternative events in terms of outlier detection(Laajala et al. 2009). In practice, researchers appear to analyze exon array data using either their own custom software or a commercially available analysis package such as EASANA (www.genosplice.com), XRAY (www.biotique.com), or PARTEK.

1.4 Focus of this work

Existing models of alternative mRNA processing test the alternative hypothesis that microarray features targeting the same gene do not come from the same distribution. In this thesis, I have framed a more specific alternative hypothesis that tests whether microarray features targeting the same gene come from two distinct distributions. By modeling alternative mRNA processing as two distinct events, we have created a more focused model that tests a specific hypothesis. Throughout the remainder of this thesis, I describe the implementation of this model and how we have tailored it to assist biologists in search of experimental models of alternative mRNA processing regulation.

In chapter 2, I describe the implementation of a biologically motivated model of alternative mRNA splicing, SplicerAV and demonstrate its ability to yield new biological insights from archival conventional gene expression microarray data.

Chapter 3 describes the adaption of SplicerAV to exon microarrays, called SplicerEX. In this chapter we extend the specific hypothesis generated by SplicerEX to include inference on the type and direction of predicted changes in mRNA processing, and use this to identify previously unobserved characteristic changes in mRNA structure in a model of B cell transformation by Epstein Barr Virus.

Chapter 4 describes areas of potential future research. Appendices A-C provide hit lists from the analysis presented in chapter 3. Appendix D provides a description of the SplicerEX categorization algorithm. Appendix E describes my role in analyzing a genome-wide siRNA screen in Dengue fever host factors.

2. SplicerAV: a tool for mining microarray expression data for changes in RNA processing

In this chapter, I describe the creation and implementation of a novel program, SplicerAV, that is capable of analyzing archival conventional 3’ gene expression arrays for evidence of changes in alternative mRNA processing. We exploit the ability of SplicerAV to analyze changes associated with clinical cancer progression.

2.1 Introduction

Large scale clinical cancer analyses of changes in alternative processing remain sparse, and there have been no high-throughput analyses of changes in mRNA processing directly associated with poor patient prognosis. Such studies require years of patient follow-up and have not been reported using the new splicing arrays, which have instead only analyzed changes between normal tissue and cancer.

Public repositories such as the Gene Expression Omnibus (GEO) currently contain conventional gene expression data from hundreds of thousands of unique biological or clinical samples ((Barrett et al. 2009)). Data previously generated by the microarray community provide an untapped source of potential insight to the regulation of alternative mRNA processing in human cancer. It is likely that well over a billion dollars have been invested in these data through reagents, facility, and personnel costs over the past two decades.

The first commercially available high-density gene expression microarrays were invented three decades ago by Affymetrix (Fodor et al. 1993) to quantify expression changes in tens of thousands of genes in a single experiment, but were not intended to detect isoform specific mRNA changes resulting from alternative processing. Two of the most commonly used human expression microarrays, the Affymetrix U95 and U133 series, use individual probesets to report expression of many genes. Each probeset is composed of 11 individual 25nt oligomers that interrogate a subsequence of the target gene. Both platforms, however, contain thousands of genes whose expression is assayed by more than one probeset. The use of multiple probesets, which often interrogate non-overlapping regions of the target gene, was originally intended to provide a robust assay of gene expression. We and others have previously observed that discrepancies between fold-changes in probesets interrogating the same gene can represent isoform-specific changes in mRNA levels [20-22]. Such isoform changes can result from alternative transcription start sites, alternative mRNA processing, or changes in mRNA isoform stability.

Methods that detect isoform-specific mRNA changes have been developed for splicing microarrays such as the Affymetrix Human Exon 1.0 ST (reviewed in (Laajala et al. 2009)), but have not been developed for or applied to conventional gene expression microarrays. In fact, it has been suggested in such reviews that “detection of disease-relevant splicing differences may be entirely missed in gene-level expression profiling studies” (Laajala et al. 2009). Although it may be possible in theory to apply such methods to conventional gene expression microarrays, to our knowledge this has not been done. To fully investigate the potential to detect isoform-specific mRNA changes in conventional gene expression microarray data, we elected to develop a novel method, SplicerAV, which we have applied to conventional Affymetrix gene expression microarray data.

For the Affymetrix GeneChip Human U133 plus 2.0 arrays, 11,193 genes, which represent 57% of uniquely annotated genes assayed by the array, are interrogated by multiple probesets and can therefore be queried for mRNA isoform changes, with an average of 3.2 probesets interrogating these genes (Table 1). For the U133A arrays, 36% are interrogated by multiple probesets, with an average of 2.7 probesets per gene for a total of 4,609 genes. The U133 series of array platforms are among the most commonly used platforms within GEO (over 40,000 samples) and have the potential to detect isoform changes in thousands of genes.

Table 1: SplicerAV related probeset features of commonly used Affymetrix microarrays.

Platform	Unique Annotated Genes	Genes w/ Mult Probesets	Fraction of genes w/ mult probesets	Avg. Probesets per gene	Unannotated Probesets	Total Probesets
U133 Plus 2.0	19,761	11,193	57%	3.2	9818	54,675
U133 A	12,737	4,609	36%	2.7	1917	22,283
U95 A	8,690	1,946	22%	2.4	1253	12,651
Mouse 430A 2	12,755	4,934	39%	2.6	2118	22,690

SplicerAV is a program created to systematically assess the likelihood of changes in alternative processing evidenced by discrepancies in probeset behavior using a Gaussian mixture model of mRNA transcript regulation. A beta version of this program, which lacked biological modifiers and the ability to generate estimates of statistical significance, was initially used to identify differential regulation of transcript isoforms by TCERG1 (Pearson et al. 2008). SplicerAV can be applied to any expression microarray platform with multiple probesets interrogating the same gene, without the need for detailed transcript annotation. The program provides a non-computationally intensive algorithm capable of analyzing probeset-summary level datasets for evidence of changes in alternative mRNA processing. We provide here a description of SplicerAV, which has been developed to provide a rigorous statistical model and incorporate biologically motivated modifications with the goal of assisting biologists in identifying alternative processing events most amenable for in-depth study from conventional gene expression microarray data.

In this study SplicerAV's unique value in detecting previously overlooked changes in mRNA processing is demonstrated using publicly available Affymetrix U133 gene expression datasets. SplicerAV was used to uncover previously uncharacterized isoform specific changes in epidermal growth factor receptor (EGFR) caused by in vitro HRAS over-expression (Bild et al. 2006). In a separate analysis, SplicerAV was used to identify changes in alternative mRNA processing associated with poor patient prognosis in over 400 breast tumors. Here we demonstrate SplicerAV's ability to examine archival data, performing the largest analysis of alternative mRNA processing in human cancer to date and the only high-throughput analysis of changes in alternative mRNA processing associated with human cancer prognosis.

2.2 Results and Discussion

SplicerAV Algorithm

There are two main steps in the SplicerAV analysis. The first step summarizes individual probeset changes in expression between a user defined group of control and treatment observations. The second step evaluates these probeset level summaries for evidence of changes in alternative processing using a Gaussian mixture model (Figure 3).

In the first step, changes in probeset expression levels are summarized by calculating their average $\log_2$fold changes and corresponding t-statistics. These metrics were taken from conventional gene expression analysis.   Probesets targeting the same gene are then grouped together and each probeset is assigned a weight. Individual probeset weights are calculated using a combination of that probeset's t-statistic, number of observations, and comparison with other probesets targeting the same gene (see methods).

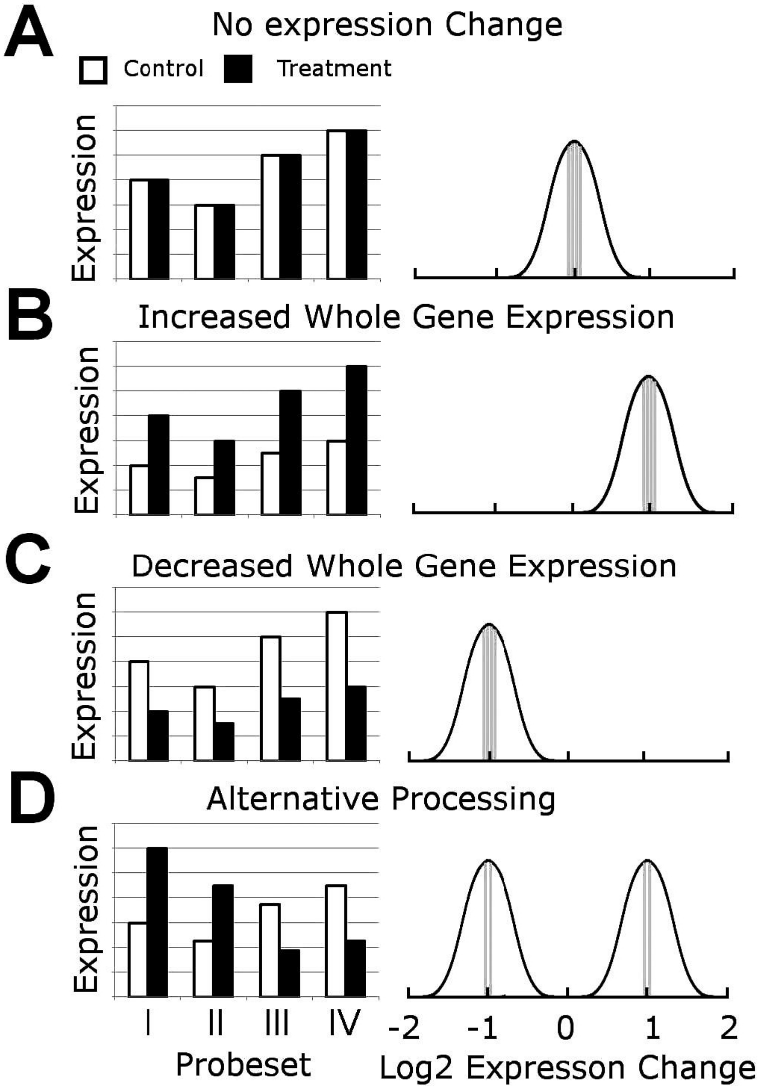

Figure 3: Gaussian mixture model of changes in alternative processing. Absolute expression of a hypothetical gene is reported by four independent probesets targeting different regions of this gene; I, II, III, IV (left panels) for control and treatment conditions (open and closed bars respectively). The idealized Gaussian mixture models representing changes in probeset behavior are illustrated in the right panels. Panels A, B, and C represent concordant probeset behaviors corresponding to no change, an increase, and a decrease, respectively. Panel D represents discordant behavior; two probesets (I, II) report an increase, while the remaining probesets (III, IV) report a decrease in expression between conditions (control and treatment). Probesets may report discrepant changes in gene expression depending on which region of the mRNA transcript they interrogate.

Once these weights are assigned, each gene is evaluated for evidence of alternative processing using a Gaussian mixture model. In the Gaussian mixture model used by SplicerAV, probesets interrogating a transcriptionally activated gene are predicted to detect the same proportional increase in expression. For example, probesets targeting an mRNA that doubles in abundance would be expected to double in intensity (Figure 3B). Conversely, probesets targeting an mRNA which is down-regulated by half would be expected to be reduced by half Figure 3C). Multiple probesets targeting a gene that is alternatively processed or undergoes isoform specific mRNA regulation would be expected to report discordant changes in probeset intensities (Figure 3D).

Plotting the same aforementioned hypothetical data as $\log_2$ fold-changes emphasizes that in alternatively processed mRNAs, summarized probeset behavior clusters into discrete groups (Figure 3, right). SplicerAV assesses this grouping mathematically assuming a Gaussian mixture model, which compares fitting the data using one vs. two Gaussian distributions. Fitting the probeset expression data with a single Gaussian curve equates to a biological model in which the gene is regulated as one expression unit (e.g., all transcripts are destabilized equally). Fitting the data with a two Gaussian model equates to a biological model in which the gene is regulated as two or more expression units, corresponding to changes in isoform specific regulation. Comparing the ratio of how well each model fits the summarized probeset data gives a maximum likelihood ratio, or MLR, which gives an indication of how well the summarized probeset data are described by changes in alternative processing relative to whole transcript regulation. The lowest possible log MLR for a gene is zero, which indicates that all probesets change proportionally and suggests no evidence of alternative processing. Log MLRs greater than zero indicate discrepancy in the expression changes in the probesets, which can be caused by an alternative processing event. The greater the value of the log MLR the more likely a gene is to be alternatively processed (see methods for more details).

$$MLR = \frac{\left(Likelihood\ of\ \ probeset\ data \,|\, Two\ Gaussian\ Curves\right)}{\left(Likelihood\ of\ \ probeset\ data \,|\, Single\ Gaussian\ Curve\right)}$$

[1]

SplicerAV uses the chip annotation file (“platform_annot.csv” for Affymetrix arrays) to determine which probesets interrogate the same gene. For most microarray platforms the gene symbol provides an appropriate annotation scheme, however any provided annotation (Transcript cluster ID, WormBase, FlyBase, Ensembl, etc.) can be used.

Probeset Annotation & Filtering

Our analyses used the default probeset annotation provided by Affymetrix. This annotation contains probesets that in some cases target multiple exons or are poorly annotated (Ferrari et al. 2007) (Lu et al. 2007) (Yu et al. 2007). Re-defining probeset definition, for example using exon-based definitions of probesets, may improve the ability of SplicerAV to detect changes in mRNA processing (Ferrari et al. 2007) (Lu et al. 2007). However, using the standard annotation provided by Affymetrix makes our findings here directly comparable to the vast majority of expression analyses conducted using the U133 series of arrays, allowing reference to specific probeset IDs and enabling us to directly analyze summarized expression datasets deposited in GEO. Roughly half of all (not limited to Affymetrix) microarray expression datasets deposited in GEO do not contain CEL files (Yu et al. 2007) and cannot be re-analyzed using custom annotation.

The use of standard Affymetrix annotation also allows us to make presence/absence probeset detection calls using previously validated methods (Warren et al. 2007). As described above, SplicerAV detects discrepancies in fold changes between probesets targeting the same gene, using these discrepancies to infer changes in alternative mRNA processing. Nevertheless, such discrepancies can also reflect the presence of negative strand matching probesets (NSMPs) or probesets that do not produce signal above background, which can be caused by low transcript levels or non-functional probes. NSMPs hybridize or detect RNAs transcribed in the opposite direction of the annotated gene; they do not reflect the expression of the target transcript and are identified and removed by SplicerAV using information available in standard Affymetrix annotation files (Warren et al. 2007). Probesets that do not produce signal can also falsely suggest isoform specific mRNA changes. These probesets are removed by SplicerAV if they are not expressed above background ($P<.05$) in either treatment or control groups using the Presence-Absence calls with Negative Probesets (PANP) algorithm (Warren et al. 2007).

Biological Modifiers

The original motivation for SplicerAV was to identify statistically significant changes in alternative processing that would also provide ideal targets for further experimental validation and study. To this end, we incorporated additional, user-modifiable parameters, which can preferentially rank events expected to be more amenable to experimental investigation. There are three biological modifiers applied to the MLR to generate the final splice score: a multiple probeset correction to adjust for total possible paired groupings of probesets, an expression cutoff modifier to specify the minimum change required between isoforms, and a centering modifier to preferentially rank genes whose probeset expression levels change in opposite directions. All modifiers are normalized by the average number of paired control and treatment observations for all probesets within a gene (Avg_Obs), so that large samples with higher statistical power will be as influenced by the modifiers as smaller samples, providing parameters that can be applied with consistent effects across varying sample sizes (see equation 2 and methods).

$$\begin{gathered} \textit{Splice Score} = \textit{MLR} + \textit{Avg\_Obs} \\ *(\textit{Multiple probeset} + \textit{Cutoff} + \textit{Centering Modifiers}) \end{gathered} \qquad [2]$$

These modifiers do not affect the p-value generated by SplicerAV, but allow the program to preferentially rank predicted changes in alternative processing that generate less complicated hypotheses, are larger in magnitude, reflect changes in expression which are qualitatively different, and are less likely to reflect probesets targeting non-transcribed regions or probesets that do not linearly reflect changes in transcript abundance. Genes that exhibit statistically significant discordant probeset behavior and are given a positive splice score represent ideal candidates for experimental investigation of isoform specific regulation.

SplicerAV generates several additional outputs with each file. These include a file containing assessment of statistically significant expression changes for all probesets, a log file containing all user set parameters and comparisons made, as well as a FASTA file for each gene. These fasta files contain the target sequences of all probesets targeting that gene, allowing quick and easy mapping to known and predicted mRNA sequences using the UCSC genome browser (http://genome.ucsc.edu) (Kent et al. 2002). All genomic analyses in this study were performed using the March 2006 release of the human genome (hg18).

SplicerAV Index Generation

To perform analyses of isoform changes within individual samples we derived an index of relative isoform abundance predicted by SplicerAV. High-throughput analyses of alternative processing have previously defined “splice index” as a quantitative measure to compare isoform abundances between individual samples. The splice index of a probeset equals its expression relative to other probesets targeting the same gene (Srinivasan et al. 2005). Using SplicerAV we defined a modified version of the splice index, referred to as the SplicerAV index. SplicerAV assumes a Gaussian mixture model, whereby all probesets are classified as belonging to one of two groups based on similarity of expression changes. The group of probesets exhibiting the largest increases in expression are referred to as the “A” (up) group and the group of probesets exhibiting the largest decreases in expression are referred to as the “B” (down) group. The

SplicerAV index of a probeset equals its expression relative to the average expression of probesets in the opposite group. For example, the SplicerAV index of a probeset in the "A" group would be calculated by subtracting the average expression of the "B" group from that probeset's log2 expression value. In our analysis, SplicerAV indexes of probesets in the "A" group were defined as increased in aggressive cancers, while indexes of probesets in the "B" group were defined as decreased in aggressive cancers. Pre-specified hypotheses generated in training datasets made unidirectional significance tests appropriate in independent validation datasets.

SplicerAV Implementation

SplicerAV was implemented in Perl, with a typical run time of 3-5 minutes on a standard personal computer and has not been tested using other operating systems. The program will only assess changes in alternative mRNA processing for genes interrogated by multiple probesets, which varies widely by microarray platform. To explore the potential for SplicerAV to identify novel changes in mRNA isform abundance in breast cancer, we applied SplicerAV to several publicly available, archival Affymetrix HG-U133 plus 2.0 datasets.

SplicerAV predicts oncogene induced changes in alternative processing of splicing factors

Studies of SRC (Neel et al. 1995), HRAS (Chandler and Bourgeois 1991; Chandler et al. 1994), and E2F family binding sites (Darville and Rousseau 1997) have demonstrated isolated roles of these oncogenes in affecting alternative mRNA processing. Nonetheless, prior to this study no large-scale examination of changes in alternative mRNA processing had been undertaken for any of these oncogenes. We examined an oncogene over-expression microarray dataset published by Nevins and colleagues (Bild et al. 2006) (GEO accession GSE3151) to demonstrate SplicerAV's ability to detect oncogene driven changes in alternative processing. In this experiment, activated HRAS, SRC, E2F3, activated β-catenin (CTNNB1), MYC, or green fluorescent protein (GFP) was over-expressed in human primary mammary epithelial cells. The Affymetrix U133 plus 2.0 microarray platform was used to assay gene expression in seven to ten replicates of each condition. Probeset level intensities were estimated using the Robust Multichip Averaging (RMA) procedure (Irizarry et al. 2003).

SplicerAV compared changes in probeset expression between GFP and over-expression of the HRAS, SRC, E2F3, CTNNB1, or MYC oncogenes. Roughly 7,000 genes were expressed above background in either GFP or oncogene over-expression, depending on the oncogene ("Total" column; Table 2). More than 2,000 of these genes were interrogated by multiple probesets, and could therefore be examined by SplicerAV for evidence of changes in alternative mRNA processing ("Multi-probeset Genes" column). More than a hundred isoform specific changes were predicted for each oncogene (Example SplicerAV output shown in Figure 4***Error! Reference source not found.***A; "Alt. Processed Genes" column Table 2). HRAS over-expression caused 645 significant isoform changes, suggesting HRAS-induced changes in alternative processing in nearly a tenth of all expressed genes. The median relative fold change between isoforms was 1.39 (log2 fold change of .48), with 61 (9%) of these genes predicted to undergo a greater than two fold change in relative isoform abundance (Figure 4B).

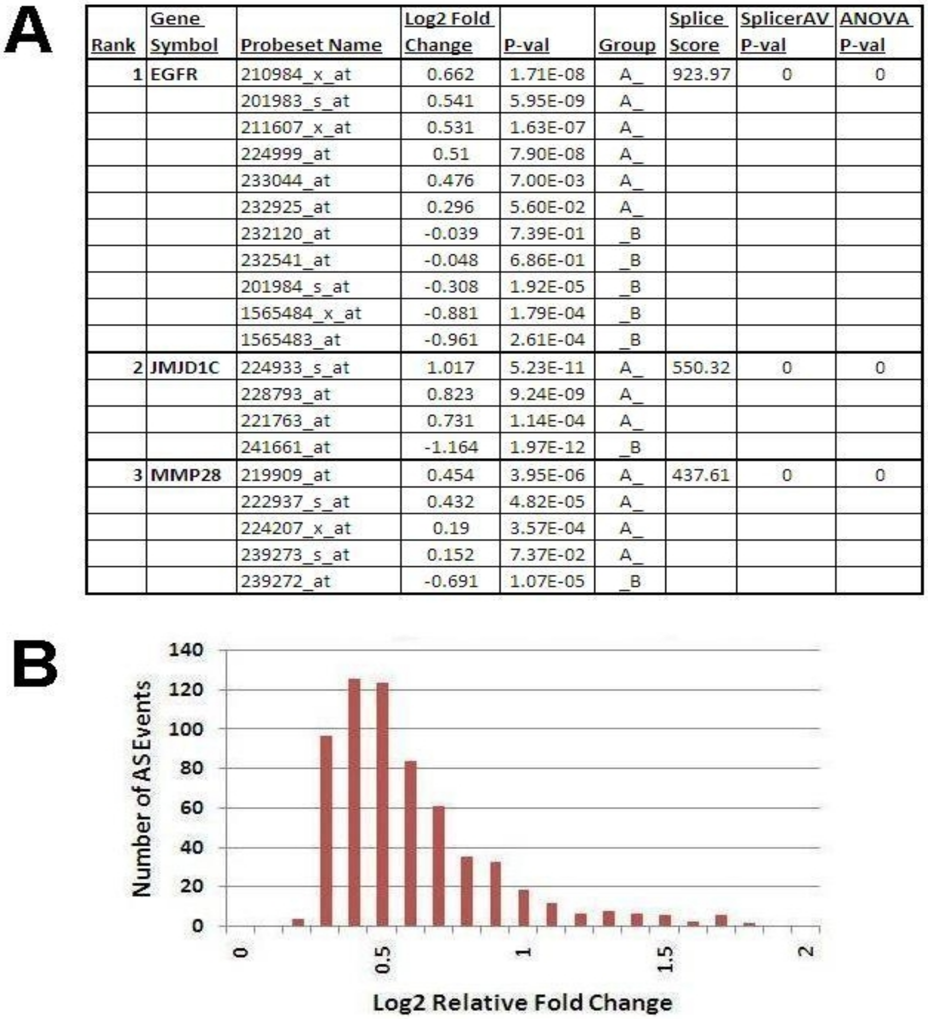

A

Rank	Gene Symbol	Probeset Name	Log2 Fold Change	P-val	Group	Splice Score	SplicerAV P-val	ANOVA P-val
1	EGFR	210984_x_at	0.662	1.71E-08	A_	923.97	0	0
		201983_s_at	0.541	5.95E-09	A_			
		211607_x_at	0.531	1.63E-07	A_			
		224999_at	0.51	7.90E-08	A_			
		233044_at	0.476	7.00E-03	A_			
		232925_at	0.296	5.60E-02	A_			
		232120_at	-0.039	7.39E-01	_B			
		232541_at	-0.048	6.86E-01	_B			
		201984_s_at	-0.308	1.92E-05	_B			
		1565484_x_at	-0.881	1.79E-04	_B			
		1565483_at	-0.961	2.61E-04	_B			
2	JMJD1C	224933_s_at	1.017	5.23E-11	A_	550.32	0	0
		228793_at	0.823	9.24E-09	A_			
		221763_at	0.731	1.14E-04	A_			
		241661_at	-1.164	1.97E-12	_B			
3	MMP28	219909_at	0.454	3.95E-06	A_	437.61	0	0
		222937_s_at	0.432	4.82E-05	A_			
		224207_x_at	0.19	3.57E-04	A_			
		239273_s_at	0.152	7.37E-02	A_			
		239272_at	-0.691	1.07E-05	_B			

Figure 4: HRAS over-expression results in substantial relative isoform changes.

Figure 4: HRAS over-expression results in substantial relative isoform changes. A) Example SplicerAV output comparing HRAS to GFP over-expression. Genes are ranked in order of descending Splice Score (top three genes shown), with EGFR receiving the top score in HRAS over-expression. Log2 fold change in expression and corresponding p-values from two tailed homoskedastic t-test of differential expression are shown for individual probesets targeting each gene. Probesets are placed into A and B groupings by SplicerAV (see text). Splice score, SplicerAV p-value, and two way ANOVA p-values are shown for each gene. (B) Distribution of the 645 isoform changes (AS Events) predicted by SplicerAV (p<.01) upon HRAS over-expression in human primary mammary epithelial cells. For each gene, SplicerAV separates probesets into two similarly behaving groups based on similar fold changes in expression. The average change in expression between probesets in these two groups (AvgChange, see Equation 8 in methods) reflects the relative fold change in isoform abundance predicted by SplicerAV. Absolute relative fold change in isoform abundance is shown in log base 2.

Gene isoform changes receiving both a significant p-value and a positive splice score indicate ideal candidates for further experimental study ("Genes with Splice Score > 0" column; Table 2). HRAS and SRC over-expression resulted in 212 and 119 such events, while MYC over-expression resulted in only 12 (Table 2). One gene, Programmed Cell Death Protein 5 (PDCD5), underwent the same change in alternative processing upon over-expression of each of the five oncogenes. PDCD5 switched from an alternative isoform (mRNA AK293486) to the major isoform (mRNA BC015519), which codes 37 isoform specific c-terminal amino acids required for PDCD5 nuclear entry & activation of apoptosis (Yao et al. 2009). Gene ontology (GO) analysis of isoform specific changes revealed a common selection for genes involved in mRNA splicing (see methods). Over-expression of all oncogenes other than MYC each resulted in significant ($p \leq .05$) enrichment of isoform specific changes in mRNA splicing, pre-mRNA splicing, or mRNA processing factors (Table 2). HRAS and SRC over-expression resulted in predicted isoform changes in 12 ($p=.009$) and seven ($p=.05$) factors involved in mRNA splicing, respectively. Both HRAS and E2F3 isoform specific changes were enriched for G-protein mediated signaling ($p = .04$; $p = .0009$) and roles in immune function ($p=.02$; $p=.01$). Sixty-seven genes were predicted to undergo isoform changes in common between two or more oncogenes. Messenger RNA processing factors (5 genes, $p=.008$; WDR33, HNRPC, SF3A1, SNRPA1, TRA2A) and mRNA splicing factors (8 genes, $p=.0003$; HNRPC, HNRPD, TARDBP, HNRPH1, SF3A1, HNRPA2B1, SNRPA1, TRA2A) were the most significant molecular function and biological process represented by these genes.

Table 2: SplicerAV predicts oncogene-induced changes in isoform specific mRNA levels.

	Unique Expressed Genes		SplicerAV Predictions (P<.01)		
GFP vs.	**Total**	**Multi-probeset Genes**	**Alt. Processed Genes**	**Genes with Splice Score > 0**	**Significant Gene Ontologies**
HRAS	7227	2185	645	212	**mRNA splicing (12)** Complement med immunity (3) G-protein mediated signaling (10)
SRC	7007	2015	291	119	Transcription Elongation (2) **mRNA splicing (7)**
CTNNB1	7023	2019	159	54	**mRNA processing factors (4)**
E2F3	7313	2139	187	45	Cell surface receptor signal (10) G-protein mediated signaling (6) Mesoderm development (6) Cell structure and motility (11) **pre-mRNA splicing (5)** Granulocyte-mediate immunity (2)
MYC	7081	2040	115	12	---

HRAS over-expression results in isoform specific EGFR mRNA regulation

Epidermal growth factor receptor (EGFR) was the top ranked gene prediction in HRAS over-expression (p< 10-5). EGFR expression was interrogated by seven probesets, providing an ideal opportunity to examine the behavior of multiple probesets targeting different regions of the same gene. Depending on the EGFR region being interrogated, probesets reported either a significant increase or decrease in expression upon HRAS over-expression (Figure 5). Four main mRNA isoforms of EGFR are annotated in the NCBI database, labeled A, B, C, and D. Isoform A encodes the full length membrane bound tyrosine kinase receptor (Ullrich et al. 1984; Kashles et al. 1991). Variants of isoform A have been observed with either long (ALong) or short (AShort) 3'UTRs (UCSC mRNA accession X00588(Ullrich et al. 1984) and AK225422

(Suzuki et al. 1997)). Isoforms B and D encode truncated intracellular domains (RefSeq NM_201282; RefSeq NM_201284) and isoform C (RefSeq NM_201283) encodes an EGFR variant that lacks a trans-membrane domain and is expected to be soluble (Reiter et al. 2001).

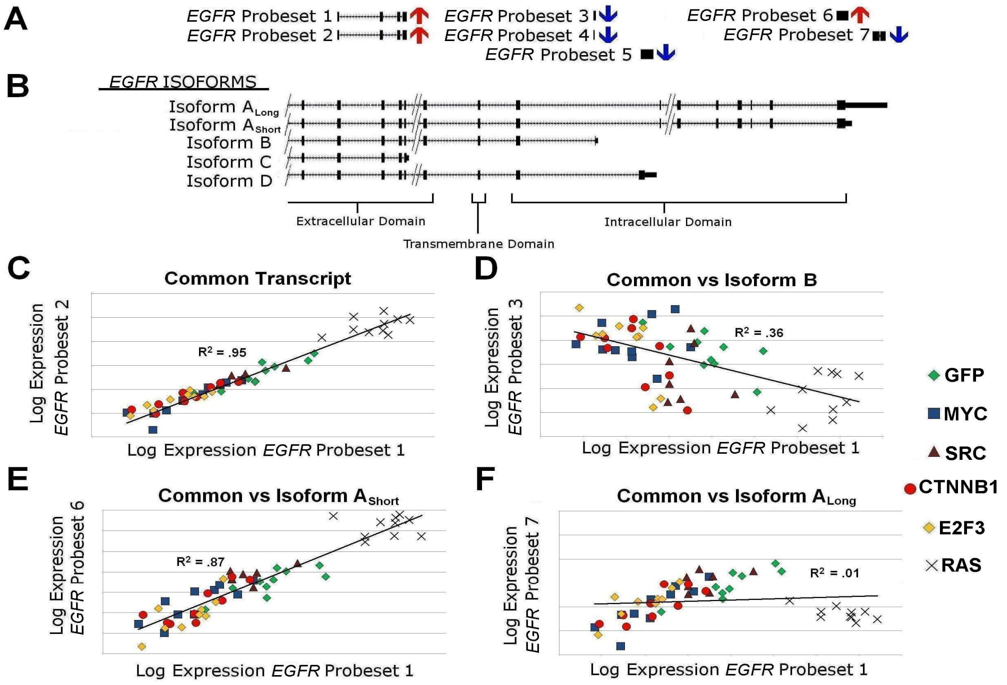

Figure 5: HRAS over-expression causes isoform specific regulation of Epidermal Growth Factor Receptor (EGFR) in human mammary epithelial cells. (A) Probesets on the Affymetrix U133 2.0 plus array interrogate EGFR expression at seven different genomic locations. Up and down arrows indicate each probeset's expression changes in HRAS over-expression compared to GFP controls. Probeset 5 experienced a significant decrease in expression with HRAS over-expression, but was not expressed above background. B) UCSC genomic alignment of probesets and EGFR isoforms. Four previously observed EGFR isoforms (A, B, C and D) are shown with exons represented as black boxes and introns as hashed lines. Extracellular, transmembrane, and intracellular domain regions are shown below the alignment. C-F) Scatter plots of logged expression levels of all 55 samples (GFP, MYC, SRC, CTNNB1, E2F3, and HRAS) for selected pairs of probesets C) Probesets 1 and 2 target a transcript region common to all major isoforms and exhibit highly correlated expression (R2 = .95). D) Probesets 1 and 3 target the common region vs. isoform B specific region and demonstrate a weak inverse relationship (R2 = .36). E) Probesets 1 and 6 interrogate the common vs. AShort isoform region, demonstrating a high degree of correlation across all samples (R2 = .87). F) In contrast, probesets 1 and 7 interrogate common and ALong isoform region and are not correlated (R2 = .01) due to the HRAS induced 3'UTR shortening of EGFR A transcripts.

Probesets 1 and 2, which target a region common to all four isoforms, reported highly concordant (R2 = .95) expression levels across all 55 samples in the dataset (Figure 5C). Probesets targeting different transcript regions (1 and 3) reported poor or even inversely correlated expression levels, (R2 = .36, Figure 5**Figure** D). Due to this "outlier" behavior these probesets would be discarded during conventional microarray expression analysis (Jaksik et al. 2009), however, SplicerAV data suggest that this behavior reflects isoform-specific regulation of EGFR expression

EGFR isoform A (AShort) appeared to be the primary transcript upregulated by HRAS over-expression, as evidenced by highly correlated expression of the probesets targeting the common and AShort isoforms (probesets 1 and 6; R2 = .87). HRAS over-expression caused a robust decrease in the probeset targeting the long 3'UTR of EGFR (probeset 7; ALong) that was not correlated with expression of the common transcript region (Figure 5**Figure** F, R2 = .01). In contrast, common and ALong expression levels were well correlated in non-HRAS samples (R2 = .70). These data suggest a HRAS-specific shortening of the isoform A 3'UTR.

We hypothesize that these HRAS-induced isoform changes promoted EGFR activation via several mechanisms. HRAS increased overall isoform A transcript levels, as evidenced by significant increases in probesets interrogating common regions of the gene (probesets 1 & 2). At the same time, HRAS over-expression resulted in selection of a shorter 3' UTR, which removes known miRNA binding sites present in the ALong UTR and likely increased translation of EGFR mRNAs (Weiss et al. 2008). Widespread 3'UTR shortening to escape miRNA regulation has been observed previously in proliferating cells (Sandberg et al. 2008). EGFR isoforms B & D code for a truncated intracellular domain, which if translated could dimerize with and inhibit activation of both EGFR and HER2 (Kashles et al. 1991). The observed down-regulation of these isoforms is predicted to promote EGFR1 and HER2 activation (Kashles et al. 1991). It should be noted, however, that the corresponding truncated receptors have not been observed. Soluble isoforms composed of the extracellular domain occur naturally and suppress ligand-dependent EGFR signaling and oncogenic transformation in a dominant negative manner (Basu et al. 1989). Our data indirectly address expression levels of the soluble isoforms, which appear to be unchanged.

Our data suggest that HRAS acts through several isoform-specific mechanisms to promote EGFR family signaling. EGFR signaling plays known roles in cell survival, proliferation, adhesion, migration, and differentiation (Adamson and Wiley 1997) . Both EGFR and HER2 are currently therapeutic targets in breast cancer (Browne et al. 2009). Our analysis here suggests that modified regulation of alternative mRNA processing could be used as a novel means of EGFR inhibition, similar to that shown recently for HER2 using splice site switching oligonucleotides (Wan et al. 2009).

SplicerAV predicted isoform changes exhibit low overlap with gene expression changes

Using the same gene expression dataset, SplicerAV was able to predict a number of previously unappreciated changes in isoform specific mRNA regulation. Genes predicted to undergo isoform changes exhibited small overlap with genes predicted to undergo expression changes by conventional analysis, consistent with previous findings in the field (Blencowe 2006) (Li et al. 2006) (Zhang et al. 2006). HRAS and SRC over-expression resulted in the largest changes in both gene expression and isoform changes. Of the212 genes predicted to undergo ideal isoform changes (significant p-value and positive splice score) in HRAS over-expression, only 8 genes (3.8%) were also among the top 212 most significant changes by conventional expression analysis (data not shown). Of the top 119 predicted isoform changes in SRC over-expression, none were in the top 119 most significant expression changes. This low degree of overlap suggests that the results obtained via SplicerAV are largely orthogonal to that of conventional gene expression analyses. This low degree of overlap provides the potential for combining traditional gene expression signatures with SplicerAV isoform-based signatures to improve signature performance.

SplicerAV predicts isoform changes in high vs. low grade breast tumors

Our analysis of oncogene regulated isoform expression demonstrated the ability to generate novel insights into cancer biology. We next determined if similar insights could be obtained from the analysis of alternative processing in clinical tumor samples. Breast cancer has been extensively studied using high-throughput analyses of gene expression at the transcriptome level (Reviewed in (Sotiriou and Pusztai 2009)). In contrast, high-throughput analysis of alternative mRNA processing in breast cancer has been addressed in only a handful of studies (Li et al. 2006) (Andre et al. 2009) (Dutertre et al. 2010). We explored the ability of SplicerAV to detect changes in alternative processing between low and high grade breast tumors in archival expression data.

Sotiriou and colleagues profiled 87 Tamoxifen treated, estrogen receptor (ER) positive tumors obtained from Guys Hospital, London (GUYT) using the Affymetrix HG-U133 PLUS2 GenechipTM(Loi et al. 2008)(GEO accession GSE6532, RMA normalized). Using this dataset, we examined changes in probeset expression between low grade (I, n=17) and high grade (III, n=16) breast tumors. Analysis was limited to probesets present on either the U133A or U133B arrays in order to validate changes in two independent data sets discussed in the next section. 11,248 unique genes were expressed above background in either the low or high grade tumor samples. Among the 4,031 genes interrogated by multiple probesets, SplicerAV predicted that 974 genes underwent significant isoform changes between aggressive and non-aggressive breast tumors (p<.01). Removing genes with negative splice scores yielded a refined list of 241 genes. GO analyses of these 241 genes revealed significant (p<.05) enrichment for several molecular functions including guanyl-nucleotide exchange factors (RAB3IP, RAPGEF2, GAPVD1, CD47, TRIO, ARHGEF7, AKAP13; p=.006), metalloprotease inhibitors(TIMP2, TIMP3; p=.007), ubiquitin-protein ligases (RNF130, TTC3 UBE3B, PML, TRIM26, RBCK1, MIB1, ZNF294, ZUBR1, TRIAD3; p=.007), and mRNA processing factors (SYNCRIP, WDR33, SFRS8, SFRS15,TAF15, SF1, SF3B1, SFPQ, PRP6; p=.01; Table 3).

Table 3: GO analysis of 241 genes predicted to undergo isoform changes between grade I and grade III breast tumors (GUYT).

Molecular Function	# Genes	P-Value	Gene Symbols
Guanyl-nucleotide exchange factor	7	6.22E-03	*RAB3IP, RAPGEF2, GAPVD1, CD47, TRIO, ARHGEF7, AKAP13*
Metalloprotease inhibitor	2	6.52E-03	*TIMP2, TIMP3*
Ubiquitin-protein ligase	10	7.40E-03	*RNF130, TTC3 UBE3B, PML, TRIM26, RBCK1, MIB1, ZNF294, ZUBR1, TRIAD3*
mRNA processing factor	9	1.27E-02	*SYNCRIP, WDR33, SFRS8, SFRS15,TAF15, SF1, SF3B1, SFPQ, PRP6*
Cytoskeletal protein	4	3.42E-02	*DNAL1, NF2, KIF5C, DYNC1H1*
Anion channel	2	3.63E-02	*PML, CLCN3*
G-protein modulator	12	4.64E-02	*RAB3IP, RAPGEF2, GAPVD1, CD47,*
mRNA splicing factor	6	4.94E-02	*TAF15, SFRS8, SF1, SF3B1, SFPQ, PRP6*
Tyrosine protein kinase receptor	4	4.97E-02	*TEK, TPR, IGF1R, PDGFRA*

SplicerAV predicted isoform changes are associated with breast cancer survival

SplicerAV probeset groupings of genes identified in the GUYT training set were used to create individual sample level indexes of relative isoform abundance. We tested an association of these SplicerAV indexes in two independent validation datasets to examine whether specific isoform changes observed in high grade tumors were also associated with poor patient prognosis (see methods). Previous datasets generated by Miller (Miller et al. 2005) (GSE3494) and Pawitan (Pawitan et al. 2005) (GSE1456) have independently profiled breast tumor gene expression using the Affymetrix U133 A and B microarrays (probeset intensities were estimated using MAS5 (69)). These studies include patient outcome, providing the opportunity to test for an association of isoform changes with survival in ER positive tumors.

We generated 687 SplicerAV Indexes from the 241 genes identified in the GUYT training set and calculated their value for each tumor sample in the validation sets. For each SplicerAV Index, tumors were sorted into the top and bottom 50th percentile of tumors. High and low SplicerAV Index groups were then tested for a difference in survival. The GUYT training set had previously determined whether a SplicerAV index was predicted to be increased or decreased in aggressive cancer (defined as Grade III vs Grade I). This pre-specified association with aggressive cancer was used to conduct one-sided logrank tests ($p<.05$) for an association with breast cancer survival for each SplicerAV index in the validation datasets. Failure in the Miller dataset was defined as death from any cause and failure in the Pawitan dataset was defined as death from breast cancer (inherent to the clinical data available). Of the 241 genes tested, 15 genes possessed indexes that were significantly associated with survival in both datasets (Table 4). Guanyl-nucleotide exchange factors (GEFs) and mRNA processing factors were both enriched among the original 241 genes tested. Interestingly, these GO categories were both represented among the 15 validated genes including ARHGEF7, a guanyl-nucleotide exchange factor, and SFPQ, an mRNA processing factor.

Table 4: Isoform changes in gene expression significantly associated with patient outcomes in both validation datasets.

SplicerAV Predictions			Association with Survival	
Gene Symbol†	**Isoform Probeset**	**Hypothesis**	**Miller**	**Pawitan**
ARHGEF7	202548_s_at	DOWN	*0.009	*0.008
DPP7	241973_x_at	DOWN	*0.001	*0.007
EIF4E2	209393_s_at	UP	**0.002	*0.003
MAPKAP1	222426_at	DOWN	*0.019	*0.003
SLC28A10	230448_at	UP	*0.007	0.032
PDXK	202671_s_at	UP	**0.001	0.025
POLI	238992_at	UP	0.037	0.052
SFPQ	201585_s_at	UP	0.062	0.041
SIVA1	203489_at	UP	*0.005	0.075
SSU72	223051_at	UP	*0.018	*0.007
TFDP2	203588_s_at	UP	0.054	*0.008
TIMP2	231579_s_at	DOWN	**0.001	0.056
TncRNA	234989_at	UP	**0.001	0.034
WDFY3	212606_at	UP	0.049	*0.010
WDR26	224897_at	UP	**0.001	0.049

†For genes possessing multiple significant SplicerAV Indices, only one isoform is shown.
*Significant association with survival (p<.01), one sided log rank test
** Significant association with survival (p<.001), one sided log rank test

Few studies have performed high-throughput examination of alternative processing in clinical tumor samples (Gardina et al. 2006; Andre et al. 2009) and to our knowledge no prior studies have examined changes in alternative mRNA processing directly associated with cancer patient survival. This study examined isoform specific mRNA levels in over 400 human clinical samples, providing support for the use of changes in alternative processing as potential prognostic markers in cancer.

ARHGEF7 & EIF4E2 isoform changes are associated with breast cancer survival

A SplicerAV index for Rho guanine nucleotide exchange factor 7 (ARHGEF7) was decreased in high vs. low grade tumors within the GUYT dataset, and was significantly associated with survival in both the Miller (p=.008) and Pawitan (p=.009) datasets. ARHGEF7 expression was assayed by three annotated probesets, providing an opportunity to compare associations of survival with either SplicerAV index or individual probeset expression. The SplicerAV index for ARHGEF7 compared the ratio of a decreasing ("Down") probeset located in the 3'UTR of ARHGEF7 to that of two increasing ("Up1" and "Up2") probesets located in shorter transcripts (Figure 6**Figure** A). We compared the ARHGEF7 SplicerAV index and each individual probeset for an association with breast cancer survival and noted that the SplicerAV index outperformed individual probeset in both datasets (Figure 6**Figure** B).

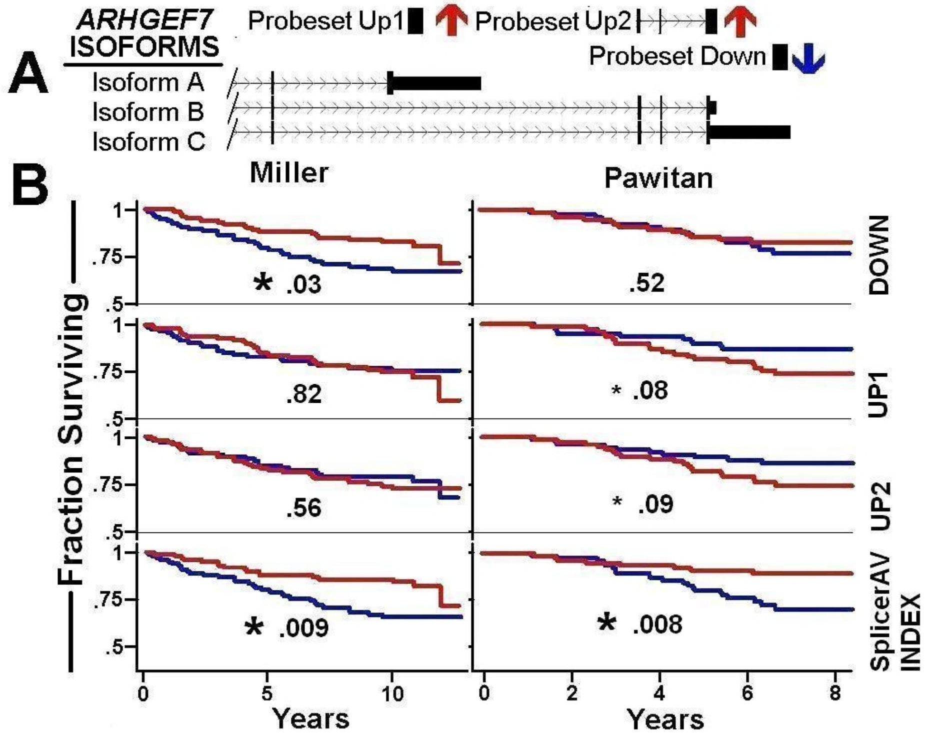

Figure 6: **SplicerAV Index of ARHGEF7 is associated with breast cancer survival.** Panel A. Schematic representation of ARHGEF7 isoforms A, B and C, with regions interrogated by probesets that increase shown as Probesets Up 1 and 2 (red arrows), and the region which decreases denoted as Probeset Down (blue arrow). Panel B. The fraction of patients surviving in each cohort (vertical axis) is shown over time in years (horizontal axis) as a function of individual probeset expression or SplicerAV index. Survival of patients in the top (red line) and bottom (blue line) 50th percentile are plotted by individual probeset expression (Down, UP1, and UP2) and the SplicerAV index within the Miller (left) and Pawitan (right) cohorts. Results of two-tailed logrank tests of survival are shown, with asterisks indicating significance at the .05 (large asterisk) and .10 (small asterisk) levels.

A SplicerAV index for Eukaryotic translation initiation factor 4E family member 2 (EIF4E2) was increased in high vs. low grade tumors within the GUYT dataset, and was significantly associated with survival in both the Miller (p=.002) and Pawitan (p=.003) datasets. The SplicerAV index for EIF4E2 compared the ratio of an increasing

“Up” probeset targeting a coding region to that of a decreasing “Down” probeset located in the 3’UTR of the longest transcript (Figure 7A). For EIF4E2, survival could be predicted by an increase in the “Up” probeset alone (Miller, p=.003; Pawitan, p=.0007; Figure 7B). Low levels of the “Down” probeset were only significantly associated with poor survival in the Pawitan cohort (p=.04).

Whether or not individual probesets could demonstrate a consistent association with survival differed by gene. Although individual probeset behavior may represent an alternative processing event, only through comparison with other probesets for that gene can SplicerAV uncover these relevant and predictive isoforms that would go unnoticed in conventional analyses.

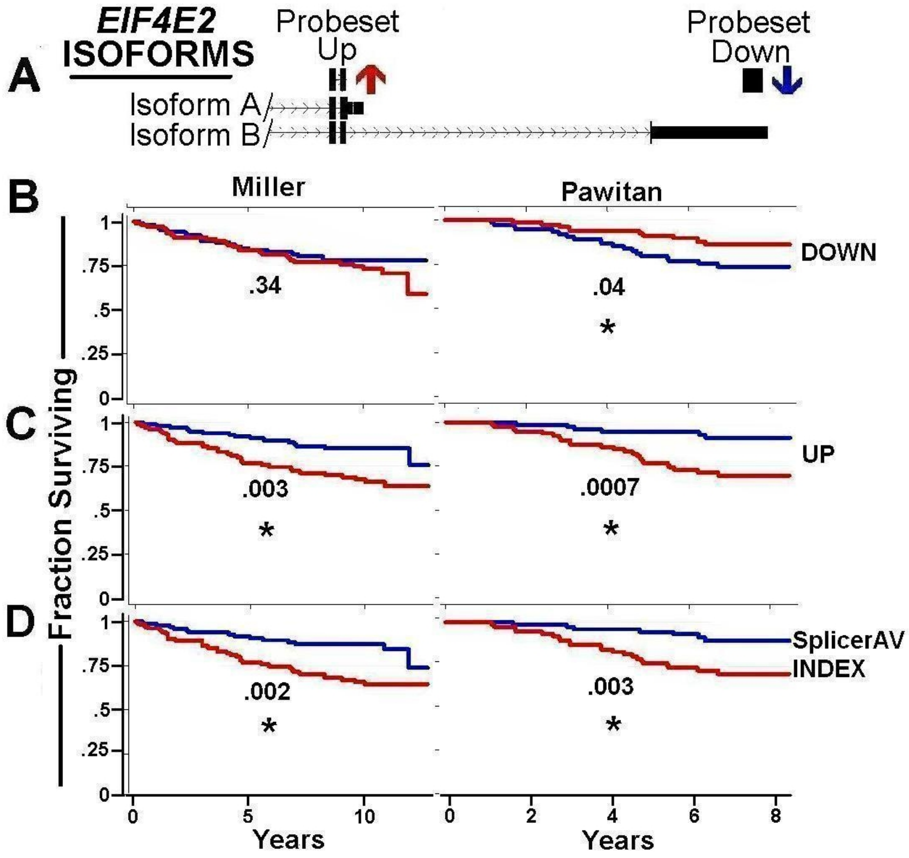

Figure 7: EIF4E2 probesets are associated with breast cancer survival. Panel A. Schematic representation of EIF4E2 isoforms A and B, with region interrogated by probesets shown as Up (red arrow), and Down (blue arrow). For panels B, C, and D, the fraction of patients surviving in each cohort (vertical axis) is shown over time in years (horizontal axis) as a function of individual probeset expression or SplicerAV index. Survival of patients in the top (red line) and bottom (blue line) 50th percentile are plotted by individual probeset expression (B,C) and the SplicerAV index (D) within the Miller (left) and Pawitan (right) cohorts. Results of two-tailed logrank tests of survival are shown, with asterisks indicating significance at the .05 level.

Combining isoform changes from multiple genes improves prediction of breast cancer survival

We chose a subset of the 15 validated isoform changes to examine the potential for generating an isoform signature that combined information from multiple isoform changes to improve prognostic accuracy. We initially chose the six genes, EIF4E2, ARHGEF7, SLC28A10, PDXK, TncRNA, and MAPKAP1, that produced the clearest separation between good and poor survival in individual prognostic analyses (data not shown). Stratifying patients by SplicerAV index for each gene demonstrated the expected association with survival (Figure 8A-F). The number of poor prognostic events was tallied for each patient. Survival was then plotted for individuals with low (0-1 events, blue), intermediate (2-4 events, black), or high (5-6 events, red) numbers of poor prognostic events (Figure 8G). This stratification of patients by total poor prognostic events demonstrated highly significant associations with survival in both the Miller (p=6e-7) and Pawitan (p=4e-7) cohorts. The combined isoform signature demonstrated prognostic value beyond that of any individual isoform or probeset change.

Similar to our in vitro analyses of oncogene over-expression, we observed low overlap between gene expression and SplicerAV changes. Of the 241 isoform changes predicted by SplicerAV in the GUYT training set that were later tested for an association with poor prognosis, only one gene (0.4%), BTD, was also among the top 241 differentially expressed genes. The orthogonality of candidate gene lists identified by SplicerAV and conventional methods suggests that these two methods detect different biological processes and may provide independent value in generating molecular classifiers. SplicerAV can generate both conventional and isoform specific gene expression analyses, and therefore provides two non-redundant datasets from one experiment.

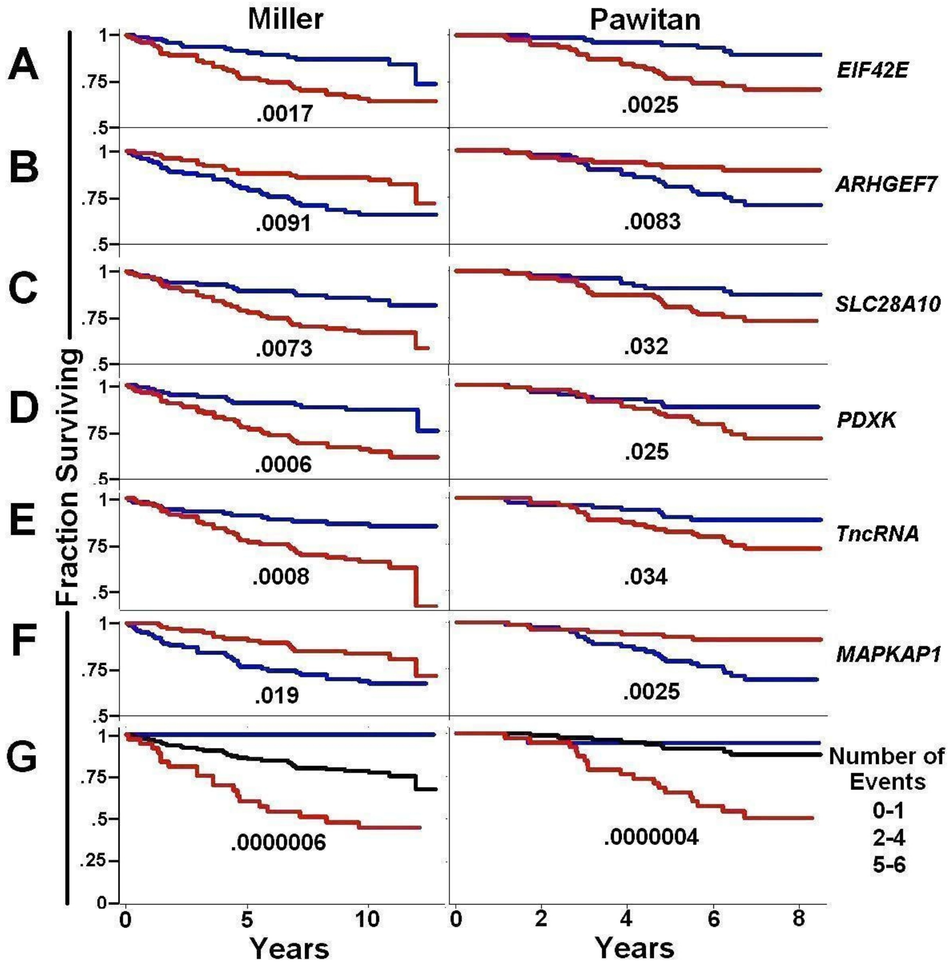

Figure 8: A six isoform signature provides improved prediction of breast cancer survival compared to individual isoforms. The fraction of patients surviving in each cohort (vertical axis) is shown over time in years (horizontal axis) as a function of individual probeset expression or SplicerAV index. Survival of patients in the top (red line) and bottom (blue line) 50th percentile are plotted by the SplicerAV index for six genes; EIF4E2 (A), ARHGEF7 (B), SLC28A10 (C), PDXK (D), TncRNA (E), MAPKAP1 (F) for the Miller (left) and Pawitan (right) cohorts. Patients survival stratified by a low(0-1), intermediate(2-4), and high (5-6) number of poor prognostic events is shown in panel G.

2.3 Methods

SplicerAV algorithm details

SplicerAV takes probeset intensities generated using conventional normalization methods (i.e. MAS5 or RMA output) as input. SplicerAV first summarizes the average $\log_2$fold change in expression and the corresponding t-statistic for each probeset on the array. Probeset changes are assigned an initial weight based on their normalized t-statistic, T_{Norm}. Conceptually, weighting by T_{Norm} counts probesets undergoing significant expression changes one time. This is because T_{Norm} equals one for probesets reporting expression changes significant at the .05 level (two tailed t-test).

$$T_{Norm} = \frac{|\,\mu_{Treatment} - \mu_{Control}\,|}{\sqrt{\sigma^2_{Treatment}\ \ \sigma^2_{Control}}} \div T_{Critical} \qquad [3]$$

Probesets targeting the same gene are next grouped together using annotation provided by the array manufacturer. Genes targeted by probesets with a T_{Norm} value greater than one scale their weights so that the maximum T_{Norm} within that gene is reduced to one. This prevents counting any probeset more than once.

$$If\ \ Max(T_{Norm}) > 1\ then\ Weight = \frac{T_{Norm}}{Max(T_{Norm})} \qquad [4]$$

$$Else\ Weight = T_{Norm}$$

At this step, individual probeset weights are raised to a user specified power (*Wt_scale*, default = 2), which allows preferential focus on more significant probeset changes in expression at the cost of removing information from less reliable probesets and reducing the power of significance tests.

This weighting scheme assigns a weight between 0 and 1 to each probset, indicating the number of times a probeset's observations will be counted in the Gaussian mixture model. In the final Gaussian mixture model, each probeset weight is multiplied by the average number of paired observations among treatment and control groups for that probeset ($N_{avg\_obs} = (N_{treat\_obs} + N_{control\_obs})/2$). The resulting model counts each effective pair of observations for a probeset at most once, with less reliable probesets being counted less.

$$\begin{aligned}&\mathit{Effective\ Weight}_{prbset}\\&= \mathit{EfWt}_{prbset}\\&= (\mathit{Weight}_{prbset})^{Wt\_Scale} * \mathit{Avg\_Obs}_{prbset}\end{aligned}$$

[5]

The Effective Weight for each probeset is used as the final probeset summary weight in the Gaussian mixture model. Average probeset log2fold changes in expression are fitted using two models, which contain one and two Gaussian distributions, respectively. Comparison of the relative fit under these two models yields a maximum likelihood ratio (MLR), which can be assessed for statistical signifance using a standard likelihood ratio (LR) test statistic, asymptotically distributed as $\chi^2(2)$, for each gene.

$$MLR = \prod_{prbset=1}^{Tot\_prbsets} \frac{\mathit{Likelihood}_A^{*IfA} * \mathit{Likelihood}_B^{*IfB}}{\mathit{Likelihood}_{Single}}$$

[6]

Where:

$$Likelihood_i = \left[\frac{1}{\sigma_i \sqrt{2\pi}} \exp\left(- \frac{(X_{prbset} - \mu_i)^2}{2\sigma_i^2} \right) \right]^{EfWt_{prbset}}$$

X_{prbset} = the log2fold expression change of that probeset

μ_A = the weighted average log2fold change in expression for probesets assigned to groupA

μ_B = the weighted average log2fold change in expression for probesets assigned to groupB

μ_{Single} = the weighted average log2fold change in expression for all probesets targeting the gene

σ_A, σ_B, and σ_{single} for groups A,B, and all probesets are determined by expectation maximization, bounded by a minimum value of 10% to prevent over-fitting by the model. The value of 10% was chosen as a conservative limit based on empirical observations of summarized significant log2fold probeset changes, which consistently exhibited standard deviations (σ) below 10% across analyzed datasets (data not shown).

Biological Modifiers

SplicerAV incorporates biologically motivated modifiers to alter the relative ranking of potential changes in alternative processing to suit the final objectives of the user. These modifiers can be adjusted by the user and do not affect the p-values reported by SplicerAV. The specified form and magnitude of these biologically motivated modifiers were empirically derived through analysis of several datasets.

Multiple Probeset Modifier

The multiprobeset modifier adjusts the splice score by the total possible ways that all the probesets targeting a given gene can be placed into groups of two. This method penalizes genes containing large numbers of probesets capable of generating a large number of alternative processing hypotheses which are difficult to interpret, using a bonferroni multiple hypothesis correction.

$$\mathit{Multiprobeset\ Modifier} = -\ln(2^{tot\_prbsets-1} - 1)$$

[7]

Expression Cutoff Modifier

The expression cutoff modifier calculates the $\log_2$ difference in average expression between the two groups of probesets, A and B. Genes whose expression between groups falls below a user specified threshold minimum fold change are penalized using a smoothed function whose steepness is set using a user specified *sharpness* parameter.

$$\mathit{If}\ \ \mathit{AvgChange} < \mathit{Cutoff}\,,$$
$$\mathit{Cutoff}\ \ \mathit{Modifier} = \mathit{Sharpness} * \ln(\mathit{AvChange} / \mathit{Cutoff}\,)$$

[8]

Centering Modifier

The centering modifier preferentially ranks genes whose probeset expression changes in opposite directions, suggesting a qualitatively different event which cannot be explained by poor annotation of probesets targeting intronic regions, saturated probeset signals, non-hybridizing probesets, or other probeset expression behavior deviating from a linear relationship with transcript abundance. Genes in which both groups of probesets change in the same direction (either both increasing or decreasing) are penalized, while genes containing groups of probesets with mean expression levels moving in opposite directions are given a bonus.

$$\begin{aligned}&If\ (Mean\Delta_{GrpA} * Mean\Delta Exp_{GrpB}) < 0,\\ &\quad then\ Centering\ Factor = -Centering\ Factor\\ \\ &Centering\ Modifier\\ &= Centering\ Factor * Min(|\,Mean\Delta_{GrpA}\,|, |\,Mean\Delta Exp_{GrpB}\,|)\end{aligned} \qquad [9]$$

Gene Ontology Analyses

Gene ontology (GO) analyses compared genes with SplicerAV predicted isoform changes (p<.01, splice score > 0) to a reference set of all genes evaluated for isoform changes in each condition using PANTHER (Thomas et al. 2003; Thomas et al. 2006). Non-overlapping GO categories with more than one gene were reported.

2.4 General Comments

Traditional analyses of gene expression data have considered the probeset as the basic unit of expression. Under this paradigm, the presence of multiple probesets has been viewed largely as a nuisance. Current approaches dealing with the issue of multiple probesets have used either probeset location or the mean, median, or largest probeset expression change to distill multiple probesets into a single gene level expression value. Each of these approaches would have yielded a different readout of *EGFR* expression changes in HRAS over-expression, making conventional interpretation inadequate for such genes. Software has even been developed whose sole purpose is the removal of discordant probeset expression values for probesets targeting the same gene (Jaksik et al. 2009).

We propose that for genes with multiple probesets, isoform specific expression changes may be a more appropriate means of interpreting standard microarray expression data than the current one gene = one probeset paradigm. Previous algorithms (Fan et al. 2006) (Hu et al. 2001) have examined the possibility of investigating changes in alternative processing using individual probe level data. These methods have relied on custom chips, or would not have detected events predicted by SplicerAV in this paper because such methods do not examine events spanning multiple probesets. SplicerAV provides a systematic means by which to detect and interpret inconsistent probeset behavior within the same gene, a situation where an oversimplified perspective may be obscuring relevant and important biological changes.

This study marks the first *en masse* analysis of mRNA isoform changes in existing conventional expression microarray data. We have shown here that re-analyzing such data using a different paradigm can uncover novel biological insights and potential prognostic markers.

Conclusion

The combination of material, personnel, and clinical costs of obtaining gene expression microarray data has resulted in a massive archive of these data accumulated over the past two decades. Many previously created datasets, particularly clinical datasets, are unique and cannot be reproduced. Numerous private and public repositories of microarray expression data exist, with the largest public repository, Gene Expression Omnibus, containing over 50,000 data samples from the Affymetrix U133 and U95 series alone. In this chapter we demonstrated the utility of SpicerAV, the first program used to analyze this existing data *en masse* for isoform specific changes that can result from alternative mRNA processing(Robinson et al. 2010).

3. Conventional Affymetrix U133 Arrays Provide Superior Detection of 3' Located Differential mRNA Processing Compared to Human Exon Arrays

In this chapter, I describe the implementation and application of SplicerAV to exon array data (SplicerEX) to analyze and characterize changes in mRNA processing during Epstein Barr Virus induced transformation of naïve B cells into lymphoblastoid cell lines (LCLs).

3.1 Introduction

Genome-wide analysis of differential mRNA processing became accessible to the general research community with the introduction of the commercially available splice-sensitive microarrays. One of the first commercially available splice-sensitive arrays was the Affymetrix Human Exon 1.0 ST array, alternatively referred to as the HuEx or Affymetrix exon array. The novelty of the Affymetrix Human Exon 1.0 ST platform has been a source of trepidation for scientists deciding whether to replace conventional 3' IVT (3' in vitro transcription) gene expression arrays with the new HuEx arrays. Commercially available 3' IVT microarrays have existed for decades and have provided a benchmark to test the ability of exon array arrays to reliably assay gene expression. The general consensus that has emerged is that the HuEx array performs reasonably well in replicating U133 assessment of differential gene expression (Bemmo et al. 2008) (Abdueva et al. 2007) (Robinson and Speed 2007). The ability of U133 and HuEx arrays to detect changes in alternative mRNA processing has not been compared previously.

In this chapter we use an expanded version of the SplicerAV algorithm, SplicerEX, to study a B cell model of EBV induced lymphoma to compare isoform changes detected using the U133 and HuEx microarrays. We have automated the characterization of predicted differential mRNA processing events, which has made it feasible to characterize widespread differences in events detected with the U133 and HuEx platforms.

We find that the U133 array is more sensitive than the HuEx platform at detecting changes in both tandem 3' UTR length and 3' terminal exon (TE) choice. This study suggests that the U133 2.0 plus array, originally designed to interrogate gene expression, may be the Affymetrix microarray of choice for detecting differential processing of 3' transcript regions. Using SplicerEX, we demonstrate significant biases in differential mRNA processing towards 3'UTR shortening and removal of internal exon content in LCLs vs. naïve B cells.

To our knowledge, the SplicerAV/EX set of programs remain the only programs currently available to analyze differential mRNA processing on U133 arrays at the level of the probeset (Robinson et al.). SplicerEX is the only program available capable of automatically categorizing differential mRNA processing events by mechanistic and directional characteristics using commercially available microarrays. SplicerEX is freely available upon request and is designed for experimental biologists interested in finding models of AS for in depth study.

3.2 Results

Sample Selection

We were able to obtain three sets of lymphoblastoid cell lines (LCL) created from matching B cell donors, and one set of unmatched LCL and B cells. RNA from all 4 LCL samples and all 4 naïve B cell samples were successfully hybridized to both the U133 2.0 plus and Human Exon arrays for a total of 16 independent hybridizations (4 LCL and 4 B cell on the U133 array and 4 LCL and 4 B cells on the exon array)(Figure 9).

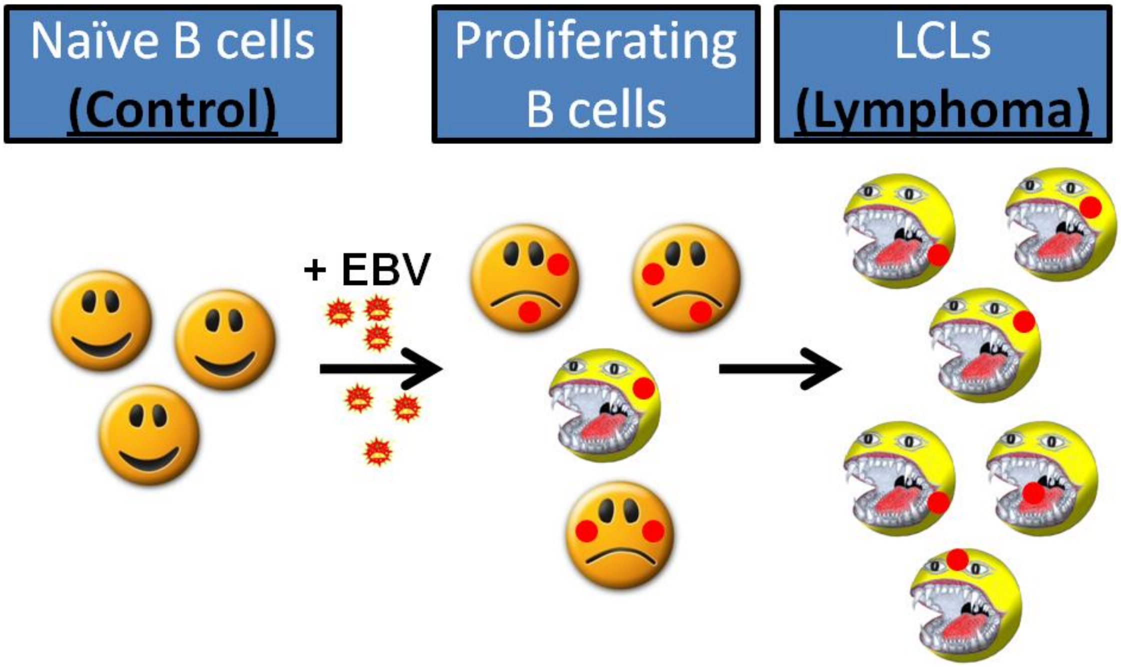

Figure 9: EBV induced transformation of Naïve B cells. B cells are infected with EBV and surviving cells are allow to proliferate. Lymphoblastoid cell lines emerge following several weeks of serial passaging.

Affymetrix U133 and HuEx arrays detect non-overlapping changes in genes undergoing changes in alternative mRNA processing

A total of 5,682 genes were detected as being expressed above background on both the U133 and HuEx array platforms in either Naïve B cells or LCLs (Figure 10). These genes composed 72% of the 7,874 genes detected by the U133 arrays and 74.3% of the 7646 genes detected by the HuEx arrays. The overlap of genes that were detected above background by both platforms was highly significant ($\chi^2 = 6122$, $p < .0001$).

Of the 5,682 genes detected on both arrays, there was considerable overlap between genes that were detected as differentially expressed. A total of 512 genes increased significantly ($p < .01$, fold change > 2) on both array platforms, corresponding to 40% of the 1,291 genes increased on the U133 and 76% of the 678 genes increased on the HuEx platform ($\chi^2 = 1219$, $p < .0001$) . Similar overlap was found among decreased genes. A total of 118 genes decreased significantly ($p < .01$, fold change > 2) on both array platforms, corresponding to 64% of the 184 genes decreased on the U133 and 53% of the 222 genes decreased on the HuEx platform ($\chi^2 = 1820$, $p < .0001$) .

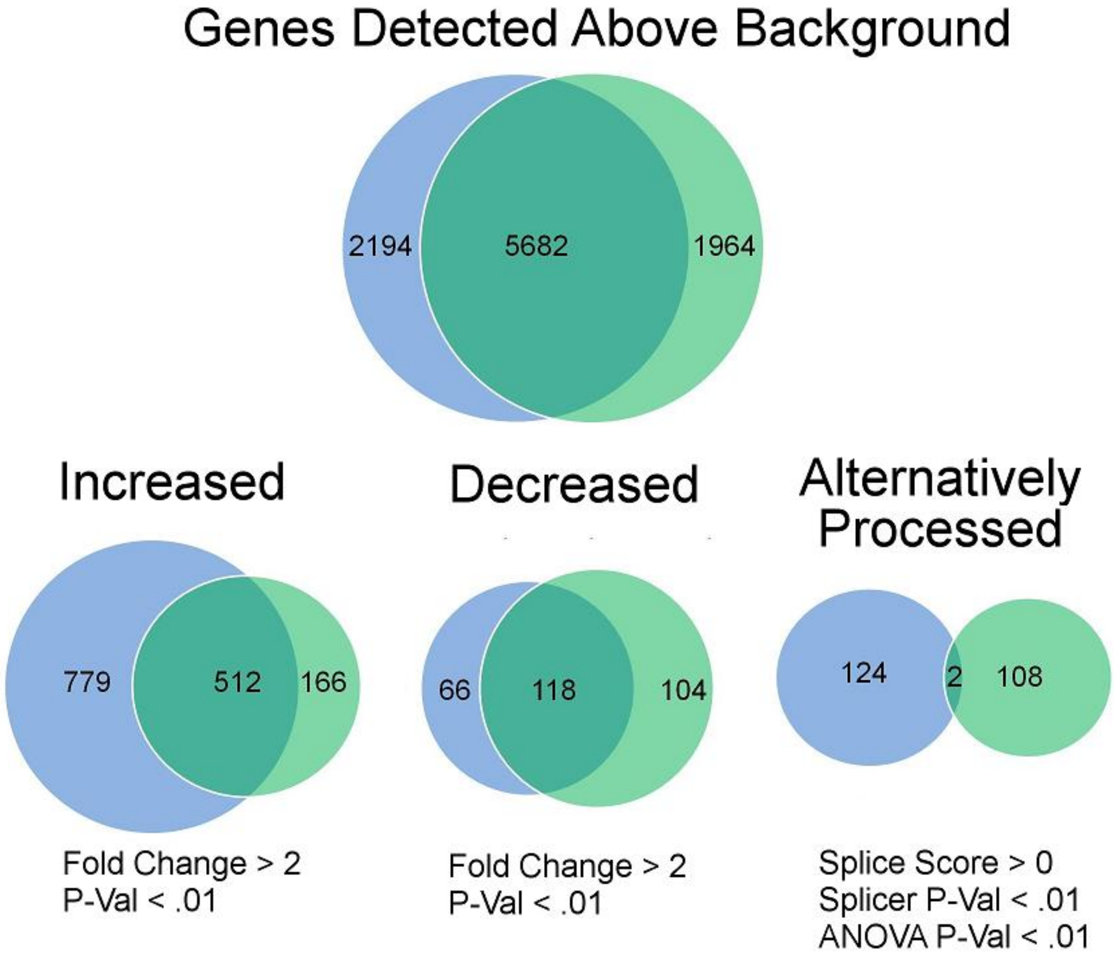

Figure 10: U133 and HuEx arrays detect non-overlapping changes in alternative mRNA processing.

In contrast, there was no significant overlap between genes that were detected to be alternatively processed by both arrays ($\chi^2 = 0$, p = 1). Only 2 genes, AURKB and TXNDC5, were independently considered hits by both arrays (splice score > 0, splicer p < .01, ANOVA p < .01). These two genes corresponded to 2% of the total genes detected by either the U133 (126 total) or HuEx (110) array.

SplicerEX reveals distinct gene ontologies regulated by transcription vs. alternative mRNA processing in B cell transformation

High confidence lists of differentially expressed genes were obtained by limiting genes to those detected as differentially increased or decreased on both the U133 and HuEx array platforms (Appendices A and B).

Ontology analyses of genes increased in LCLs vs. naïve B cells revealed enrichment for biological processes involved in cell cycle and cell structure (both P <.001;Table 5). Among the list of 512 genes increased within LCLs vs. naïve B cells, only one gene with functions in mRNA splicing, *HNRPLL*, was found. This indicated a significant depletion of genes involved in mRNA splicing among the list of 512 genes, which was expected to contain nine such genes (P < .001). Enrichment of molecular functions were observed in cytoskeletal proteins, oxidoreductases, and reductases (all P < .002).

Table 5: Gene ontology enrichment in genes increased in LCLs vs. naïve B cells

Biological Process	**P value**	**Genes**
Cell cycle	1.7E-06	*ASPM,AURKA,AURKB,BRCA1,BUB1,BUB1B,C14orf166,CALM3,CCNA2,CCNB1,CCNB2,CCND2,CCNE1,CDC25A,CDC45L,CDC6,CDCA4,CDK6,CENPE,CENPF,CHEK1,NEDD9,NUF2,ORC1L,PLK4,PRC1,PTTG1,RCBTB2,RFC3,RPN2,SESN2,SLFN13,STK38L,SUMO3,TFDP1,TOP2A,TRIM69,TRIP10,TTF2,TTK,TUBA8,TUBGCP5,UBE2C*
mRNA splicing (depleted)	9.0E-04	*HNRPLL*
Cell structure	9.2E-04	*ACTN1,CKAP5,CORO1C,CTNNAL1,DBN1,DCTN5,FOXM1,GTSE1,KIF14,KIF20A,KIF21A,KLHL2,LCP1,LIMA1,LMNB1,LMNB2,MX2,SCARB1,STK38L,TJP2,TMOD1*

Table 5, continued.

Molecular Function	**P value**	**Gene**
Cytoskeletal protein	3.1E-04	*ACTN1,ASPM,CCIN,CENPE,CKAP5,CORO1C,CSRP1,CTNNAL1,DBN1,DCTN5,KIF11,KIF14,KIF20A,KIF21A,KIF23,KIF2C,KLHL2,LCP1,LIMA1,LMNB1,LMNB2,MX2*
Oxidoreductase	1.1E-03	*ACADM,AHRR,ALDH18A1,BLVRA,CRYZ,CYBRD1,DECR1,DHCR24,DHCR7,FAR2,FAS,HSD17B12,HSDL2,IDH1,IDH2,LOXL1,MDH2,ME1*
Reductase	1.4E-03	*CRYZ,CYBRD1,DECR1,DHCR24,DHCR7,FAR2,HSD17B12,HSDL2,MSRB2,NDUFS3,NDUFV1,RRM1,UQCRC2*

Ontology analyses of genes decreased in LCLs vs. naïve B cells revealed enrichment for pathways involved in JAK/STAT signaling, apoptosis, and inflammation mediated by chemokines (all P < .007; Table 6). Biological processes among decreased genes were enriched for B cell and antibody mediated immunity, cytokine signaling, and cell surface receptor signaling (all P < .001). Molecular functions among decreased genes were enriched for receptors, homeobox transcription factors, and signaling molecules (all P < .005).

Table 6: Gene ontology enrichment in genes decreased in LCLs vs. naïve B cells

Pathway	**P value**	**Genes**
JAK/STAT signaling pathway	5.07E-03	*JAK1,PTPRC,STAT4*
Apoptosis signaling pathway	5.20E-03	*BCL2L11,CASP8,LTB,MALT1,REL,TNFRSF10A,*
Inflammation mediated by chemokine and cytokine signaling pathway	6.11E-03	*CXCR4,CXCR5,INPP5D,JAK1,NFATC1,REL,STAT4,VAV3,*

Table 6, continued.

Biological Process	**P value**	**Genes**
B-cell- and antibody-mediated immunity	8.1E-06	*CXCR5,FCRL2,FCRL3,IL13RA1,LTB,LY9,VAV3*
Cell surface receptor mediated signal transduction	1.2E-05	*CXCR4,CXCR5,ECE1,FOXP1,GABBR1,IL13RA1,IL4R,INPP5D,JAK1,LTB,PTPRO,RASGRP2,SLA,STAT4,TAGAP,TGFBR2,TNFRSF10A,TRAF5,VAV3*
Cytokine and chemokine mediated signaling pathway	1.4E-05	*CXCR4,CXCR5,IL13RA1,IL4R,INPP5D,LTB,STAT4,TGFBR2,TRAF5*

Molecular Function	**P value**	**Genes**
Receptor	3.7E-04	*CXCR4,CXCR5,FCRL2,FCRL3,GABBR1,IL13RA1,IL4R,KIAA0999,LY9,NOTCH2,NR4A1,PTPRC,PTPRO,TGFBR2,TNFRSF10A*
Homeobox transcription factor	4.2E-03	*HHEX,SATB1,ZHX2*
Signaling molecule	4.5E-03	*IL16,INPP5D,LTB,LY9,NOTCH2,RASGRP2,SLA,STAT4,TRAF5*

Because of the small degree of overlap between alternative mRNA processing changes detected by the two arrays, ontology analyses for alternatively processed genes were performed on the combined list of genes that were alternatively processed according to either platform (N = 281). This included genes that were detected on one platform but not the other. Among the 281 genes differentially processed between LCLs and naïve B cells, there was enrichment of molecular functions involving cysteine proteases (P = .006), transcription factors (P = .009), and RNA binding proteins (P = .01). Alternatively processed cysteine proteases included CASP6 and CASP7. Transcription factors included TCF3, TCF4, and TCFL5. RNA-binding proteins included STAU1 and STAU2.

Table 7: Gene ontology enrichment in genes differentially processed between LCLs vs. naïve B cells

Molecular Function	P value	Genes
Cysteine protease	5.71E-03	CASP6,CASP7,CTSS,PGPEP1,USP30,USP48,USP6
Basic helix-loop-helix transcription factor	8.76E-03	MSC,MXD4,TCF3,TCF4,TCFL5
Other RNA-binding protein	1.18E-02	C1orf107,CPSF6,CUGBP2,RBM19,RBM8A,RCL1,RTCD1,STAU1,STAU2

B cell transformation reduces 3'UTR length and internal exon content

SplicerEX assigned one of the following six mutually exclusive categories to genes detected as alternatively processed: 1) Alternative 5' initiation 2) Internal Event 3) Tandem 3' UTR 4) Alternative 3' Terminal Exon choice 5) Alternative transcript length, and 6) unclassified (Table 8). All classified categories generated specific hypotheses that agreed with subjective assessments and could be directly tested using experimental validation methods such as RT-PCR or northern blot. Of the top 20 hypotheses automatically generated by SplicerEX for both the U133 and HuEx platforms, all 40 automated hypotheses agreed with the subjective categorization assigned by the researchers.

Table 8: Categories of mRNA processing events assigned by SplicerEX

Category	Description	Directional Subtypes	Optimal Detection Platform
5’ Initiation	Change in 5’ transcription initiation site. Considered to result in coding changes if 5’ isoform possess three or more exons prior to the start of the 3’ isoform.	Relative increase in 5’ most initiation site (more 5’)	Exon Array
		Relative decrease in 5’ most initiation site (more 3’)	
Internal Event	Changes in internal exon content. Includes primarily cassette exons, alt 5’ SS, alt 3’ SS, and intron retention.	Inclusion	Exon Array
		Exclusion	
Tandem 3’ Terminal Exons	Change in length of 3’ TE. Almost universally results in non-coding changes in 3’ UTR length.	Shorten	U133
		Lengthen	
3’ Terminal Exon Choice	Change in choice of 3’ TE. Almost universally results in protein coding changes.	More 5’	U133
		More 3’	
Alternative Transcript Length	1) Metaprobeset 1 or 2 interrogates 3’ TE	N/A	
Unclassified/ No class	Unable to be categorized using above	N/A	

These general categories reflect basic mechanistic descriptions of each alternative processing event, and are the same regardless of which condition is considered the reference group. SplicerEX also assigns directional subtypes, which describe a change in processing associated with a specific phenotype. Alternative 5’ initiation start sites and alternative 3’ terminal exons were subcategorized as being more 5’ or 3’ located within UCSC gene transcripts. Internal cassette exons made up the bulk of observed internal events, and were succesfully characterized with regards to inclusion vs. exclusion.

Tandem 3’ terminal exon events were uniformly observed to result in 3’UTR length changes, which were either lengthened or shortened.

B cell transformation reduces 3’UTR length and internal exon content

Alternative mRNA processing categories differed significantly by platform ($\chi2$ = 141, 5 df, P < .001; Figure 11). The U133 array detected primarily changes in 3’ UTR length (50%) and alternative 3’ terminal exon choice (26%), while the HuEx array detected mostly internal cassette exons (45%) and alternative 5’ initiation sites (21%).

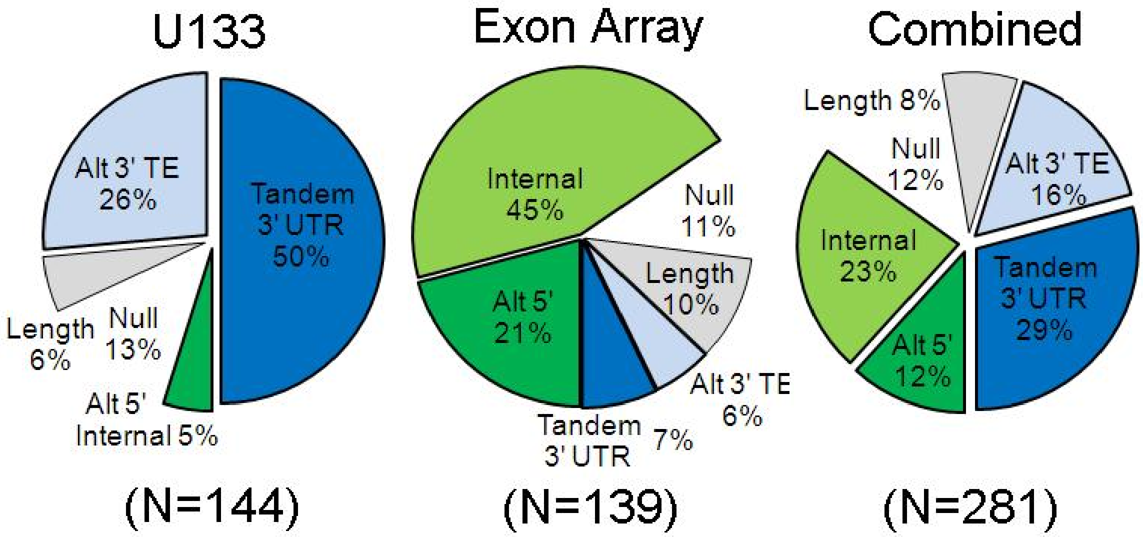

Figure 11: Distribution of events observed by array platform.

The U133 and HuEx platforms exhibited similar performance with regards to the total number of events detected and hypotheses created. Testable hypotheses could be automatically generated for the majority of genes on both the U133 (125/ 144, 87%) and HuEx (123/139, 88%) arrays. Of the 125 hypotheses created by the U133 array, 39 (31%) were predicted to result in alternative ORF usage and subsequent isoform specific protein coding changes. Of the 139 hypotheses created by the HuEx array, 69 (56%) were predicted to result in changes in protein coding transcript regions.

As expected, the U133 arrays displayed a strong tendency to detect changes in mRNA processing at the 3’ end of genes. HuEx arrays displayed an equally strong tendency to detect events in the 5’ and internal portions of genes (Figure 12).

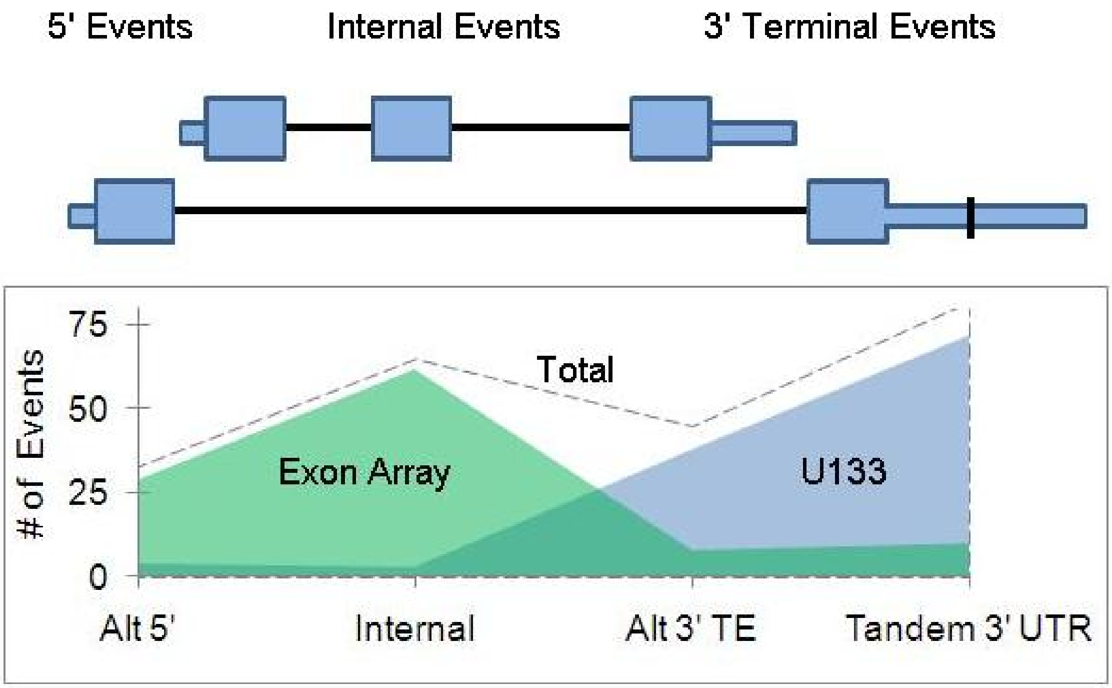

Figure 12: U133 and HuEx arrays preferentially detect changes in mRNA processing in 3’ vs. 5’/internal transcript regions

Relative to naïve B cells, LCLs preferentially shortened mRNA 3’UTR lengths (P = 2e-15) and excluded internal exon content (both P = 3e-8; Figure 13).

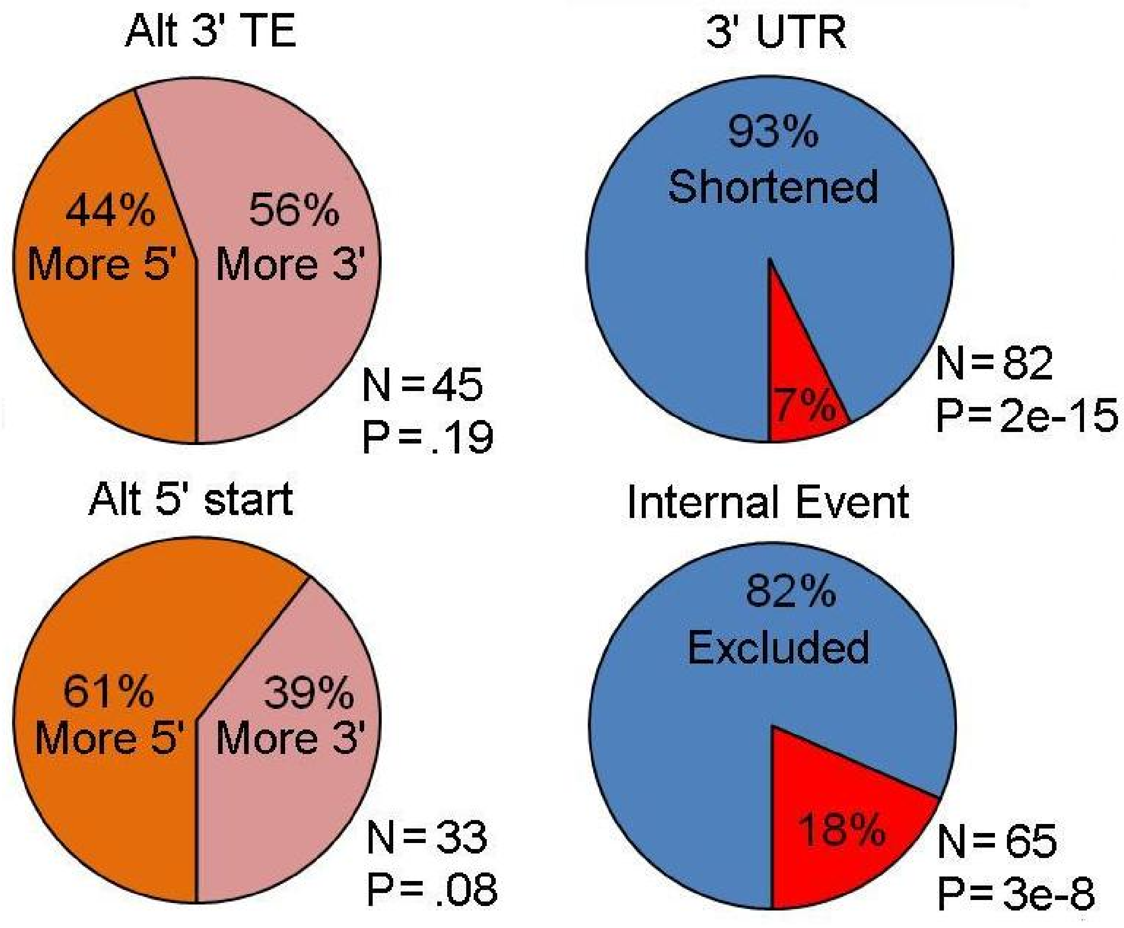

Figure 13: B cell transformation reduces 3'UTR length and internal exon content

Of the 82 changes in tandem 3'UTR length detected by SplicerEX, 76 (93%) shortened the 3'UTR (P = 2e-15). Of the 65 internal splicing events detected by SplicerEX, 53 (82%) excluded internal exon content (P = 3e-8). There was no preference towards more 5' or more 3' located terminal exon choice in LCLs vs. naïve B cells (P=.19). There was no significant preference towards choosing a more 5' located alternative start site, however a weak trend (P = .08) was observed for choosing more 5' located initiation sites in LCLs vs. Bcells.

3.3 Methods

Adaption of SplicerAV to exon array data

Previously, we created a program, SplicerAV, which employs a Gaussian mixture model to detect changes in mRNA processing from conventional Affymetrix 3' IVT expression microarrays. We adapted our original Gaussian mixture model to efficiently function on a wider array of newer splicing arrays, in particular the Affymetrix Human Exon 1.0 ST (HuEx). The updated algorithm has been tested on both conventional and exon array data, and is capable of both detecting and categorizing changes in alternative mRNA processing. To differentiate this algorithm from the previous SplicerAV program, we refer to the new program as SplicerEX.

Creation of an algorithm capable of correctly categorizing alternative mRNA processing event types in both conventional and exon array data posed several challenges. Within the U133 2.0 plus series, genes are targeted by an average of 3.2 probesets per gene, with few genes interrogated by more than four or five probesets. In contrast, the HuEx series uses an average of 10 probesets per gene, with the majority of genes targeted by 4-40 probesets per gene. This raised two concerns 1) excessive multiple hypothesis testing and 2) difficulty identifying specific isoform ratios.

The large number of hypotheses being tested per gene presented two issues. First, each gene on the exon array was receiving a large penalty for multiple hypothesis testing, likely resulting in a increased rate of false negatives. Second, the sheer number of hypotheses tested raised a simultaneous concern of overtesting and may have increased the number of false positive results.

As a separate issue, the large number of probesets present on exon arrays made identification of specific isoform ratios and subsequent categorization of splicing events difficult. Isoform ratios within the original U133 array were calculated by identifying the single most significant increasing probeset (Group A) and contrasting it the single most significant decreasing probeset (Group B). We found that with the U133 arrays, these single probesets provided the appropriate level of focus to accurately categorize mRNA processing events, described in the next section. In contrast, categorization using single probesets within the exon arrays resulted in largely arbitrary selection of transcript features that were too focused on single internal exons to reliably identify commonly observed isoform changes. We attempted isoform categorization using the entire group A and group B probesets, but found that the inclusion of all interrogated probesets provided too large a focus and incorporated many non-changing or irrelevant probesets.

Metaprobeset feature definition

We resolved these challenges by collapsing highly correlated probesets together into metaprobeset features. Analyzing exon array data at the metaprobeset feature level both reduced multiple hypothesis testing and simultaneously focused feature selection by collapsing related probeset changes together and ignoring irrelevant probesets. By adjusting the correlation threshold used to collapse probesets, we were able to tune our analysis to the appropriate level of focus. We found that the original SplicerAV algorithm was able to operate well on exon array data analyzed at the metaprobeset feature level, allowing us to combine these approaches into a single program, SplicerEX, that was capable of analyzing both U133 and exon array data by simply changing the level of feature selection.

Metaprobeset Implementation and Selection of Correlation Threshold

Metaprobeset feature selection was accomplished in several steps. First, pairwise Pearson correlations were calculated between all probesets targeting the same gene. If this correlation exceeded a user set threshold, these two probesets would be joined together into a single probeset. Correlations between the joined probesets and remaining probesets would then be averaged to create a new pairwise correlation matrix. The process was then repeated until no remaining features were correlated above the set threshold. The resulting features, each made up of one or multiple probesets, each constituted a metaprobeset.

Metaprobeset collapse using an empirically derived correlation threshold of .7 maximized our ability to effectively categorize mRNA processing events and greatly reduced the average number of features per gene (Figure 14). Within each gene, the single largest metaprobeset was considered to be interrogating the main isoform, and was used to calculate changes in overall gene expression.

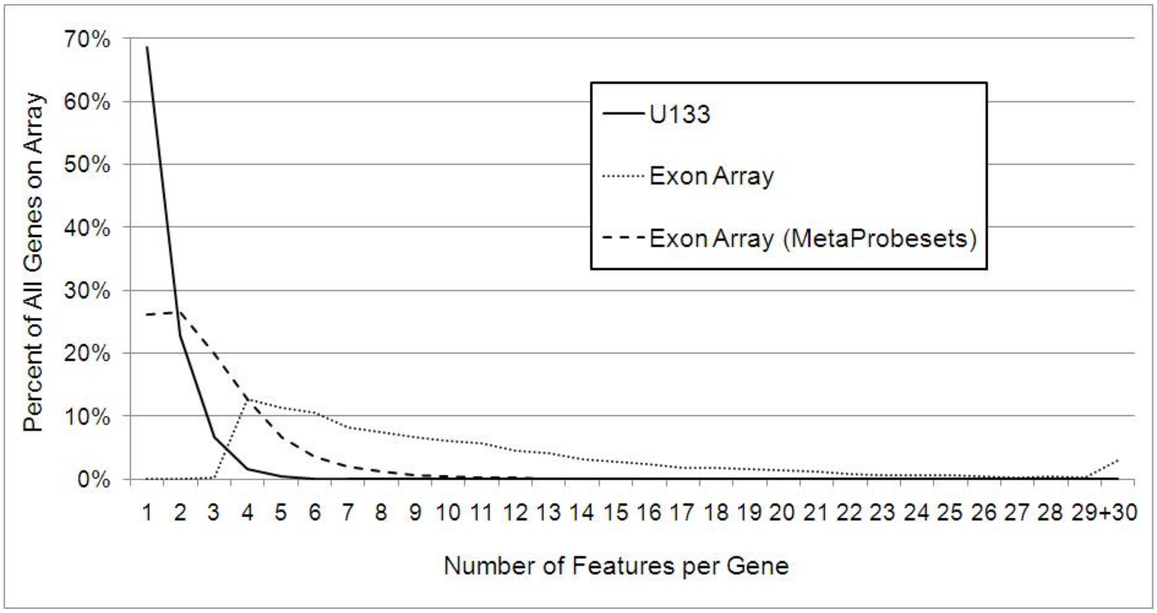

Figure 14: Number of features targeting individual genes by array platform.

Automated categorization of mRNA processing events

In order to fully benefit from large scale analyses of mRNA processing, we devised an algorithm capable of automatically categorizing SplicerEX hits into mechanistically distinct categories: 1) Tandem 3'UTR choice 2) Alternative 3' terminal exon choice 3) Alternative 5' transcript initiation 4) Internal exon choice 5) Alternative transcript length and 6) Unclassified. These categories were chosen to correspond loosely to event categories described previously in deep sequencing studies of alternative mRNA processing by Burge and colleagues (Wang et al. 2008): The Burge categories were adapted to what we were able to reliably differentiate within the framework of event inference based on two single metaprobesets. At the same time, we wanted to keep the classification scheme reasonably simple to promote transparency and encourage external adoption.

In addition to categorizing AS events by mechanistic class, SplicerEX also assessed directional changes in treatment vs. control conditions for categories 1-4. Specifically, SplicerEX differentiates 1) lengthened vs. shortened 3'UTR choice, 2) 5' prime vs. 3' located TE choice, 3) 5' vs. 3' located alternative 5' initiation start site, and 4) Internal event inclusion vs. exclusion. The detailed schema used to categorize alternative processing events into mechanistic and directional categories is described in detail in Appendix D.

Preprocessing and implementation Details

SplicerEX takes normalized probe or probeset intensities as input, which can be generated using a number of existing software options. Readily available options for probeset level normalization of U133 and exon array data include the Affymetrix Expression Console, bioconductor R packages, Partek, XRAYS, and others. For our exon array analysis, we used XRAY (Biotique Systems, Inc.) to check for quality control, limit analysis to the "core" probeset level, generate probeset level normalized expression values, and filter out probesets not detected above background. Background detection in XRAY was assessed by removing individual probes with high or low GC content, low variance, or expression below background and probesets for which three or more probes were retained were included for analysis. Median derived probeset expression levels for 81,828 probesets were used as input for SplicerEX. As an additional background expression filter, SplicerEX further removed any probesets with $\log_2$ expression below 6. For the U133 analysis, we used RMA Express to generate probeset level normalized expression values and PANP (described in chapter 2) to filter out probesets not detected above background. The full set of 54,675 U133 probesets were used as input for the SplicerEX program.

To improve the quality of hypotheses generated by SplicerEX, the program can limit the analysis to a user-specified set of probesets. We have generated default probeset lists for both the U133 and exon array platforms that limit analysis to probesets that overlap one or more UCSC gene transcripts. Overlap was determined using Affymetrix annotated target probeset sequence coordinates and comparing them to the March 2006 (hg18) version of the human genome and checking for overlap with known UCSC genes. Genomic coordinates of U133 probeset target coordinates were not publicly available from Affymetrix or from the UCSC genome browser, and were generated using BLAT to align Affymetrix probeset sequences against the March 2006 genome and will be provided as supplemental material in a later publication..

SplicerEX was implemented in Perl, with typical PC run times of 3-5 minutes for U133 2.0 plus data and 10-15 minutes for exon aray data using metaprobeset features. Perl is a freely available programming language that is widely available for most operating systems: SplicerEX has only been tested using a PC.

EBV-induced B cell transformation and mRNA preparation

Human B cells were obtained from normal donor buffy coats through the Carolina Red Cross and peripheral blood mononuclear cells (PBMC) were isolated by Ficoll Hystopaque gradient (Sigma #H8889). CD19+ B cells were purified from PBMC using the BD iMag Negative Isolation Kit (BD,cat #558007). Purity was routinely greater than 90% as determined by flow cytometry. Total mRNA was prepared from four normal donors in two conditions: 1) uninfected purified CD19+ B cells and 2) monoclonal LCL derived by limiting B95-8 virus dilution on PBMC. B95-8 virus was produced from the B95-8 Z-HT cell line as previously described (Johannsen et al. 2004).

cDNA preparation, labeling, and fragmentation was performed using the Gene Chip wt cDNA synthesis and amplification kit (Affymetrix cat# 900673) and Exon Array labeling kits (Affymetrix cat# 900671). Eight samples (4 of each condition) were hybridized to HuEx 1.0ST Exon Arrays (Affymetrix cat# 900650) and the chips were scanned in the Duke Microarray Facility.

Gene ontology and hit lists of increased, decreased, and differentially processed genes

To compare the performance of U133 and HuEx platforms, the set of genes differentially detected, expressed, and processed were compared. Comparisons of differential gene expression and processing were limited to genes detected by both arrays to provide a fair assessment of overlap. All gene ontology analyses were performed using PANTHER(Thomas et al. 2003). The set of genes detected above background by both platforms (N=5,682) was used as the reference list for increased and decreased gene expression lists. The set of genes detected above background on either platform (N=9,838) was used as the reference list the differentially processed gene list.

3.4 Discussion

In this chapter, I have described the first comparison of the ability of U133 and Exon arrays to detect changes in alternative mRNA processing using a novel program, SplicerEX. We found that both the U133 and HuEx platforms were capable of detecting comparable numbers of overall changes in differential mRNA processing, but detected almost no events in common. We attribute the low overlap between the platforms to biases in the types of events detected by each array.

We found that the U133 array was superior to the HuEx platform for detecting changes in both 3’ UTR length (72 vs 10 events) and 3’ TE choice (38 vs. 8 events). This study suggests that the U133 2.0 plus array, originally designed to interrogate overall gene expression, is currently the most sensitive Affymetrix microarray for detecting differential processing of 3’ transcript regions.

It is well known that the U133 array design preferentially targets probesets towards the 3’ ends of genes. Among U133 probesets that target any known UCSC gene, we found that 90% interrogated a 3’ terminal exon. U133 arrays use cDNA prepared using oligo dT reverse transcription, which provides the strongest amplification of the 3’ ends of transcripts.

A somewhat surprising finding of this analysis was the relative inability of HuEx arrays to detect differential processing at the 3’ end of genes. There are several likely explanations as to why this might be the case. An analysis by Bemmo et al previously examined the ability of HuEx arrays to detect changes in differential mRNA processing and found that a large number of false positive events were detected at the 5’ and 3’ ends of genes (Bemmo et al. 2008). The authors demonstrated that the signal strength of the HuEx arrays was particularly weak at the 3’ ends of genes, and hypothesized that the lack of signal was due as a consequence of using random primed cDNAs. A study by Robinson and Speed suggested that individual HuEx array probeset signals are less reliable than U133 probesets as a result of smaller probe feature size and the use of fewer probes per probeset (Robinson and Speed 2007). Lastly, it is possible that HuEx array probeset target locations within the genome do not represent all 3' UTRs. However, we found in preliminary analyses that HuEx probesets interrogated 90% of all U133 probeset target sequences, suggesting that this is unlikely.

The analysis presented here suggests that researchers deciding between the U133 and HuEx platforms should choose which platform to use based on their specific research objectives. Changes in 3' terminal processing may be of particular interest in studying gene regulation by miRNAs, known to largely target the 3' UTRs of most transcripts (Friedman et al. 2009) (Sandberg et al. 2008). Changes in 5' transcript initiation may be of interest to studying using of alternative promoters. Internal processing events, composed largely of cassette exons, may be of interest to those interested in identifying splicing events that result in changes in ORFs and resultant encoded protein structure. We found that roughly half of events detected by exon array were hypothesized to result in protein coding changes in transcript structure, compared with only a quarter of U133 predictions.

We combined both HuEx and U133 arrays to demonstrate highly significant biases towards 3' UTR shortening and internal exon exclusion in LCLs vs. naïve B cells. A previous study has demonstrated widespread 3' UTR shortening in proliferating cell types (Sandberg et al. 2008), which agrees with the highly significant 3'UTR shortening we observed in the rapidly proliferating LCLs relative to naïve B cells. In addition to reproducing this observation, our study finds a comparably significant preference for exclusion of internal exon content in LCLs vs. B cells. Reduction of 3'UTR length in proliferating cells has been suggested as a mechanism of global evasion of regulatory inhibition by miRNAs (Sandberg et al. 2008). We speculate that removal of internal exons may provide a similar role in avoiding miRNA inhibition in proliferating cell types. Confirmation of this hypothesis would mark a significant change in our current understanding of miRNA message inhibition, which has not been observed within internally located exons on a genome wide scale (Bartel 2009).

There are a number of programs that have been developed to analyze Affymetrix exon array data for changes in alternative mRNA processing, discussed in chapter 1. Of these programs, PLATA (Sandberg et al. 2008) has been previously been used to calculate changes in tandem 3'UTR length within proliferating cell types, but is not capable of otherwise characterizing differential processing events. Previous algorithms have been used to deconvolute relative abundance of specific splice variants (Li and Wong 2001; Wang et al. 2003). However, these algorithms have only been applied to a handful of well-characterized genes and are not applicable to commercially available microarrays.

To our knowledge, the SplicerAV/EX set of programs remain the only programs currently available to analyze differential mRNA processing on U133 arrays at the level of the probeset (Robinson et al. 2010). SplicerEX is the only program available capable of automatically categorizing differential mRNA processing events by mechanistic and directional characteristics using commercially available microarrays. SplicerEX is freely available upon request and is designed for experimental biologists interested in finding models of AS for in depth study. RT-qPCR experimental validation of events predicted in this chapter is currently underway.

4. Future Directions

The SplicerAV and SplicerEX programs are designed to generate biological hypotheses that provide potential areas of future research. One such thread is the story of Oncostatin M Receptor (OSMR), which was originally detected by SplicerAV and confirmed by RT-PCR to be alternatively processed in a model of breast tumor microenvironment.

4.1 Proposed Role for the Alternative mRNA processing of Oncostatin M Receptor in the Tumor Microenvironment

In solid tumors, unrestricted and unorganized cell growth leads to an environment in which the supply of oxygen, nutrients, and waste removal afforded by local vasculature becomes limited. This so-called tumor microenvironment is characterized by spatially and temporally fluctuating hypoxia, acidosis, and nutrient deprivation(Gatenby and Gilles 2004; Bristow and Hill 2008; Dewhirst et al. 2008). Cancer cells within this harsh environment are prone to apoptosis, decreased cell survival, and stress-related signaling, all of which act to promote the evolution of more aggressive tumors (Gatenby and Gilles 2004; Bristow and Hill 2008; Dewhirst et al. 2008; Dewhirst 2009).

In order to identify and study potential alternative processing events of interest in the tumor microenvironment, SplicerAV was used to analyze U133 2.0 plus microarray data generated from primary human mammary epithelial cells exposed to both lactic acidosis (25mM, pH 6.7) and hypoxia (.5%) for 24 hours (Chen et al. 2008). Oncostatin M receptor was the top hit detected as undergoing changes in mRNA processing, which was validated by RT-PCR (Figure 15).

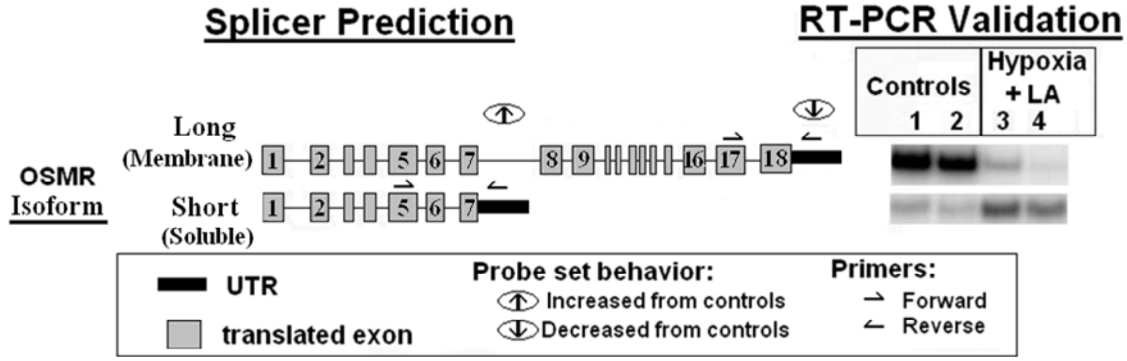

Figure 15: Splicer AV predicted alternative processing of OSMR validated by RT-PCR. OSMR isoform specific regulation was predicted by Splicer AV as shown on the left. The location and expression change of each Affymetrix probeset interrogating the OSMR transcript is shown as a circle with arrows indicating changes in that probeset's expression level upon exposure to hypoxia and lactic acid. The relative abundance of each predicted transcript (left) was confirmed by semi-quantitative P^{32} labeled RT-PCR (right). PCR primer locations are indicated with left and right arrows.

Overexpression of the OSM receptor has been associated with poor patient outcomes in cervical cancer (Ng et al. 2007) and knockout mice lacking the OSM receptor have deficiencies in maintaining specific progenitor cell populations (Tanaka et al. 2003; Nakamura et al. 2004). OSMR's principle ligand, oncostatin M (OSM), was initially discovered as a soluble protein able to inhibit melanoma proliferation and survival without affecting normal fibroblasts (Zarling et al. 1986). It is an inflammatory cytokine produced by activated human T-lymphocytes, monocytes, macrophages, and neutrophils (Miles et al. 1992; Nair et al. 1992) that has been shown to inhibit growth of a number of human tumor cell lines (Zarling et al. 1986; Horn et al. 1990) and stimulate tumor invasion (Holzer et al. 2004; Queen et al. 2005; Jorcyk et al. 2006), epithelial-mesenchymal transition (Queen et al. 2005; Pollack et al. 2007), fibroblast, endothelial, and vascular smooth muscle cell proliferation (Brown et al. 1991; Grove et al. 1993), angiogenesis and VEGF production (Vasse et al. 1999; Repovic et al. 2003; Weiss et al. 2003; Queen et al. 2005; Ehashi et al. 2007; Rega et al. 2007), and coagulation (Mirshahi et al. 2002).

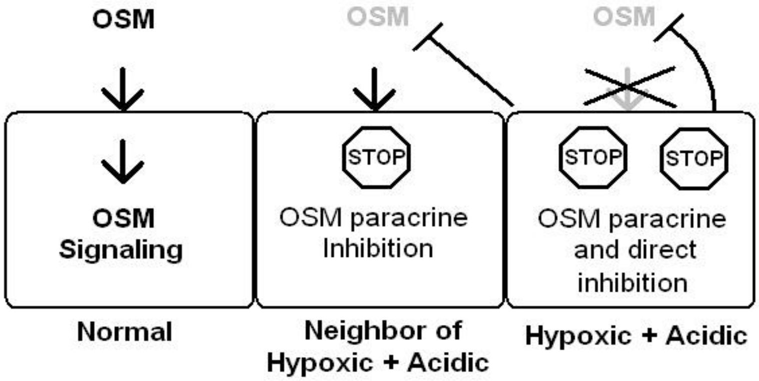

Figure 16: Schematic of hypothesized OSMR regulation of OSM signaling within the tumor microenvironment. Normally, OSM signals through the OSMR:gp130 heterodimeric receptor to promote tumor invasion and angiogenesis of cancer cells (left). As cells near hypoxic and acidic regions of a tumor, they encounter soluble OSMR (sOSMR), which sequesters and inactivates OSM via paracrine inhibition (middle). Breast cancer cells directly exposed to hypoxia and lactic acidosis not only produce the antagonistic sOSMR, but also reduce membrane expression of membrane bound OSMR (right).

Regulation of OSMR and related gene pre-mRNA processing could be involved in the angiogenic switch from benign to malignant solid cancers and may function as an important mechanism of regulating angiogenesis, metastases, and inflammatory responses in the breast tumor microenvironment. Future investigation into regulation of OSMR at the level of alternative mRNA processing may provide novel opportunities for therapeutic interventions in the treatment of breast and other solid tumors.

4.2 Isoform signature generation

Gene expression signatures are now being used clinically to help assess breast cancer patient prognosis through the application of tests such as Oncotype DX and Mammoprint. The creation of such signatures follows a standard process. Typically one or two gene expression data sets are used to select and refine a set of genes that are individually associated with patient prognosis or some other phenotype (chemoresistant, etc). A summary statistic is created using a weighted sum of these genes' expression values. The equation for this summary statistic, which is often referred to as a gene signature, is then tested for the ability to generate a summary statistic that is reproducibly associated with prognosis or another phenotype in one or more validation cohorts.

Gene signatures are created typically by choosing some subset of genes whose expression levels are most significantly correlated with the phenotype of interest in the training sets. In our analyses of oncogene over-expression, breast cancer prognosis, and B cell transformation, we observed minimal overlap between the most significant gene expression changes and the top scored isoform ratio changes. The creation of an isoform signature, analogous to a gene signature, could be created in the same way that a gene signature is created. This isoform signature could be created and tested on the same set of data as the original gene signature. Because of the low overlap between top isoform ratios and top genes, this isoform signature could have the potential to represent an independent biological dimension of the phenotype of interest.

By providing an orthogonal indicator of prognosis, isoform signatures could in theory be used in the future to augment existing gene signatures to possibly provide a more robust phenotypic indicator.

4.3 Automated sequence extraction and motif finding

Part of the novelty of the SplicerEX algorithm relates to its ability to generate specific hypotheses associated with a mechanistic category and directionality. Further work on the SplicerEX algorithm may be able to automate extraction of relevant regulatory sequences of top targets. With adequate numbers of top hits or relaxation of top hit criteria, the program may be used to find cis-acting regulatory elements involved in the regulation of alternative mRNA processing, including miRNA seed sequences.

4.4 Concluding Remarks

As our current understanding of biology and our ability to generate data become increasingly more complex, there will be an ever increasing need for biologically motivated mathematical models. As mathematical models become increasingly more complex in their structure and ability to generate data, there will be an ever increasing need for experimental biology. Also, never put a bacteria plate in the cell culture incubator.

Appendix A: Genes increased in LCLs vs. naïve B cells

Fold Increase	P-Val	Gene	TCluster ID
8.4	4.4E-03	LAMP3	2707876
8.2	6.8E-05	CD226	3812385
6.8	6.4E-04	IL32	3645626
6.6	2.9E-03	CHI3L2	2351687
6.5	3.6E-03	TXNDC5	2940826
6.2	3.1E-04	CCND2	3401704
6.2	4.1E-04	SLC12A8	2693014
6.0	2.5E-03	FCER2	3848492
5.8	3.7E-04	SCARB1	3476665
5.7	9.9E-04	UBE2C	3887049
5.6	4.9E-03	IFI44L	2343473
5.4	7.0E-03	CD300A	3734379
5.1	8.1E-04	SLAMF7	2363202
5.0	1.3E-03	EBI3	3817380
4.9	6.1E-05	USP18	3936550
4.9	4.0E-05	LTA	2902407
4.9	1.8E-03	CD38	2719656
4.9	2.3E-03	IFITM1	3315675
4.8	6.7E-03	UCHL1	2725013
4.7	9.2E-03	ZWINT	3290210
4.7	2.9E-03	C12orf75	3429857
4.7	1.5E-04	BLVRA	2999544
4.6	5.2E-04	BUB1	2570616
4.6	2.2E-04	CCNA2	2784113
4.6	1.7E-06	HDGFRP3	3636522
4.6	1.1E-03	HJURP	2604254
4.5	3.8E-04	P4HB	3774241
4.5	6.0E-05	AICDA	3443206
4.5	2.1E-03	HSPA5	3225398
4.4	8.0E-05	MKI67	3312490
4.4	2.8E-03	DUSP4	3129731
4.4	3.9E-04	ZMAT3	2706791
4.4	7.1E-06	CYBRD1	2515240
4.3	2.2E-05	MSC	3140213

Fold Change	P-Value	Gene	TCluster ID
2.5	1.7E-03	ACAT2	2934131
2.5	5.6E-04	C1orf85	2438093
2.5	2.4E-05	ANLN	2997376
2.5	1.3E-03	NCOR2	3476457
2.5	4.9E-03	STARD13	3508898
2.5	7.1E-03	CCT3	2438125
2.5	1.8E-04	DUSP16	3444958
2.5	2.7E-04	SGMS1	3289235
2.5	4.5E-03	NCALD	3147173
2.5	8.9E-04	AK3	3197318
2.5	1.0E-04	FLOT1	2948587
2.5	1.4E-07	MBOAT1	2944491
2.4	4.9E-04	ZFAT	3154700
2.4	7.6E-03	MX2	3922037
2.4	2.6E-04	AACS	3436571
2.4	5.3E-03	ZNF215	3318989
2.4	2.2E-04	ACADM	2342576
2.4	8.2E-04	EBP	3976670
2.4	2.7E-04	PBK	3129149
2.4	8.1E-05	SEC61A1	2641032
2.4	2.7E-06	AIG1	2928690
2.4	7.7E-04	TMEM55A	3144235
2.4	4.7E-04	TNFRSF8	2320683
2.4	1.1E-03	PSMD14	2512701
2.4	1.6E-03	LMAN2	2888698
2.4	2.3E-04	CHEK1	3354799
2.4	1.8E-04	DENND1A	3224650
2.4	4.1E-04	PDIA6	2540317
2.4	1.7E-05	TPM4	3823511
2.4	6.2E-04	PCBD1	3293537
2.4	1.7E-04	IDH1	2597010
2.4	9.0E-03	ANXA4	2487412
2.4	6.8E-04	INSIG1	3033209
2.4	5.9E-03	LRRC59	3762355

4.3	4.7E-05	TJP2	3173880
4.3	1.1E-04	DST	2958325
4.3	1.0E-03	NEK6	3188697
4.3	1.1E-03	AHRR	2798586
4.3	8.2E-05	GTSE1	3949055
4.3	1.2E-04	AURKB	3744263
4.2	8.0E-04	DHCR24	2413907
4.2	5.0E-03	CCNB2	3595979
4.2	1.5E-03	TNFRSF17	3648391
4.2	9.0E-04	OAS1	3432438
4.1	7.7E-04	HYOU1	3394123
4.1	5.1E-03	KIAA0101	3629103
4.1	2.9E-03	PSAT1	3175971
4.1	1.1E-03	LAP3	2720145
4.1	2.7E-04	FAS	3257098
4.1	1.4E-03	FEZ1	3396593
4.0	6.0E-04	DHCR7	3380697
4.0	2.9E-04	KCNN3	2436826
4.0	2.4E-05	CDC20	2333136
4.0	5.6E-04	BST2	3854454
4.0	1.0E-04	RCN1	3325503
4.0	2.0E-03	IDH2	3638760
3.9	6.2E-05	MACC1	3040518
3.9	1.2E-04	RHOC	2428405
3.9	1.2E-03	LY6E	3119339
3.9	3.8E-06	ARNTL2	3409127
3.8	8.9E-05	LIMA1	3454331
3.8	1.5E-05	LDLR	3821015
3.8	2.4E-04	TNIK	2705266
3.8	5.4E-04	NUSAP1	3590388
3.8	8.5E-05	CCNB1	2813414
3.8	8.6E-03	ENOSF1	3795866
3.8	6.0E-05	SMAD1	2746119
3.8	3.0E-03	TOP2A	3756193
3.7	5.1E-04	PCCB	2644014
3.7	4.7E-06	TRPV2	3712062
3.7	3.0E-04	MAP2K6	3733065
3.7	5.0E-03	ENTPD1	3259253
2.4	8.5E-05	PBX3	3189311
2.4	1.3E-04	HSDL2	3185205
2.4	5.1E-04	ORC1L	2412799
2.4	6.7E-03	DUSP2	2565119
2.4	1.8E-05	KIF11	3258168
2.4	2.0E-04	NT5DC1	2922521
2.4	4.2E-05	UBE2J1	2964200
2.4	7.0E-03	RAB35	3474228
2.4	6.7E-04	GAS7	3744965
2.4	4.5E-03	CUTA	2950714
2.4	9.2E-04	SLC16A1	2428501
2.4	1.2E-05	RAD54B	3144973
2.4	4.3E-04	ALDH18A1	3301512
2.4	8.1E-04	NIPSNAP1	3956909
2.4	2.1E-04	RCBTB2	3513549
2.4	6.1E-04	HMMR	2838656
2.4	3.4E-06	STIL	2411228
2.4	9.6E-05	RAD51AP1	3401804
2.4	8.3E-04	SRM	2396461
2.4	1.2E-03	SLC31A1	3185522
2.4	5.6E-07	PLK1	3653072
2.4	2.7E-04	SLC1A4	2485636
2.3	1.5E-05	ABCC4	3521174
2.3	3.5E-03	CLPP	3818376
2.3	6.7E-04	PDIA5	2639225
2.3	2.5E-03	C22orf9	3963676
2.3	2.3E-03	NUP62	3868183
2.3	4.6E-04	TRIM69	3592054
2.3	2.8E-03	TMEM106C	3413278
2.3	5.6E-04	TFRC	2712632
2.3	1.5E-04	MRPL53	2560141
2.3	5.2E-05	PLK4	2742985
2.3	9.1E-05	FNDC3A	3489212
2.3	1.8E-03	HSD17B12	3328069
2.3	8.1E-05	LGALS9	3715274
2.3	2.2E-04	YES1	3795942
2.3	2.8E-05	RRM1	3318009
2.3	1.6E-03	SCPEP1	3728037

3.6	5.2E-03	TACC1	3094778
3.6	2.2E-03	MTHFD1	3540007
3.6	4.3E-04	MRPL4	3820414
3.6	4.8E-04	WDR40A	3203855
3.6	1.4E-04	GNA15	3816815
3.6	6.3E-06	SESN2	2327391
3.6	1.9E-04	CDK6	3061319
3.6	1.2E-03	MTHFD2	2489172
3.5	5.6E-04	DLGAP5	3565663
3.5	2.9E-03	CD274	3161082
3.5	1.1E-04	SEC24D	2783316
3.5	1.1E-04	CORO1C	3470549
3.5	1.0E-03	IRF4	2891341
3.5	5.0E-03	PTTG1	2838201
3.5	2.3E-03	DUSP5	3263743
3.4	3.2E-03	PPIB	3628994
3.4	3.5E-03	DDB2	3329649
3.4	8.8E-03	SRGN	3250146
3.3	8.4E-04	CREB3L2	3075136
3.3	7.6E-05	SPATS2	3413950
3.3	1.0E-03	NCAPG	2720251
3.3	5.4E-04	PIK3R3	2410470
3.3	1.2E-03	FOXM1	3440598
3.3	1.6E-03	MYL6B	3417435
3.3	2.6E-04	WSB2	3473727
3.3	1.6E-03	GLCCI1	2989537
3.3	2.1E-04	HMGB2	2793951
3.3	8.4E-06	CEP55	3258444
3.3	1.3E-03	MRPS15	2406766
3.3	1.4E-04	DPP3	3336238
3.3	1.9E-03	OASL	3474831
3.2	2.9E-05	NCAPH	2494484
3.2	5.0E-05	ZNRF1	3668834
3.2	1.1E-03	DTL	2378937
3.2	2.9E-04	NCAPD2	3402571
3.2	4.4E-06	HDLBP	2607110
3.2	1.6E-03	GINS1	3880827
3.2	2.1E-03	B4GALT6	3803120
2.3	3.2E-04	CARM1	3820865
2.3	1.4E-05	HS2ST1	2345196
2.3	1.8E-04	MCM10	3235789
2.3	1.1E-05	BRCA1	3758317
2.3	8.4E-06	SYT11	2361154
2.3	1.9E-03	C14orf166	3535674
2.3	7.3E-04	WHSC1	2715076
2.3	2.9E-04	PRDM1	2919669
2.3	2.4E-04	CALU	3023060
2.3	2.1E-03	SSR4	3995975
2.3	6.9E-04	SAMHD1	3904691
2.3	1.3E-03	HNRPLL	2548871
2.3	2.8E-04	AIFM1	4021469
2.3	1.2E-03	F11R	2440476
2.3	8.5E-04	FH	2463425
2.3	1.5E-04	TYW3	2342391
2.3	1.8E-04	ARF3	3453370
2.3	1.0E-03	ATIC	2526759
2.3	2.9E-04	TTF2	2353773
2.3	2.7E-04	BAIAP2L1	3062868
2.3	2.3E-03	CYB5B	3666732
2.3	2.3E-05	DEPDC1	2417528
2.3	3.2E-04	ACLY	3757433
2.3	5.2E-03	CRELD2	3950452
2.3	5.0E-03	RAC2	3960061
2.3	3.6E-04	RSU1	3279575
2.3	7.0E-05	TRAPPC1	3744039
2.3	9.7E-04	NCAPG2	3082181
2.3	3.8E-04	AARS	3697015
2.3	3.4E-03	SLC25A1	3952543
2.3	5.8E-05	PCK2	3529508
2.2	3.9E-05	SH3RF1	2793137
2.2	2.0E-04	MTDH	3108433
2.2	7.9E-05	WDR41	2863535
2.2	5.5E-04	SUSD1	3220846
2.2	9.0E-06	GALNT10	2836518
2.2	1.1E-03	ALCAM	2634494
2.2	5.5E-04	ME1	2962820

3.2	1.2E-03	BATF	3544605
3.2	2.2E-04	BSG	3815014
3.2	2.1E-03	IFI44	2343511
3.2	7.6E-04	B3GNT2	2484841
3.1	6.3E-04	PLA1A	2638077
3.1	7.0E-03	CRYZ	2418451
3.1	5.2E-04	SLC1A1	3160658
3.1	7.6E-04	IGF2BP3	3041409
3.1	1.8E-03	RGL1	2371346
3.1	9.9E-05	TUBG1	3721926
3.1	4.2E-05	40429	2875454
3.1	7.2E-04	SEC24A	2829416
3.1	4.0E-03	SSR3	2702154
3.1	5.5E-04	SLAMF1	2440327
3.1	2.5E-04	KIF2C	2334098
3.1	3.6E-03	ITM2C	2531589
3.1	3.1E-03	DOK3	2888879
3.0	5.5E-06	KIF23	3599811
3.0	9.4E-06	TWSG1	3778372
3.0	1.3E-04	LMNB1	2827185
3.0	1.6E-04	SPARC	2882098
3.0	7.8E-04	TMEM97	3715489
3.0	1.9E-04	GFPT1	2558045
3.0	4.6E-04	CDC6	3720896
3.0	2.8E-04	CDC45L	3936913
3.0	9.4E-05	SPAG5	3750785
3.0	3.6E-04	40432	2732273
3.0	1.9E-03	CYFIP1	3583638
3.0	6.1E-05	PRC1	3639031
3.0	1.8E-03	MELK	3168508
3.0	7.0E-03	PMAIP1	3790704
3.0	7.1E-04	SEMA4A	2361342
3.0	4.0E-03	PLOD1	2320581
3.0	2.3E-03	IL10	2452948
3.0	8.8E-04	SORD	3592109
2.9	1.7E-04	SORBS2	2796995
2.9	2.9E-04	FEN1	3333226
2.9	1.3E-04	DBI	2502821
2.2	1.2E-03	ATF3	2379132
2.2	6.6E-04	ACSL4	4017810
2.2	2.8E-05	NUF2	2364438
2.2	2.3E-03	CBX5	3456630
2.2	4.7E-04	MAPKAP1	3225456
2.2	2.8E-04	TFDP1	3502710
2.2	2.4E-03	TRAM2	2957227
2.2	3.1E-06	RFC3	3485074
2.2	3.6E-03	RRBP1	3899173
2.2	3.5E-04	RDX	3390542
2.2	3.4E-03	UCHL3	3494102
2.2	4.1E-03	CHMP2A	3872983
2.2	4.1E-03	THOC4	3774331
2.2	2.3E-05	CENPE	2780172
2.2	2.9E-05	CASC5	3590014
2.2	9.2E-03	PSMC3	3372209
2.2	3.8E-03	CTNNAL1	3219621
2.2	1.7E-03	COPG	2641532
2.2	2.7E-04	TTK	2914777
2.2	2.4E-04	CALM3	3836841
2.2	5.7E-04	POMP	3483348
2.2	2.1E-06	CCDC88A	2553771
2.2	5.9E-05	AP2S1	3866302
2.2	2.3E-04	MRPS33	3076489
2.2	5.2E-04	FECH	3809621
2.2	7.6E-03	ORMDL3	3755934
2.2	3.2E-03	SC4MOL	2750594
2.2	1.4E-03	NDUFV1	3337196
2.2	1.3E-03	LRP8	2413203
2.2	1.2E-04	PHF19	3223687
2.2	1.1E-03	GINS2	3703112
2.2	1.7E-05	E2F8	3365776
2.2	1.6E-04	CBX3	2993639
2.2	3.5E-03	TCEAL4	3985615
2.2	3.8E-03	RAD54L	2334646
2.2	6.8E-05	NFE2L1	3725035
2.2	9.1E-03	NOMO3	3682893
2.2	1.8E-04	LRRC42	2336913

2.9	2.5E-04	OAS2	3432514
2.9	2.8E-04	CDCA2	3090697
2.9	7.3E-03	ASF1B	3852565
2.9	1.3E-04	TLR7	3969081
2.9	5.5E-04	AAK1	2558150
2.9	7.1E-04	ASPM	2449559
2.9	3.3E-04	BCL2L12	3838795
2.9	4.2E-03	SLC43A3	3373845
2.9	1.2E-03	KIAA1797	3164601
2.9	9.5E-03	TMOD1	3181240
2.9	4.8E-03	OPTN	3235726
2.9	1.0E-03	CAMK4	2823880
2.9	3.2E-03	TRAF1	3223738
2.9	6.5E-05	STK38L	3409081
2.8	3.7E-04	DSG2	3783529
2.8	1.7E-03	PTPN6	3403092
2.8	6.8E-04	GMDS	2938636
2.8	6.0E-04	FNDC3B	2652410
2.8	1.4E-03	ST7	3020496
2.8	4.4E-03	GOT1	3302990
2.8	3.6E-04	HN1	3770606
2.8	6.2E-04	CDR2	3684782
2.8	1.3E-03	HMGA1	2904000
2.8	6.3E-03	PAK1	3382861
2.8	1.9E-04	SHCBP1	3689880
2.8	1.7E-04	BIRC5	3736290
2.8	1.2E-03	MGC29506	2877893
2.8	6.3E-04	NUCB2	3322251
2.8	2.0E-03	ATP1B1	2366422
2.8	7.7E-06	DEPDC1B	2858592
2.8	1.5E-04	UBE2T	2451200
2.7	1.1E-04	MCM4	3097152
2.7	8.2E-05	CDCA4	3581386
2.7	4.6E-03	AHCY	3903361
2.7	7.8E-03	LMNB2	3845909
2.7	8.7E-05	RPS27L	3628469
2.7	1.1E-03	MLEC	3434525
2.7	3.0E-04	CCNE1	3828112
2.2	1.6E-04	MCM2	2640855
2.2	2.7E-05	MREG	2598496
2.2	2.1E-03	KEAP1	3850363
2.2	6.8E-03	ETV5	2709132
2.2	6.4E-05	NETO2	3690154
2.2	5.2E-04	DDOST	2400220
2.2	2.3E-04	PML	3601387
2.2	8.1E-03	RAPGEF2	2749699
2.2	4.3E-04	CCNG1	2838598
2.2	6.4E-03	FADS2	3333247
2.2	1.1E-03	CDC25A	2673085
2.1	1.4E-03	CLTA	3168415
2.1	5.2E-04	ILDR1	2691850
2.1	7.8E-04	THOP1	3816611
2.1	3.4E-03	RHOBTB3	2820925
2.1	1.3E-04	NDFIP2	3495076
2.1	2.2E-03	MBD2	3808600
2.1	2.7E-04	PMM1	3962000
2.1	1.6E-04	DRAP1	3335736
2.1	5.5E-03	ERH	3570049
2.1	3.6E-03	NDUFAB1	3685306
2.1	2.2E-05	RAD51	3590086
2.1	4.2E-05	DECR1	3106310
2.1	1.9E-05	PGRMC1	3988740
2.1	1.9E-03	ARHGAP18	2973694
2.1	9.4E-04	GPHN	3540862
2.1	3.8E-05	ECT2	2652675
2.1	2.6E-04	WDHD1	3565571
2.1	8.8E-04	CKAP5	3371719
2.1	9.3E-03	DPAGT1	3394192
2.1	8.7E-04	TXNDC11	3680479
2.1	5.1E-03	CABLES1	3781531
2.1	6.6E-04	CTNNA1	2830946
2.1	7.9E-03	PPP1R15A	3838004
2.1	2.8E-03	GRN	3722917
2.1	5.7E-03	FUCA1	2401643
2.1	6.1E-04	SLC39A14	3089360
2.1	4.6E-03	TARS	2805786

2.7	7.1E-04	TRIB3	3873160
2.7	7.8E-04	KIF20A	2830638
2.7	7.9E-05	CENPF	2379863
2.7	7.3E-03	SCD	3260586
2.7	1.9E-03	APOBEC3B	3945545
2.7	2.5E-03	RPN2	3884100
2.7	7.3E-03	DNAJB11	2656569
2.7	1.9E-04	TRIP13	2798915
2.7	1.4E-03	VASH2	2379314
2.7	5.3E-03	SLC25A23	3847873
2.7	3.4E-03	LGALS3	3536706
2.7	3.2E-05	HSPA4L	2742935
2.7	4.1E-04	FAR2	3409605
2.7	6.8E-04	SUMO3	3934669
2.7	4.1E-03	OAS3	3432467
2.7	2.0E-05	C13orf3	3504617
2.7	9.4E-03	PLEK	2486811
2.7	6.8E-04	STAG3	3015338
2.7	4.6E-04	CKS1B	2360452
2.7	2.0E-05	AURKA	3910785
2.6	3.1E-04	TBC1D4	3518086
2.6	7.8E-04	PFKM	3413344
2.6	3.1E-04	MOXD1	2974413
2.6	6.4E-04	SH3KBP1	4001850
2.6	3.5E-04	ICAM1	3820443
2.6	4.5E-04	OBFC2B	3417485
2.6	1.2E-04	FAM33A	3764738
2.6	5.4E-03	TUBB	2901913
2.6	2.9E-03	TUBA1B	3453732
2.6	6.6E-04	TM7SF3	3448481
2.6	9.2E-03	CDCA7	2516023
2.6	5.6E-04	MCOLN2	2420642
2.6	4.8E-04	CLIC2	4027769
2.6	6.8E-07	TNFRSF10B	3127703
2.6	5.3E-04	STOM	3223928
2.6	1.2E-04	MYO6	2914070
2.6	3.6E-05	CTSC	3385769
2.6	3.2E-03	FGR	2403215
2.1	1.1E-05	XRCC4	2818454
2.1	4.5E-03	LHFPL2	2863885
2.1	1.4E-03	SNX4	2693149
2.1	1.2E-05	MSRB2	3238761
2.1	4.9E-03	TCF19	2902178
2.1	2.5E-03	CMAS	3407926
2.1	1.0E-03	ATP5J2	3063305
2.1	5.1E-03	PPIL1	2952065
2.1	2.1E-03	DNMT3A	2544662
2.1	2.3E-03	TIPARP	2649113
2.1	2.1E-03	SELS	3642137
2.1	6.5E-03	TMEM184B	3960440
2.1	1.8E-04	CAMSAP1L1	2374345
2.1	4.8E-04	MTMR2	3387483
2.1	4.2E-04	MPZL1	2365958
2.1	3.7E-04	RABGAP1L	2367963
2.1	9.4E-04	HRSP12	3145980
2.1	1.5E-04	KIF14	2450345
2.1	1.4E-03	CSRP1	2450865
2.1	2.1E-03	PNPO	3724969
2.1	3.5E-05	HERC5	2735409
2.1	8.6E-03	SEC23B	3878467
2.1	8.3E-04	SLFN13	3753568
2.1	2.8E-04	CPEB4	2841699
2.1	5.4E-03	GTPBP4	3231774
2.1	1.0E-03	BPNT1	2456805
2.1	2.0E-03	EIF2B2	3544387
2.1	5.0E-03	NUS1	2923060
2.1	1.6E-03	NEDD9	2941784
2.1	5.8E-04	DMXL2	3624145
2.1	1.0E-03	XPOT	3419807
2.1	7.8E-03	GRAMD3	2827057
2.1	5.5E-04	DDX49	3825446
2.1	1.2E-04	MRPL37	2337003
2.1	1.1E-03	OSTC	2738949
2.1	5.2E-04	OSBPL9	2336099
2.0	1.5E-05	SEL1L	3574207
2.0	4.0E-05	CD99L2	4025771

2.6	2.5E-04	HELLS	3258910
2.6	4.7E-03	BOLA3	2559792
2.6	8.8E-04	ACTN1	3569814
2.6	7.6E-04	TRIP10	3818515
2.6	6.6E-04	MAPK6	3594129
2.6	2.9E-03	LSS	3935243
2.6	1.6E-03	PRDX3	3309383
2.6	4.7E-04	FBN1	3623031
2.6	7.1E-04	MDH2	3009299
2.6	2.3E-03	EIF2AK2	2548402
2.6	1.2E-04	TRIM14	3217123
2.5	1.7E-04	EXO1	2388219
2.5	1.6E-03	SIAE	3396003
2.5	7.0E-04	LMAN1	3810472
2.5	5.0E-04	KIF21A	3450775
2.5	3.6E-05	FUT8	3540552
2.5	7.4E-03	LCK	2328841
2.5	2.3E-03	MLLT3	3200982
2.5	1.0E-03	CHMP5	3166844
2.5	3.3E-04	SLC7A11	2786322
2.5	3.6E-04	SLC38A5	4007437
2.5	1.1E-03	MNDA	2362333
2.5	1.9E-05	C19orf48	3868659
2.5	5.7E-04	RBM47	2766788
2.5	2.2E-03	YARS	2405192
2.5	1.2E-03	FERMT3	3334257
2.5	2.6E-04	BUB1B	3589697
2.5	2.0E-04	FANCI	3607537
2.5	7.4E-04	TNFSF10	2705706
2.5	1.0E-04	ACAT1	3347615
2.5	2.3E-03	CD80	2690900
2.5	6.0E-04	ANXA6	2881747
2.0	2.3E-04	FBXO5	2980241
2.0	6.4E-04	PPIF	3253880
2.0	1.3E-03	SMARCA4	3820921
2.0	6.8E-04	GSK3B	2691014
2.0	9.9E-03	BUD31	3014742
2.0	2.9E-04	C12orf4	3441215
2.0	4.3E-04	UQCRC2	3652218
2.0	7.0E-03	LCP1	3512874
2.0	5.7E-03	CPNE8	3450655
2.0	3.8E-04	GNS	3460127
2.0	2.8E-03	MRPL48	3340032
2.0	4.4E-03	MRPS9	2497892
2.0	8.3E-03	EBNA1BP2	2409220
2.0	1.3E-03	BTG3	3926080
2.0	8.8E-04	PRKAG1	3453556
2.0	3.5E-05	AGK	3027808
2.0	3.8E-03	NDUFS3	3329904
2.0	7.0E-03	ACP2	3372097
2.0	2.3E-05	MOV10	2352275
2.0	2.4E-04	NUP37	3468261
2.0	1.3E-03	ASNA1	3821847
2.0	2.2E-03	SURF4	3228674
2.0	1.4E-04	SRA1	2878347
2.0	1.6E-04	NOD2	3660175
2.0	2.4E-03	TTC35	3111375
2.0	9.7E-03	TROAP	3413875
2.0	7.3E-04	GALK2	3593339
2.0	1.3E-03	RAB11A	3598482
2.0	6.3E-03	RTN3	3333942
2.0	5.2E-04	NDUFA8	3224197
2.0	5.3E-05	GMNN	2898597
2.0	7.7E-03	ZMYND8	3908149

Appendix B: Genes decreased in LCLs vs. naïve B cells

Fold Decrease	P-Value	Gene	TCluster ID
15.5	1.0E-04	FAM129C	3824427
15.2	6.8E-05	TGFBR2	2615360
11.1	1.2E-07	ADAM28	3090209
11.0	3.0E-04	CXCR4	2578028
11.0	7.1E-06	ARRDC2	3824713
9.2	2.8E-06	FOXP1	2681753
7.7	1.0E-03	TAGAP	2982076
7.7	6.2E-04	BANK1	2737596
7.5	2.5E-03	C13orf18	3512948
7.3	3.9E-05	BACH2	2964553
6.5	7.7E-03	KIAA0746	2764192
6.5	4.7E-05	GALNAC4S-6ST	3268940
6.2	1.2E-04	RASGRP2	3376976
5.9	5.6E-04	ARHGAP25	2486927
5.5	7.3E-06	HHEX	3258221
5.5	2.8E-06	NOTCH2	2431112
5.2	1.2E-03	BCL6	2709778
5.2	1.0E-03	FCRL3	2439001
5.0	6.0E-03	HIP1R	3435548
5.0	5.3E-05	MTSS1	3151970
4.9	5.9E-03	CD83	2895841
4.9	3.6E-03	TXNIP	2356115
4.8	1.9E-07	COBLL1	2584787
4.8	2.7E-03	CD72	3204648
4.8	6.4E-03	APLP2	3356115
4.8	7.1E-05	NUAK2	2452405
4.4	3.6E-05	MAP4K4	2496727
4.4	8.5E-06	CMTM7	2615938
4.4	1.6E-03	SATB1	2665199
4.3	1.1E-03	LTB	2949118
4.3	3.8E-05	OSBPL10	2667809
4.1	3.6E-05	PFKFB3	3233605
3.9	2.7E-03	FADS3	3375582

Fold Decrease	P-Value	Gene	TCluster ID
2.9	1.1E-03	FAM65B	2945741
2.9	3.0E-03	KIAA0999	3392996
2.9	7.8E-04	FAM53B	3311269
2.9	7.9E-03	RASA3	3526831
2.9	7.2E-04	DCK	2730714
2.8	7.6E-05	FCRL2	2439052
2.8	2.6E-03	IL13RA1	3988538
2.7	3.0E-04	TMEM71	3154185
2.7	3.5E-04	PLEKHA1	3268274
2.7	6.8E-04	VAV3	2426385
2.7	3.1E-04	SLC6A16	3867734
2.6	3.7E-03	GABBR1	2947889
2.6	5.5E-03	BANP	3673091
2.6	8.4E-03	EZR	2981912
2.6	4.4E-03	HLA-DMB	2950263
2.6	1.5E-03	IL16	3604287
2.6	2.0E-03	BCL2L11	2500275
2.6	4.2E-03	DGKD	2532894
2.5	6.1E-03	PTPRC	2373842
2.5	1.1E-03	RASSF2	3896034
2.5	1.2E-03	KIAA0226	2713555
2.5	1.5E-03	TNFRSF10A	3127775
2.5	1.7E-03	SLA	3154263
2.5	1.5E-04	NBPF14	2433686
2.5	7.2E-04	RP11-94I2.2	2432851
2.4	2.4E-03	ZNF238	2388794
2.4	3.9E-04	RP11-94I2.2	2355365
2.4	3.1E-03	GGA2	3685183
2.4	1.9E-04	USP24	2413943
2.3	3.4E-03	MLXIP	3435192
2.3	1.8E-03	FAM65A	3665550
2.3	1.4E-04	TRAK1	2619120
2.3	4.7E-03	SH3BP5	2664209

3.9	6.7E-03	NDRG1	3154317
3.7	4.9E-04	ARHGAP24	2734421
3.6	4.2E-05	JAZF1	3043264
3.6	4.7E-03	IL4R	3654175
3.6	4.4E-04	TGIF1	3776504
3.5	6.3E-03	MED13L	3473083
3.5	5.8E-04	IGF1R	3610804
3.5	1.0E-03	ZNF395	3129304
3.3	2.6E-05	COL9A3	3892974
3.3	5.9E-04	PMEPA1	3911217
3.2	4.0E-04	PDE3B	3321512
3.2	1.9E-04	CXCR5	3351675
3.2	6.4E-04	JAK1	2416522
3.2	1.8E-03	REL	2484358
3.2	2.8E-03	LY9	2363248
3.2	3.9E-04	QSOX2	3229797
3.2	6.7E-03	ADAM19	2883440
3.1	6.7E-03	STAT4	2592356
3.1	3.0E-03	PTPRO	3406329
3.1	2.0E-03	CHMP7	3089853
3.1	6.6E-03	ZHX2	3113894
3.1	1.9E-03	PXK	2626167
3.0	9.6E-04	INPP5F	3267382
3.0	2.8E-04	NFATC1	3795184
3.0	4.3E-04	EBF1	2883878
2.9	4.7E-03	C12orf42	3468610
2.3	5.1E-04	---	3734966
2.2	2.7E-03	BACE2	3921933
2.2	2.9E-04	SIDT2	3350775
2.2	8.4E-03	ABLIM1	3307939
2.2	4.6E-03	CSGALNACT1	3126504
2.2	6.7E-03	NT5E	2915828
2.2	6.9E-03	MLL5	3017547
2.2	1.3E-03	ECE1	2400518
2.2	1.4E-04	FLOT2	3751121
2.2	9.7E-03	CASP8	2522728
2.2	2.1E-03	ZNF532	3790361
2.2	1.2E-05	BZW2	2991103
2.1	1.6E-04	PRDM2	2321238
2.1	9.1E-03	NR4A1	3415229
2.1	9.1E-04	ABCA1	3218528
2.1	5.2E-03	ZMAT1	4016001
2.1	2.6E-03	FYN	2969886
2.1	9.2E-03	KIAA0355	3829638
2.1	8.7E-03	KDM6B	3709153
2.0	4.5E-04	TRAF5	2378662
2.0	2.7E-03	KMO	2388085
2.0	1.0E-03	ADAM6	3581637
2.0	7.1E-04	EZH1	3758078
2.0	2.5E-03	ABCB4	3060117
2.0	7.5E-05	EVL	3551566
2.0	1.7E-03	INPP5D	2532699

Appendix C: Genes alternatively processed in LCLs vs. naïve B cells

Array	Rank	Gene	TCluster ID	Hyp	Prot	Category	Subtype
Exon	1	KIAA1797	3164601	Yes	No	Alt 5' Init	More 3' start
U133	2	TRIM37	3764680	Yes	Yes	Internal Event	Exclusion
U133	2	NFYA	2906607	No	No	Unclassified	---
U133	3	CPSF2	3548788	Yes	No	Tandem 3' UTR	Shorten
Exon	4	CASC5	3590014	Yes	Yes	Internal Event	Exclusion
Exon	5	ADFP	3200648	Yes	No	Alt 5' Init	More 5' start
U133	5	ZNF277	3019401	Yes	Yes	Alt 3' TE – APA	More 3' TE
Exon	6	PRKDC	3134034	Yes	Yes	Internal Event	Exclusion
U133	6	DDX59	2450416	Yes	Yes	Alt 3' TE - Alt 3' SS	More 5' TE
Exon	7	RRBP1	3899173	Yes	Yes	Internal Event	Inclusion
U133	7	DDX58	3203086	Yes	No	Tandem 3' UTR	Shorten
U133	8	WDR33	2575054	Yes	Yes	Alt 3' TE – APA	More 5' TE
U133	9	HAUS2	3591044	Yes	No	Tandem 3' UTR	Shorten
U133	10	PHC3	2704894	Yes	No	Tandem 3' UTR	Shorten
U133	11	CTSS	2434575	Yes	No	Tandem 3' UTR	Shorten
Exon	12	MYO3B	2514745	Yes	Yes	Internal Event	Exclusion
U133	12	ATXN3	3576889	Yes	No	Tandem 3' UTR	Shorten
U133	13	MARCH6	2801608	Yes	No	Transcript Length	---
Exon	14	DYNC1H1	3552847	No	No	Unclassified	---
U133	14	FAM36A	2389062	Yes	No	Tandem 3' UTR	Shorten
U133	15	MXD4	2757751	Yes	No	Tandem 3' UTR	Shorten
Exon	16	TMEM135	3343546	Yes	Yes	Alt 3' TE - Alt 3' SS	More 3' TE
U133	16	UBE2I	3643703	No	No	Unclassified	---
Exon	17	STAU1	3908786	Yes	Yes	Internal Event	Exclusion
U133	17	N4BP2L2	3508696	No	No	Unclassified	---
U133	18	RUNX1	3930360	No	No	Unclassified	---
U133	19	6-Sep	4019486	Yes	Yes	Alt 3' TE - Alt 3' SS	More 5' TE
U133	20	RRP7B	3962469	No	No	Unclassified	---
Exon	21	CDC2L5	2998536	Yes	No	Alt 5' Init	More 5' start
U133	21	DBT	2425212	Yes	No	Tandem 3' UTR	Shorten
U133	22	ZNF207	3717635	Yes	Yes	Alt 3' TE – APA	More 5' TE
U133	24	NASP	2334404	Yes	No	Tandem 3' UTR	Shorten
U133	25	C17orf69	3723572	No	No	Unclassified	---

Exon	27	PASK	2607055	Yes	Yes	Alt 3' TE – APA	More 3' TE
U133	27	NUB1	3032017	Yes	No	Tandem 3' UTR	Shorten
Exon	29	FAM111A	3331926	Yes	No	Internal Event (3' TE)	Exclusion
U133	29	ALMS1	2488785	No	No	Unclassified	---
U133	30	TXNL4B	3698055	Yes	No	Tandem 3' UTR	Shorten
U133	31	JMJD7	3590709	Yes	Yes	Alt 3' TE – APA	More 5' TE
U133	32	RER1	2316558	Yes	No	Tandem 3' UTR	Shorten
U133	33	POLR1B	2500838	Yes	No	Tandem 3' UTR	Shorten
Exon	34	TCFL5	3913483	Yes	No	Alt 5' Init	More 5' start
U133	36	HEXA	3632152	Yes	No	Internal Event (3' TE)	Exclusion
U133	37	ALPK1	2739792	Yes	Yes	Alt 3' TE - Alt 3' SS	More 3' TE
Exon	38	CCDC90A	2942578	Yes	Yes	Internal Event	Exclusion
U133	38	PCTK1	3976124	Yes	No	Tandem 3' UTR	Shorten
U133	39	LRCH4	3064082	No	No	Unclassified	---
U133	40	TPCN2	3337918	No	No	Unclassified	---
Exon	41	SH2B3	3431892	No	No	Unclassified	---
U133	41	CDC42SE2	2828146	Yes	No	Tandem 3' UTR	Shorten
U133	42	PHF17	2743315	Yes	Yes	Alt 3' TE – APA	More 5' TE
Exon	43	CRTAP	2616166	Yes	No	Tandem 3' UTR	Shorten
Both	43	TXNDC5	2940826	Yes	Yes	Alt 3' TE - Alt 3' SS	More 3' TE
U133	44	SYMPK	3865715	Yes	Yes	Alt 3' TE – APA	More 3' TE
U133	45	ATF7IP	3406015	Yes	Yes	Alt 3' TE – APA	More 3' TE
U133	46	RBBP6	3653317	Yes	No	Alt 5' Init	More 3' start
Exon	47	SCMH1	2408499	Yes	Yes	Internal Event	Exclusion
U133	47	VKORC1	3688197	Yes	Yes	Alt 3' TE - Alt 3' SS	More 5' TE
Exon	48	SYNE1	2979871	Yes	Yes	Alt 5' Init	More 5' start
U133	48	PPP2R5C	3552729	Yes	Yes	Alt 3' TE – APA	More 5' TE
U133	50	UBOX5	3895232	Yes	Yes	Alt 3' TE - Alt 3' SS	More 5' TE
U133	51	CLPTM1	3835935	Yes	No	Internal Event (3' TE)	Exclusion
U133	52	TRIOBP	3944922	Yes	Yes	Alt 3' TE - Alt 3' SS	More 3' TE
Exon	53	PGPEP1	3824963	Yes	Yes	Internal Event	Exclusion
Exon	54	ARCN1	3351531	Yes	No	Alt 5' Init	More 5' start
U133	54	PNO1	2486740	Yes	No	Tandem 3' UTR	Shorten
Exon	56	CASP7	3264948	Yes	Yes	Internal Event	Exclusion
U133	56	HAUS5	3830571	Yes	No	Tandem 3' UTR	Shorten
Exon	57	TCL6	3550139	No	No	Unclassified	---
U133	57	CRAMP1L	3643966	Yes	No	Tandem 3' UTR	Shorten
U133	59	ATG5	2967550	Yes	No	Tandem 3' UTR	Shorten

U133	61	AGGF1	2816563	Yes	No	Tandem 3' UTR	Shorten
U133	62	FLYWCH1	3645402	Yes	Yes	Alt 3' TE – APA	More 5' TE
U133	64	PRMT2	3924783	Yes	No	Transcript Length	---
Exon	65	SCLT1	2785282	Yes	Yes	Internal Event	Exclusion
U133	65	BCL2	3811339	Yes	No	Tandem 3' UTR	Shorten
U133	66	PPHLN1	3412008	Yes	Yes	Alt 3' TE – APA	More 5' TE
Exon	68	PFAS	3709540	Yes	No	Tandem 3' UTR	Shorten
U133	68	C2orf64	2566383	Yes	No	Tandem 3' UTR	Shorten
U133	70	CBR4	2793054	Yes	Yes	Alt 3' TE – APA	More 3' TE
U133	72	ARGLU1	3524618	Yes	No	Alt 5' Init	More 5' start
U133	73	TRIM4	3063536	Yes	No	Tandem 3' UTR	Shorten
Exon	74	PTER	3236786	Yes	Yes	Internal Event	Exclusion
U133	75	TRIM27	2947572	Yes	No	Tandem 3' UTR	Shorten
Exon	77	ARHGAP26	2833286	Yes	Yes	Internal Event	Exclusion
U133	77	MBNL1	2648141	No	No	Unclassified	---
Exon	78	MTRF1	3511189	Yes	Yes	Internal Event	Exclusion
U133	78	LONP2	3659306	No	No	Unclassified	---
Exon	79	ZNF3	3063646	Yes	No	Alt 5' Init	More 3' start
U133	80	HPS1	3302805	Yes	Yes	Alt 3' TE – APA	More 5' TE
U133	83	CPT1B	3966057	Yes	Yes	Alt 3' TE – APA	More 3' TE
Exon	85	BRCA1	3758317	Yes	No	Transcript Length	---
U133	87	TRMT61A	3553803	Yes	No	Tandem 3' UTR	Shorten
U133	88	GNL3L	3978453	Yes	No	Tandem 3' UTR	Shorten
U133	89	CHCHD7	3099089	Yes	No	Tandem 3' UTR	Shorten
U133	90	C10orf4	3300793	No	No	Unclassified	---
U133	91	BTN2A2	2899340	Yes	No	Tandem 3' UTR	Lengthen
U133	92	HNRNPH1	2890148	Yes	No	Transcript Length	---
U133	94	MBNL2	3497586	No	No	Unclassified	---
Exon	95	DCTN1	2559967	Yes	Yes	Internal Event	Exclusion
Exon	96	SAP18	3480657	Yes	No	Tandem 3' UTR	Shorten
U133	96	TMEM97	3715489	Yes	No	Tandem 3' UTR	Shorten
U133	97	TTLL4	2528020	Yes	No	Transcript Length	---
Exon	99	C19orf54	3862785	Yes	No	Internal Event (3' TE)	Exclusion
U133	101	PECR	2598606	Yes	No	Tandem 3' UTR	Shorten
U133	102	ANP32E	2434319	Yes	No	Tandem 3' UTR	Shorten
U133	106	TMC8	3736162	Yes	No	Tandem 3' UTR	Shorten
U133	108	STXBP2	3819016	Yes	Yes	Alt 3' TE – APA	More 3' TE
U133	112	TCP11L1	3325839	Yes	No	Tandem 3' UTR	Lengthen

Exon	114	MOSPD1	4022833	Yes	No	Tandem 3' UTR	Shorten
U133	115	TRNAU1AP	2327542	Yes	No	Tandem 3' UTR	Shorten
Exon	116	IFT81	3431426	Yes	Yes	Internal Event	Exclusion
U133	117	SLC35E1	3854000	Yes	Yes	Alt 3' TE – APA	More 3' TE
U133	119	GCOM1	3595441	Yes	Yes	Alt 3' TE - Alt 3' SS	More 3' TE
U133	120	CALM3	3836841	Yes	No	Tandem 3' UTR	Shorten
U133	126	FAM129C	3824427	Yes	Yes	Alt 3' TE – APA	More 5' TE
U133	127	LIMK2	3942838	Yes	No	Tandem 3' UTR	Lengthen
U133	128	FCRL5	2438892	Yes	Yes	Alt 3' TE – APA	More 5' TE
Exon	129	FBXL17	2870113	Yes	Yes	Internal Event	Exclusion
U133	131	SFRS15	3928866	Yes	Yes	Alt 3' TE – APA	More 3' TE
Exon	132	IFT20	3750595	Yes	Yes	Internal Event	Exclusion
U133	132	DENND1A	3224650	Yes	Yes	Alt 3' TE - Alt 3' SS	More 5' TE
U133	133	MTSS1	3151970	Yes	No	Tandem 3' UTR	Shorten
Exon	135	E2F2	2401448	Yes	No	Tandem 3' UTR	Shorten
U133	136	ACSL4	4017810	No	No	Unclassified	---
U133	137	C1orf107	2378180	Yes	No	Tandem 3' UTR	Shorten
U133	142	CASP6	2781693	Yes	No	Internal Event (3' TE)	Inclusion
U133	145	TRIM69	3592054	Yes	Yes	Alt 3' TE - Alt 3' SS	More 3' TE
Exon	147	PDIA6	2469529	Yes	Yes	Internal Event	Exclusion
U133	148	C18orf25	3787031	Yes	No	Tandem 3' UTR	Shorten
U133	150	PRKRIP1	3016692	Yes	No	Tandem 3' UTR	Shorten
U133	153	STAU2	3140640	Yes	Yes	Alt 3' TE – APA	More 5' TE
U133	154	DGCR8	3937183	Yes	No	Alt 5' Init	More 3' start
U133	157	STAT5B	3757770	Yes	Yes	Alt 3' TE – APA	More 3' TE
Exon	160	RAB3IP	3421706	Yes	Yes	Internal Event	Exclusion
Exon	165	EPS15L1	3853814	Yes	Yes	Internal Event	Exclusion
Exon	166	STAB1	2623922	No	No	Unclassified	---
U133	166	RBM19	3472468	Yes	Yes	Alt 3' TE – APA	More 5' TE
Exon	167	PLD2	3707214	Yes	Yes	Internal Event	Exclusion
Exon	169	SLFN11	3753500	Yes	No	Internal Event (3' TE)	Inclusion
U133	172	CCDC88C	3576441	No	No	Unclassified	---
U133	175	SOS1	2549092	No	No	Unclassified	---
Exon	176	TCF4	3808854	Yes	Yes	Alt 5' Init	More 3' start
U133	177	XRCC4	2818454	Yes	Yes	Alt 3' TE - Alt 3' SS	More 3' TE
U133	179	ST7	3020496	Yes	Yes	Alt 3' TE - Alt 3' SS	More 3' TE
U133	181	TRIM14	3217123	Yes	No	Tandem 3' UTR	Lengthen
U133	182	STS	3967689	Yes	No	Tandem 3' UTR	Lengthen

Exon	183	VGLL4	2662956	No	No	Unclassified	---
U133	183	CACYBP	2368198	Yes	No	Tandem 3' UTR	Shorten
U133	184	PHF19	3223687	Yes	Yes	Alt 3' TE – APA	More 5' TE
U133	187	MLF1IP	2796510	Yes	No	Tandem 3' UTR	Lengthen
U133	188	ZKSCAN5	3014855	Yes	No	Tandem 3' UTR	Shorten
Exon	189	PTPRE	3270270	Yes	Yes	Internal Event	Inclusion
U133	189	TRMT5	3567469	Yes	No	Tandem 3' UTR	Shorten
U133	192	SLC25A17	3961622	Yes	No	Tandem 3' UTR	Shorten
U133	193	EIF1	3721400	No	No	Unclassified	---
Exon	198	C21orf7	3917204	Yes	Yes	Internal Event	Exclusion
Exon	199	C20orf27	3895679	Yes	No	Transcript Length	---
U133	201	CCDC25	3129121	Yes	No	Tandem 3' UTR	Shorten
Exon	203	USP30	3430894	Yes	Yes	Internal Event	Exclusion
Exon	207	ANKRD20B	2564520	Yes	Yes	Internal Event	Exclusion
Exon	208	FZR1	3816988	No	No	Unclassified	---
Exon	209	TERF1	3103187	Yes	No	Alt 5' Init	More 5' start
Exon	211	LILRB2	3870733	Yes	Yes	Internal Event	Inclusion
U133	216	MYO19	3754227	Yes	Yes	Alt 3' TE – APA	More 3' TE
U133	219	RCL1	3160773	Yes	No	Tandem 3' UTR	Shorten
U133	220	EXOC7	3771336	Yes	Yes	Alt 3' TE – APA	More 3' TE
U133	224	KIAA1715	2588319	Yes	No	Tandem 3' UTR	Shorten
U133	231	CPSF6	3421446	Yes	No	Tandem 3' UTR	Shorten
U133	233	C16orf35	3674886	Yes	No	Transcript Length	---
Exon	239	WDR74	3376235	No	No	Unclassified	---
U133	243	MGEA5	3304012	Yes	Yes	Alt 3' TE – APA	More 3' TE
Exon	246	RTCD1	2348854	Yes	Yes	Internal Event	Exclusion
Exon	249	USP6	3707498	Yes	No	Alt 5' Init	More 3' start
Both	250	AURKB	3744263	Yes	No	Transcript Length	---
U133	252	DIS3	3517594	Yes	No	Tandem 3' UTR	Shorten
U133	253	CLCC1	2426791	Yes	No	Tandem 3' UTR	Shorten
Exon	255	TJAP1	2908008	Yes	No	Alt 5' Init	More 5' start
Exon	256	BTG3	3926080	Yes	Yes	Internal Event	Exclusion
U133	258	MSH3	2817837	Yes	No	Transcript Length	---
Exon	261	PPIL5	3534785	Yes	Yes	Internal Event	Exclusion
Exon	270	ZNF215	3318989	Yes	No	Transcript Length	---
Exon	271	---	2563785	Yes	Yes	Internal Event	Inclusion
Exon	283	ITPA	3874249	Yes	Yes	Internal Event	Exclusion
Exon	287	C12orf48	3428845	Yes	Yes	Internal Event	Exclusion

Exon	290	LTB	2949118	Yes	No	Alt 5' Init	More 5' start
Exon	291	KAT2A	3757630	Yes	No	Alt 5' Init	More 5' start
U133	303	COPZ1	3416522	Yes	No	Tandem 3' UTR	Shorten
Exon	309	LPAL2	2982630	Yes	No	Transcript Length	---
U133	317	ZMYM4	2329752	Yes	No	Tandem 3' UTR	Shorten
Exon	327	---	3850832	Yes	No	Alt 5' Init	More 3' start
Exon	328	ZNHIT6	2420958	Yes	No	Alt 5' Init	More 5' start
Exon	333	CTCF	3665603	Yes	Yes	Internal Event	Inclusion
Exon	340	APBB2	2766893	Yes	Yes	Alt 5' Init	More 5' start
U133	346	ETNK1	3408018	Yes	No	Tandem 3' UTR	Shorten
U133	348	KLHDC5	3409364	Yes	No	Tandem 3' UTR	Shorten
Exon	356	ABCC4	3521174	Yes	Yes	Alt 3' TE - Alt 3' SS	More 3' TE
Exon	358	FAM160B2	3089140	Yes	Yes	Internal Event	Exclusion
U133	367	PDXK	3923257	Yes	No	Tandem 3' UTR	Shorten
Exon	375	MESDC2	3635456	Yes	Yes	Alt 3' TE – APA	More 5' TE
Exon	381	ZNF613	3839955	Yes	Yes	Internal Event	Exclusion
U133	397	CAST	2821194	Yes	No	Tandem 3' UTR	Shorten
Exon	399	MARK3	3553690	Yes	No	Alt 5' Init	More 5' start
Exon	400	GKAP1	3212189	Yes	No	Transcript Length	---
U133	401	TCF3	3845365	Yes	No	Tandem 3' UTR	Shorten
U133	412	SRR	3706219	Yes	No	Tandem 3' UTR	Shorten
Exon	421	PRKAR1A	3732885	Yes	No	Alt 5' Init	More 5' start
U133	423	SMARCA4	3820921	Yes	Yes	Alt 3' TE – APA	More 3' TE
U133	427	TPR	2448232	Yes	No	Transcript Length	---
Exon	434	RABGAP1L	2367963	Yes	Yes	Alt 3' TE - Alt 3' SS	More 3' TE
Exon	444	ATMIN	3670668	Yes	No	Alt 5' Init	More 5' start
U133	449	RAD50	2828564	No	No	Unclassified	---
Exon	455	SF1	3377044	Yes	Yes	Internal Event	Inclusion
Exon	481	SMYD5	2488680	Yes	No	Alt 5' Init	More 5' start
U133	488	RABL3	2691475	Yes	No	Tandem 3' UTR	Shorten
Exon	490	STAG3	3015338	Yes	Yes	Internal Event	Exclusion
Exon	493	PSMD12	3768103	Yes	Yes	Internal Event	Exclusion
U133	493	RAB35	3474228	Yes	No	Tandem 3' UTR	Shorten
Exon	496	OBFC2B	3417485	Yes	No	Internal Event (3' TE)	Exclusion
Exon	498	H3F3B	3770944	Yes	No	Tandem 3' UTR	Shorten
Exon	500	SLC25A45	3377569	Yes	Yes	Internal Event	Inclusion
U133	503	MSI2	3728147	Yes	Yes	Alt 5' Init	More 3' start
Exon	505	C19orf28	3846238	Yes	Yes	Internal Event	Exclusion

U133	518	CUGBP2	3234760	No	No	Unclassified	---
U133	522	FBXO9	2910477	Yes	No	Tandem 3' UTR	Shorten
Exon	537	ACD	3695786	Yes	Yes	Internal Event	Exclusion
Exon	550	COL9A3	3892974	Yes	No	Transcript Length	---
Exon	556	DPEP2	3696142	Yes	Yes	Internal Event	Exclusion
U133	568	GRK6	2843163	Yes	No	Tandem 3' UTR	Shorten
Exon	572	GARNL4	3706439	No	No	Unclassified	---
U133	575	DENR	3435490	Yes	No	Tandem 3' UTR	Shorten
Exon	578	KDM4B	3817733	Yes	No	Transcript Length	---
Exon	580	ZNF335	3907561	Yes	Yes	Internal Event	Exclusion
Exon	593	SLFN13	3753568	Yes	No	Tandem 3' UTR	Shorten
Exon	602	PRDM1	2919669	Yes	Yes	Internal Event	Exclusion
U133	606	---	3717052	Yes	No	Tandem 3' UTR	Shorten
Exon	607	MSC	3140213	Yes	No	Alt 5' Init	More 3' start
Exon	614	RAD54L	2334646	Yes	Yes	Internal Event	Exclusion
Exon	616	HOMER2	3636391	Yes	Yes	Internal Event	Inclusion
Exon	622	PKD2	2735221	Yes	Yes	Internal Event	Exclusion
Exon	645	ELMO1	3046197	Yes	Yes	Alt 5' Init	More 3' start
Exon	648	MRPL35	2492015	Yes	No	Alt 5' Init	More 3' start
U133	664	OGT	3981120	Yes	No	Tandem 3' UTR	Shorten
Exon	665	C2orf18	2473965	Yes	No	Transcript Length	---
Exon	667	ZFAT	3154700	Yes	Yes	Alt 3' TE – APA	More 3' TE
U133	671	SYT11	2361154	Yes	No	Tandem 3' UTR	Shorten
Exon	672	TNS1	2599153	Yes	Yes	Internal Event	Inclusion
Exon	675	ACSF2	3726406	Yes	Yes	Internal Event	Exclusion
Exon	678	RABEP2	3686750	No	No	Unclassified	---
Exon	679	STAP2	3846709	Yes	Yes	Internal Event	Exclusion
Exon	692	BAI1	3119017	Yes	Yes	Internal Event	Exclusion
Exon	713	C1orf85	2438093	Yes	Yes	Internal Event	Exclusion
Exon	714	PIP5K1A	2358761	Yes	No	Alt 5' Init	More 5' start
Exon	719	ENTPD5	3571667	No	No	Unclassified	---
Exon	731	ZEB2	2579572	Yes	No	Internal Event (3' TE)	Inclusion
U133	766	OTUB1	3334137	Yes	No	Tandem 3' UTR	Shorten
U133	787	USP48	2400718	Yes	No	Tandem 3' UTR	Shorten
Exon	797	YES1	3795942	Yes	Yes	Internal Event	Exclusion
Exon	806	SPNS1	3655172	Yes	No	Transcript Length	---
Exon	885	KIAA0513	3672059	Yes	Yes	Internal Event	Exclusion
Exon	886	ZWINT	3290210	Yes	Yes	Internal Event	Exclusion

Exon	899	IL10	2452948	Yes	No	Alt 5' Init	More 3' start
Exon	907	HIST2H4A	2357891	Yes	No	Tandem 3' UTR	Shorten
Exon	939	PDE2A	3381150	Yes	No	Alt 5' Init	More 3' start
Exon	988	C11orf51	3380996	No	No	Unclassified	---
Exon	1019	CCDC48	2641449	No	No	Unclassified	---
Exon	1055	NBEA	3485292	Yes	No	Alt 5' Init	More 5' start
Exon	1071	ALG13	3987446	Yes	No	Tandem 3' UTR	Shorten
Exon	1238	SH3PXD2A	3304853	Yes	No	Transcript Length	---
Exon	1252	HIST2H4A	2434102	Yes	Yes	Alt 3' TE - Alt 3' SS	More 5' TE
Exon	1256	MAP3K12	3456212	Yes	No	Alt 5' Init	More 5' start
Exon	1263	METTL8	2586744	Yes	No	Transcript Length	---
Exon	1264	MAN1B1	3195174	No	No	Unclassified	---
Exon	1275	DNM2	3820758	No	No	Unclassified	---
Exon	1316	FAM63A	2434746	Yes	No	Transcript Length	---
Exon	1399	PCMTD1	3134922	No	No	Unclassified	---
Exon	1449	NSDHL	3995371	Yes	Yes	Internal Event	Exclusion
Exon	1601	SNAP29	3937755	Yes	No	Transcript Length	---
Exon	1639	RBM8A	2356181	No	No	Unclassified	---
Exon	1672	RRAS2	3363868	Yes	No	Alt 5' Init	More 5' start
Exon	1724	MRPS25	2664099	Yes	No	Tandem 3' UTR	Shorten

Appendix D: SplicerEX Categorization Algorithm

We devised an algorithm to categorize SplicerEX predicted changes in alternative mRNA processing into distinct mechanistic and directional categories. This algorithm was created with two main goals 1) to provide biologically useful distinct categories and 2) to provide an algorithm that was as simple as possible to promote transparency of the method.

Algorithm Input

To categorize AS events, the algorithm uses two sources of input for each gene 1) the genomic coordinates of the two features used to generate the isoform ratio (chapter 2) and 2) a database of all known UCSC gene transcript genomic coordinates. The two features used to generate isoform ratios come from the single most significant probesets/metaprobesets found in the A and B probeset groups. The program uses single probesets as features for the U133 array and single metaprobesets for the HuEx array. The UCSC known gene list has been developed and maintained by the University of California, Santa Cruz, which also runs the UCSC genome browser (Kent et al. 2002). The UCSC known gene list contains predictions based on data from RefSeq, Genbank, CCDS and UniProt and contains about 10% more protein coding genes than RefSeq and about twice as many splice variants.

Categorization Decision Tree

The categorizer works by stepping through a binary decision tree that asks questions about the two probesets (or metaprobesets) and their overlap with known UCSC genes (Figure 17). The categorizer sequentially asks a set of five questions. If the answer to any of these questions is no, the program assigns a category and then terminates. If no category has been assigned after these five questions, the common transcript inference algorithm is used to assign a category.

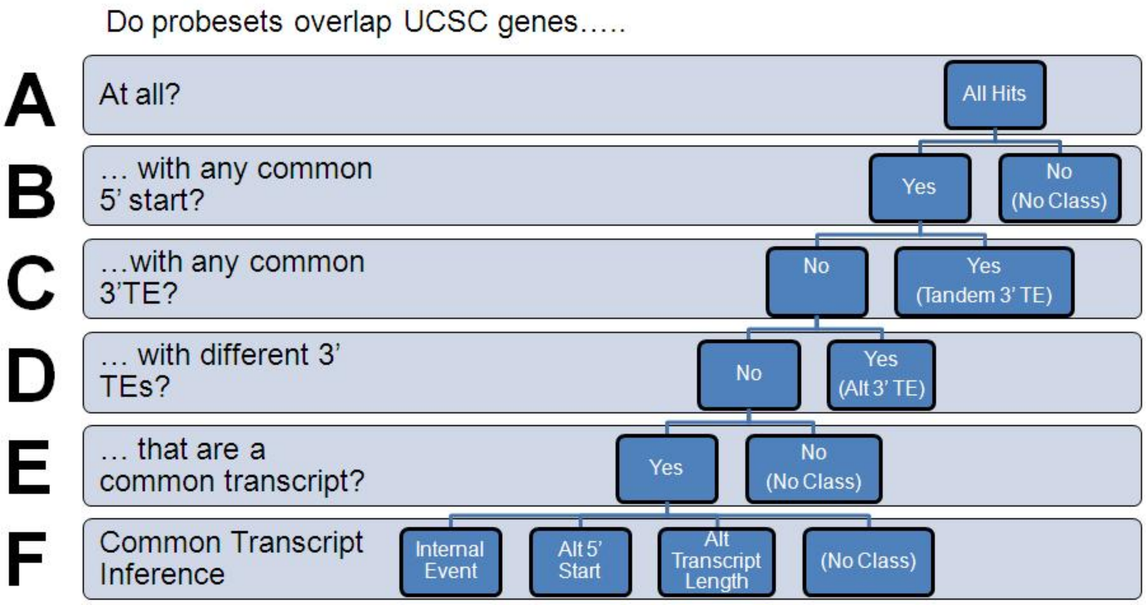

Figure 17: Binary decision tree used to categorize alternative mRNA processing events into discrete categories.

The first question (panel A) asks whether both probesets interrogate any known UCSC genes. Because we filter out probesets that do not meet this criteria, this first step does not exclude any possible categories for our analysis. This step would, however, allow others to run the program where such a filter was unavailable, such as on a novel platform. In this case, events where either probeset did not interrogate a UCSC gene would be unclassified.

The second question (panel B) asks if interrogated UCSC genes share any common 5' start location. This removes poorly annotated events in which probesets are targeting unrelated transcripts that begin in two separate locations and for which no overlapping transcript has ever been observed. Events that do not pass this criteria are placed into the unclassified (no class) category.

The next question (panel C) asks if the probesets target a common 3’ TE. In this case, we have evidence that the same 3’TE is undergoing different changes in abundance, which is most commonly explained by changes in 3’UTR length. Changes in 3’TE regional abundance can also be explained by two other events 1) inclusion/exclusion of internal 3’TE content and 2) use of an alternative 3’ SS. The program checks for internal inclusion/exclusion (described in common transcript inference). If an internal inclusion/exclusion is ruled out, then the program assigns this category as “Tandem 3’ TE”. All events categorized in this step are assumed to result in non-coding changes (the ORF is not altered), as they are typically limited to the 3’ UTR.

Step 4 (panel D) asks if each probeset interrogates a different 3’TE. In this case, the suggestion is that a gene is undergoing mutually exclusive selection of which 3’ end of the gene it will use. These events almost uniformly result in changes in transcript ORF. All events identified in this step are categorized as affecting protein coding regions.

The next question asks if both probesets interrogate any common UCSC known transcript. If the answer is no, the event is unclassifiable and the program terminates. If the answer is yes, the categorizer attempts categorization using only the common UCSC transcript. In the case where there are multiple common UCSC transcripts interrogated, these transcripts are combined into a single representative transcript that comprises only common exons.

Common Transcript Inference (CTI)

Events placed in the common transcript inference (CTI) category are categorized based on each probeset’s exon count and location within the common transcript. CTI events can be categorized as internal events, alternative 5’ initiation, alternative transcript length, or uncategorized (Table 9).

Table 9: Common transcript inference (CTI) categories

Category	Criteria	SubTypes	Criteria
Internal Event	1) probeset1: Contained internally within probeset2 OR 2) probeset1: Single exon, internal probeset2: Multiple exons	Inclusion	Probeset1 is from Group A
		Exclusion	Probeset1 is from Group B
5’ Alt Initiation	1) Probeset1: Single 5’ located exon OR 2)Probesets 1 &2 each target 3 or more exons & do not overlap	More 5’	Group A probeset is more 5’
		More 3’	Group A probeset is more 3’
Alt Transcript Length	1) Probeset 1 or 2 interrogates 3’ TE	N/A	
Unclassified/ No class	Unable to be categorized using above	N/A	

Of events not assigned hypotheses, only a handful of events had reasonably clear hypotheses that could be assessed subjectively by the researchers. These additional events could be accurately categorized by SplicerEX with additional modifications to the categorization algorithm. However, it was felt that the increased additional complexity required to categorize these few events was not worth the loss in transparency. These modifications were not included in the final SplicerEX program.

Appendix E: Discovery of Dengue virus host factors in insects and humans

In 2009, Sessions et al. published the first genome wide siRNA screen for Dengue virus host factors in Drosophila (Sessions et al. 2009). I performed the data analysis to select hits from the first round of the screen, which required the development of a nonparametric screen statistic to deal with data that violated assumptions of normality and was subject to several sources of bias and noise.

Screen/Data Structure

The Dengue screen was performed in duplicate using 384 well plates. Each of the 384 wells had a unique dsRNA printed on it from the screening library. After 72 hours of infection by Dengue, the percent of cells that had been infected and total cell counts within each well were assayed in order to determine the effect of each dsRNA on infectivity. The primary goal of the screen was to identify Dengue host factors, defined by factors required by Dengue. Knockdown of a Dengue host factor in a well would be expected to decrease infectivity in that well. The primary goal of the study was therefore to identify wells with unusually low levels of infectivity as a result of dsRNA knockdown of a required Dengue host factor.

Data Analysis

We observed that the infectivity rates within each plate were not normally distributed and had highly variable infection rates from plate to plate and day to day. This us to approach the data analysis using a nonparametric approach, which was similar in theme to quantile normalization. I developed the Sum Rank algorithm to deal with data we encountered during the analysis of the drosophila dengue siRNA screen.

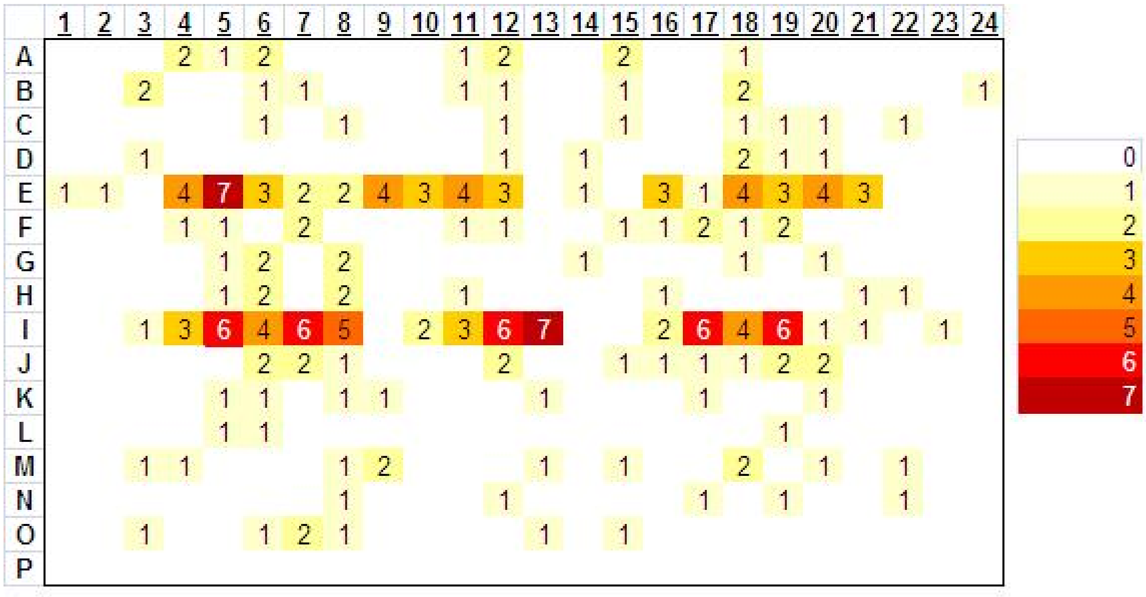

	1	2	3	4	5	6	7	8	9	10	11	12	13	14	15	16	17	18	19	20	21	22	23	24
A				2	1	2					1	2			2			1						
B			2			1	1				1	1			1			2						1
C						1		1				1			1			1	1	1		1		
D			1									1		1				2	1	1				
E	1	1		4	7	3	2	2	4	3	4	3		1		3	1	4	3	4	3			
F				1	1		2				1	1			1	1	2	1	2					
G					1	2		2						1				1		1				
H					1	2		2			1					1					1	1		
I			1	3	6	4	6	5		2	3	6	7			2	6	4	6	1	1		1	
J						2	2	1				2			1	1	1	1	2	2				
K					1	1		1	1				1				1			1				
L					1	1													1					
M			1	1				1	2				1		1			2		1		1		
N								1				1					1		1			1		
O			1			1	2	1					1		1									
P																								

Figure 18: Heat map of low infectivity hits detected from the screen by plate positition. The number of total hits detected within each position ranged between 0 and 7. Clear enrichment of hit selection (low infectivity) was seen in rows E and I. Only a single hit per column was selected from columns 1, 2, 23, and 24. The probability of having 7 or more hits come from any well on the plate was p=6e-5, demonstrating highly significant plate effects. Non-random distribution of genes on the plate may have also been partially responsible for observed spatial biases. Plate effects are a common practical problem in genome wide siRNA screens and deserve more discussion in the published accounts of siRNA screens.

The Sum Rank algorithm functions to produce a single summary statistic for each siRNA tested in duplicate using two separate 384 well plates and is implemented as follows:

Exclusion Criteria

First each siRNA well on both plates is examined for sufficient cell growth. Any well with less than 2000 cells/field is removed from the analysis, along with its duplicate in the other plate. The 16 control wells are also removed prior to analysis. For each pair of 384 well plates, up to 368 (= 384 – 16) wells are included in the analysis.

Sum Rank algorithm

Within each plate, wells are ranked by the percent of infected cells, with the least infected well being given rank 1. For each siRNA, its rank from each plate is summed to yield that well's Sum Rank statistic.

Sum Rank = Rank on plate #1 + Rank on plate #2 [1]

For each pair of duplicate plates, we obtain a distribution of Sum Ranks. For an experiment with no excluded wells (368), the Sum Ranks can potentially range from 2 to 734 (= 368 * 2). In generally the Sum Rank can range from 2 to (#Valid Wells * 2). In order to assess the significance of observing a given Sum Rank, we calculated a null distribution for the Sum Rank statistic.

All possible ranks are present on every plate. For example, every plate will contain one well ranked #1, one well ranked #, etc on up to the # of valid wells. When the ranks from a duplicate plate are added to this first plate, there is only one way that a Sum Rank of 2 can be achieved. The #1 ranked well from plate must also be ranked #1 on the duplicate plate. Since there are 368 wells on this second plate, there is only 1/368 ways that a Sum Rank of 2 would be observed. On average, a Sum Rank of 2 would be expected to be observed in 1/368 (= .0027) plate pairs. This is the expected number of times we would observe a Sum Rank of 2 by chance alone. There are two possible ways to achieve a Sum Rank of 3 (Ranked #1 on plate A and #2 on plate B, or #2 on plate A and #1 on plate B). The resulting expectation is 2/368 (= .0054). In this way, the expectation of Sum Rank for the lowest infected wells is given by the following equation:

$$E[SR] = (SR - 1) / 368 \qquad [2]$$

For the highest infected wells, within a pair of plates with no excluded wells, the distribution mirrors that of the low infected wells with the maximum Sum Rank being least likely:

$$E[SR] = (734 - SR) / 368 \qquad [3]$$

These equations can be generalized to apply to all pair plates, regardless of the number of valid wells:

Expectation of observing lowest Sum Ranks:

$$E[SR] = (SR - 1) / (\#\ Valid\ Wells) \qquad [4]$$

Expectation of observing highest Sum Ranks:

$$E[SR] = ((\#Valid\ Wells * 2) - (SR - 1)) / (\#\ Valid\ Wells) \qquad [5]$$

I confirmed this theoretical distribution using computational simulations in R. The key assumption of this null distribution is that ranks within a plate are randomly distributed. This assumption can be invalid if there are local biases in infectivity within a plate, for example if edges are infected more than center wells. Such affects are likely present in our assay, and we therefore expect a slightly higher false discover rate than would be predicted by theory alone. We have not yet assessed the magnitude or implication of such spatial biases within duplicate plates. Such spatial biases would affect any statistical analyses and not just the Sum Rank method.

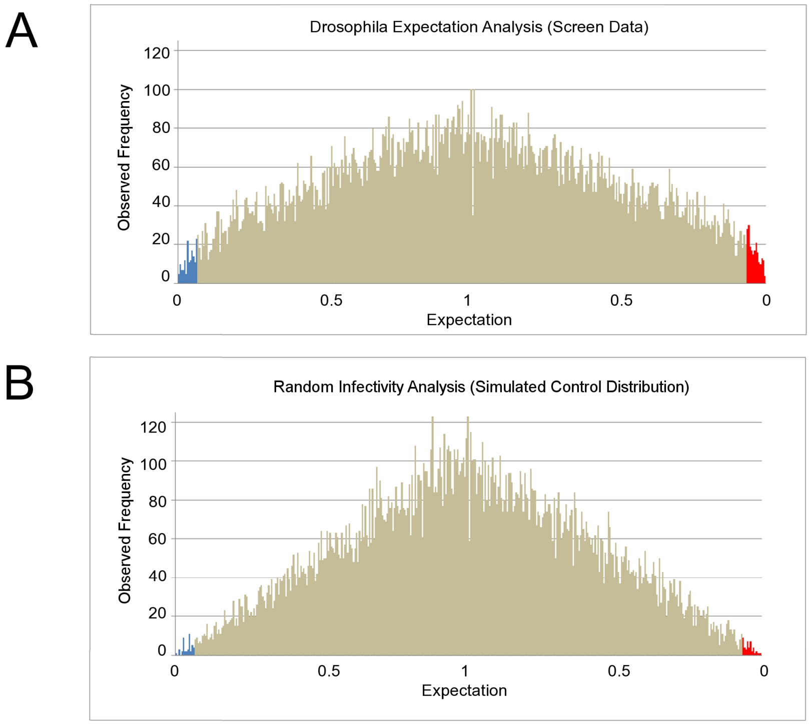

Figure 19: Histogram of empirical and theoretical distributions of expected Sum Rank values. For each paired well in the screen, a Sum Rank statistic was calculated. Each Sum Rank's expected frequency by random chance is shown on the horizontal axis, with uncommon extremes in low infectivity to the left and high infectivity to the right. The vertical axis indicates the frequency with which each expectation value was actually observed during the screen (A) and during a simulation of random infectivity (B). Sum Ranks expected to occur fewer than 0.065 times per paired duplicate plates are highlighted in blue and red, representing extremes of low and high infectivity, respectively. Wells from the Drosophila screen (A) yielded a significantly larger number of wells with extremes of low ($\chi 2 = 62.8$, $p<.0001$) and high ($\chi 2 = 108$, $p<.0001$) infectivity compared to that expected by wells assigned random infectivity (B), suggesting significant departures from random biological variation upon treatment of cells with dsRNAs. Using the random infectivity analysis to determine the false discovery rate suggests approximately 24% of detected "hits" (expectation less than 0.065) were due to random chance alone, in rough agreement with the validation rate of putative hits.

References

Affymetrix (2001) Microarray Suite User Guide, Version 5. Affymetrix, http://www.affymetrix.com/support/technical/manuals.affx.

Abdueva, D., M. R. Wing, et al. (2007). "Experimental comparison and evaluation of the Affymetrix exon and U133Plus2 GeneChip arrays." PLoS One **2**(9): e913.

Adamson, E. D. and L. M. Wiley (1997). "The EGFR gene family in embryonic cell activities." Curr Top Dev Biol **35**: 71-120.

Affymetrix (2005). "Alternative transcript analysis methods for exon arrays. Affymetrix Whitepaper 2005 [http://www.affymetrix.com/support/technical/whitepapers.affx]."

Andre, F., S. Michiels, et al. (2009). "Exonic expression profiling of breast cancer and benign lesions: a retrospective analysis." Lancet Oncol **10**(4): 381-90.

Barrett, T., D. B. Troup, et al. (2009). "NCBI GEO: archive for high-throughput functional genomic data." Nucleic Acids Res **37**(Database issue): D885-90.

Bartel, D. P. (2009). "MicroRNAs: target recognition and regulatory functions." Cell **136**(2): 215-33.

Basu, A., M. Raghunath, et al. (1989). "Inhibition of tyrosine kinase activity of the epidermal growth factor (EGF) receptor by a truncated receptor form that binds to EGF: role for interreceptor interaction in kinase regulation." Mol Cell Biol **9**(2): 671-7.

Bemmo, A., D. Benovoy, et al. (2008). "Gene expression and isoform variation analysis using Affymetrix Exon Arrays." BMC Genomics **9**: 529.

Bhasi, A., R. V. Pandey, et al. (2007). "EuSplice: a unified resource for the analysis of splice signals and alternative splicing in eukaryotic genes." Bioinformatics **23**(14): 1815-23.

Bild, A. H., G. Yao, et al. (2006). "Oncogenic pathway signatures in human cancers as a guide to targeted therapies." Nature **439**(7074): 353-7.

Black, D. L. (2003). "Mechanisms of alternative pre-messenger RNA splicing." Annu Rev Biochem **72**: 291-336.

Blencowe, B. J. (2006). "Alternative splicing: new insights from global analyses." Cell **126**(1): 37-47.

Bristow, R. G. and R. P. Hill (2008). "Hypoxia and metabolism. Hypoxia, DNA repair and genetic instability." Nat Rev Cancer. **8**(3): 180-92.

Brown, T. J., J. M. Rowe, et al. (1991). "Regulation of IL-6 expression by oncostatin M." J Immunol **147**(7): 2175-80.

Browne, B. C., N. O'Brien, et al. (2009). "HER-2 signaling and inhibition in breast cancer." Curr Cancer Drug Targets **9**(3): 419-38.

Castrignano, T., M. D'Antonio, et al. (2008). "ASPicDB: a database resource for alternative splicing analysis." Bioinformatics **24**(10): 1300-4.

Chandler, L. A. and S. Bourgeois (1991). "Posttranscriptional down-regulation of fibronectin in N-ras-transformed cells." Cell Growth Differ **2**(8): 379-84.

Chandler, L. A., C. P. Ehretsmann, et al. (1994). "A novel mechanism of Ha-ras oncogene action: regulation of fibronectin mRNA levels by a nuclear posttranscriptional event." Mol Cell Biol **14**(5): 3085-93.

Chen, J. L., J. E. Lucas, et al. (2008). "The genomic analysis of lactic acidosis and acidosis response in human cancers." PLoS Genet **4**(12): e1000293.

Cheung, H. C., K. A. Baggerly, et al. (2008). "Global analysis of aberrant pre-mRNA splicing in glioblastoma using exon expression arrays." BMC Genomics **9**: 216.

Clark, T. A., A. C. Schweitzer, et al. (2007). "Discovery of tissue-specific exons using comprehensive human exon microarrays." Genome Biol **8**(4): R64.

Cline, M. S., J. Blume, et al. (2005). "ANOSVA: a statistical method for detecting splice variation from expression data." Bioinformatics **21 Suppl 1**: i107-15.

Cooper, T. A., L. Wan, et al. (2009). "RNA and disease." Cell **136**(4): 777-93.

Darville, M. I. and G. G. Rousseau (1997). "E2F-dependent mitogenic stimulation of the splicing of transcripts from an S phase-regulated gene." Nucleic Acids Res **25**(14): 2759-65.

de la Grange, P., M. Dutertre, et al. (2007). "A new advance in alternative splicing databases: from catalogue to detailed analysis of regulation of expression and function of human alternative splicing variants." BMC Bioinformatics **8**: 180.

de la Grange, P., M. Dutertre, et al. (2005). "FAST DB: a website resource for the study of the expression regulation of human gene products." Nucleic Acids Res **33**(13): 4276-84.

Dewhirst, M. W. (2009). "Relationships between cycling hypoxia, HIF-1, angiogenesis and oxidative stress." Radiat Res. **172**(6): 653-65.

Dewhirst, M. W., Y. Cao, et al. (2008). "Cycling hypoxia and free radicals regulate angiogenesis and radiotherapy response." Nat Rev Cancer. **8**(6): 425-37.

Dutertre, M., M. Lacroix-Triki, et al. (2010). "Exon-based clustering of murine breast tumor transcriptomes reveals alternative exons whose expression is associated with metastasis." Cancer Res **70**(3): 896-905.

Ehashi, T., T. Koyama, et al. (2007). "Effects of oncostatin M on secretion of vascular endothelial growth factor and reconstruction of liver-like structure by fetal liver cells in monolayer and three-dimensional cultures." J Biomed Mater Res A **82**(1): 73-9.

Fan, W., N. Khalid, et al. (2006). "A statistical method for predicting splice variants between two groups of samples using GeneChip expression array data." Theor Biol Med Model **3**: 19.

Ferrari, F., S. Bortoluzzi, et al. (2007). "Novel definition files for human GeneChips based on GeneAnnot." BMC Bioinformatics **8**: 446.

Fodor, S. P., R. P. Rava, et al. (1993). "Multiplexed biochemical assays with biological chips." Nature **364**(6437): 555-6.

Foissac, S. and M. Sammeth (2007). "ASTALAVISTA: dynamic and flexible analysis of alternative splicing events in custom gene datasets." Nucleic Acids Res **35**(Web Server issue): W297-9.

Friedman, R. C., K. K. Farh, et al. (2009). "Most mammalian mRNAs are conserved targets of microRNAs." Genome Res **19**(1): 92-105.

Garcia-Blanco, M. A., A. P. Baraniak, et al. (2004). "Alternative splicing in disease and therapy." Nat Biotechnol **22**(5): 535-46.

Gardina, P. J., T. A. Clark, et al. (2006). "Alternative splicing and differential gene expression in colon cancer detected by a whole genome exon array." BMC Genomics **7**: 325.

Gatenby, R. A. and R. J. Gilles (2004). "Why do cancers have high aerobic glycolysis?" Nat Rev Cancer. **4**(11): 891-9.

Grove, R. I., C. Eberhardt, et al. (1993). "Oncostatin M is a mitogen for rabbit vascular smooth muscle cells." Proc Natl Acad Sci U S A **90**(3): 823-7.

He, C., F. Zhou, et al. (2009). "A global view of cancer-specific transcript variants by subtractive transcriptome-wide analysis." PLoS ONE **4**(3): e4732.

Holzer, R. G., R. E. Ryan, et al. (2004). "Oncostatin M stimulates the detachment of a reservoir of invasive mammary carcinoma cells: role of cyclooxygenase-2." Clin Exp Metastasis **21**(2): 167-76.

Horn, D., W. C. Fitzpatrick, et al. (1990). "Regulation of cell growth by recombinant oncostatin M." Growth Factors **2**(2-3): 157-65.

Hu, G. K., S. J. Madore, et al. (2001). "Predicting splice variant from DNA chip expression data." Genome Res **11**(7): 1237-45.

Irizarry, R. A., B. Hobbs, et al. (2003). "Exploration, normalization, and summaries of high density oligonucleotide array probe level data." Biostatistics **4**(2): 249-64.

Jaksik, R., J. Polanska, et al. (2009). "Calculation of reliable transcript levels of annotated genes on the basis of multiple probe-sets in Affymetrix microarrays." Acta Biochim Pol.

Johannsen, E., M. Luftig, et al. (2004). "Proteins of purified Epstein-Barr virus." Proc Natl Acad Sci U S A **101**(46): 16286-91.

Jorcyk, C. L., R. G. Holzer, et al. (2006). "Oncostatin M induces cell detachment and enhances the metastatic capacity of T-47D human breast carcinoma cells." Cytokine **33**(6): 323-36.

Kan, Z., E. C. Rouchka, et al. (2001). "Gene structure prediction and alternative splicing analysis using genomically aligned ESTs." Genome Res **11**(5): 889-900.

Kashles, O., Y. Yarden, et al. (1991). "A dominant negative mutation suppresses the function of normal epidermal growth factor receptors by heterodimerization." Mol Cell Biol **11**(3): 1454-63.

Kent, W. J., C. W. Sugnet, et al. (2002). "The human genome browser at UCSC." Genome Res **12**(6): 996-1006.

Kim, N., A. V. Alekseyenko, et al. (2007). "The ASAP II database: analysis and comparative genomics of alternative splicing in 15 animal species." Nucleic Acids Res **35**(Database issue): D93-8.

Koscielny, G., V. Le Texier, et al. (2009). "ASTD: The Alternative Splicing and Transcript Diversity database." Genomics **93**(3): 213-20.

Krawczak, M., J. Reiss, et al. (1992). "The mutational spectrum of single base-pair substitutions in mRNA splice junctions of human genes: causes and consequences." Hum Genet **90**(1-2): 41-54.

Laajala, E., T. Aittokallio, et al. (2009). "Probe-level estimation improves the detection of differential splicing in Affymetrix exon array studies." Genome Biol **10**(7): R77.

Lee, C., L. Atanelov, et al. (2003). "ASAP: the Alternative Splicing Annotation Project." Nucleic Acids Res **31**(1): 101-5.

Li, C., M. Kato, et al. (2006). "Cell type and culture condition-dependent alternative splicing in human breast cancer cells revealed by splicing-sensitive microarrays." Cancer Res **66**(4): 1990-9.

Li, C. and W. H. Wong (2001). "Model-based analysis of oligonucleotide arrays: expression index computation and outlier detection." Proc Natl Acad Sci U S A **98**(1): 31-6.

Loi, S., B. Haibe-Kains, et al. (2008). "Predicting prognosis using molecular profiling in estrogen receptor-positive breast cancer treated with tamoxifen." BMC Genomics **9**: 239.

Lopez-Bigas, N., B. Audit, et al. (2005). "Are splicing mutations the most frequent cause of hereditary disease?" FEBS Lett **579**(9): 1900-3.

Lu, J., J. C. Lee, et al. (2007). "Transcript-based redefinition of grouped oligonucleotide probe sets using AceView: high-resolution annotation for microarrays." BMC Bioinformatics **8**: 108.

Miles, S. A., O. Martinez-Maza, et al. (1992). "Oncostatin M as a potent mitogen for AIDS-Kaposi's sarcoma-derived cells." Science **255**(5050): 1432-4.

Miller, L. D., J. Smeds, et al. (2005). "An expression signature for p53 status in human breast cancer predicts mutation status, transcriptional effects, and patient survival." Proc Natl Acad Sci U S A **102**(38): 13550-5.

Mirshahi, F., M. Vasse, et al. (2002). "Oncostatin M induces procoagulant activity in human vascular smooth muscle cells by modulating the balance between tissue factor and tissue factor pathway inhibitor." Blood Coagul Fibrinolysis **13**(5): 449-55.

Nair, B. C., A. L. DeVico, et al. (1992). "Identification of a major growth factor for AIDS-Kaposi's sarcoma cells as oncostatin M." Science **255**(5050): 1430-2.

Nakamura, K., H. Nonaka, et al. (2004). "Hepatocyte proliferation and tissue remodeling is impaired after liver injury in oncostatin M receptor knockout mice." Hepatology **39**(3): 635-44.

Neel, H., P. Gondran, et al. (1995). "Regulation of pre-mRNA processing by src." Curr Biol **5**(4): 413-22.

Ng, G., D. Winder, et al. (2007). "Gain and overexpression of the oncostatin M receptor occur frequently in cervical squamous cell carcinoma and are associated with adverse clinical outcome." J Pathol **212**(3): 325-34.

Pawitan, Y., J. Bjohle, et al. (2005). "Gene expression profiling spares early breast cancer patients from adjuvant therapy: derived and validated in two population-based cohorts." Breast Cancer Res **7**(6): R953-64.

Pearson, J. L., T. J. Robinson, et al. (2008). "Identification of the cellular targets of the transcription factor TCERG1 reveals a prevalent role in mRNA processing." J Biol Chem **283**(12): 7949-61.

Pickrell, J. K., J. C. Marioni, et al. "Understanding mechanisms underlying human gene expression variation with RNA sequencing." Nature.

Pollack, V., R. Sarkozi, et al. (2007). "Oncostatin M-induced effects on EMT in human proximal tubular cells: differential role of ERK signaling." Am J Physiol Renal Physiol **293**(5): F1714-26.

Queen, M. M., R. E. Ryan, et al. (2005). "Breast cancer cells stimulate neutrophils to produce oncostatin M: potential implications for tumor progression." Cancer Res **65**(19): 8896-904.

Rega, G., C. Kaun, et al. (2007). "Vascular endothelial growth factor is induced by the inflammatory cytokines interleukin-6 and oncostatin m in human adipose tissue in vitro and in murine adipose tissue in vivo." Arterioscler Thromb Vasc Biol **27**(7): 1587-95.

Reiter, J. L., D. W. Threadgill, et al. (2001). "Comparative genomic sequence analysis and isolation of human and mouse alternative EGFR transcripts encoding truncated receptor isoforms." Genomics **71**(1): 1-20.

Repovic, P., C. Y. Fears, et al. (2003). "Oncostatin-M induction of vascular endothelial growth factor expression in astroglioma cells." Oncogene **22**(50): 8117-24.

Robinson, M. D. and T. P. Speed (2007). "A comparison of Affymetrix gene expression arrays." BMC Bioinformatics **8**: 449.

Robinson, T. J., M. A. Dinan, et al. (2010). "SplicerAV: A tool for mining microarray expression data for changes in RNA processing." BMC Bioinformatics **11**(1): 108.

Sandberg, R., J. R. Neilson, et al. (2008). "Proliferating cells express mRNAs with shortened 3' untranslated regions and fewer microRNA target sites." Science **320**(5883): 1643-7.

Sessions, O. M., N. J. Barrows, et al. (2009). "Discovery of insect and human dengue virus host factors." Nature **458**(7241): 1047-50.

Sotiriou, C. and L. Pusztai (2009). "Gene-expression signatures in breast cancer." N Engl J Med **360**(8): 790-800.

Srinivasan, K., L. Shiue, et al. (2005). "Detection and measurement of alternative splicing using splicing-sensitive microarrays." Methods **37**(4): 345-59.

Suzuki, Y., K. Yoshitomo-Nakagawa, et al. (1997). "Construction and characterization of a full length-enriched and a 5'-end-enriched cDNA library." Gene **200**(1-2): 149-56.

Takeda, J., Y. Suzuki, et al. (2006). "Large-scale identification and characterization of alternative splicing variants of human gene transcripts using 56,419 completely sequenced and manually annotated full-length cDNAs." Nucleic Acids Res **34**(14): 3917-28.

Tanaka, M., Y. Hirabayashi, et al. (2003). "Targeted disruption of oncostatin M receptor results in altered hematopoiesis." Blood **102**(9): 3154-62.

Thomas, P. D., M. J. Campbell, et al. (2003). "PANTHER: a library of protein families and subfamilies indexed by function." Genome Res **13**(9): 2129-41.

Thomas, P. D., A. Kejariwal, et al. (2006). "Applications for protein sequence-function evolution data: mRNA/protein expression analysis and coding SNP scoring tools." Nucleic Acids Res **34**(Web Server issue): W645-50.

Thorsen, K., K. D. Sorensen, et al. (2008). "Alternative splicing in colon, bladder, and prostate cancer identified by exon array analysis." Mol Cell Proteomics **7**(7): 1214-24.

Ullrich, A., L. Coussens, et al. (1984). "Human epidermal growth factor receptor cDNA sequence and aberrant expression of the amplified gene in A431 epidermoid carcinoma cells." Nature **309**(5967): 418-25.

Vasse, M., J. Pourtau, et al. (1999). "Oncostatin M induces angiogenesis in vitro and in vivo." Arterioscler Thromb Vasc Biol **19**(8): 1835-42.

Venables, J. P. (2006). "Unbalanced alternative splicing and its significance in cancer." Bioessays **28**(4): 378-86.

Venables, J. P., R. Klinck, et al. (2009). "Cancer-associated regulation of alternative splicing." Nat Struct Mol Biol **16**(6): 670-6.

Wan, J., P. Sazani, et al. (2009). "Modification of HER2 pre-mRNA alternative splicing and its effects on breast cancer cells." Int J Cancer **124**(4): 772-7.

Wang, E. T., R. Sandberg, et al. (2008). "Alternative isoform regulation in human tissue transcriptomes." Nature **456**(7221): 470-6.

Wang, H., E. Hubbell, et al. (2003). "Gene structure-based splice variant deconvolution using a microarray platform." Bioinformatics **19 Suppl 1**: i315-22.

Warren, P., D. Taylor, et al. (2007). "PANP - a New Method of Gene Detection on Oligonucleotide Expression Arrays." Proc. 2007 IEEE 7th International Symposium on BioInformatics & BioEngineering,Cambridge, USA, 2007, pp.108-115.

Weiss, G. J., L. T. Bemis, et al. (2008). "EGFR regulation by microRNA in lung cancer: correlation with clinical response and survival to gefitinib and EGFR expression in cell lines." Ann Oncol **19**(6): 1053-9.

Weiss, T. W., W. S. Speidl, et al. (2003). "Glycoprotein 130 ligand oncostatin-M induces expression of vascular endothelial growth factor in human adult cardiac myocytes." Cardiovasc Res **59**(3): 628-38.

Xi, L., A. Feber, et al. (2008). "Whole genome exon arrays identify differential expression of alternatively spliced, cancer-related genes in lung cancer." Nucleic Acids Res **36**(20): 6535-47.

Xing, Y., P. Stoilov, et al. (2008). "MADS: a new and improved method for analysis of differential alternative splicing by exon-tiling microarrays." Rna **14**(8): 1470-9.

Xu, Q. and C. Lee (2003). "Discovery of novel splice forms and functional analysis of cancer-specific alternative splicing in human expressed sequences." Nucleic Acids Res **31**(19): 5635-43.

Yao, H., L. Xu, et al. (2009). "Structure-function correlation of human programmed cell death 5 protein." Arch Biochem Biophys **486**(2): 141-9.

Yu, H., F. Wang, et al. (2007). "Transcript-level annotation of Affymetrix probesets improves the interpretation of gene expression data." BMC Bioinformatics **8**: 194.

Zarling, J. M., M. Shoyab, et al. (1986). "Oncostatin M: a growth regulator produced by differentiated histiocytic lymphoma cells." Proc Natl Acad Sci U S A **83**(24): 9739-43.

Zhang, C., H. R. Li, et al. (2006). "Profiling alternatively spliced mRNA isoforms for prostate cancer classification." BMC Bioinformatics **7**: 202.

Zheng, C. L., Y. S. Kwon, et al. (2005). "MAASE: an alternative splicing database designed for supporting splicing microarray applications." Rna **11**(12): 1767-76.

Zhu, L., Y. Zhang, et al. (2009). "Patterns of exon-intron architecture variation of genes in eukaryotic genomes." BMC Genomics **10**: 47.

Biography

Timothy John Robinson was born on October 11, 1981 in Chesapeake, Virginia. Tim attended Engineering School at the University of Virginia as a Rodman Scholar. He graduated with a Bachelor's of Science in Engineering Sciences with an emphasis and minor in Biomedical Engineering in 2003. During his time at UVA, Tim worked in a computational neurosurgery laboratory under Dr. William Levy studying computational simulations of action potential dynamics and spent his summers working at NASA Langley studying atmospheric sciences. In the fall of 2003, Tim began medical school at Duke University as part of the Medical Scientist Training (MD/PhD) Program. In 2005, Tim began his PhD studies in Molecular Cancer Biology where he joined the laboratories of both Dr. Mariano Garcia-Blanco and Dr. Mark Dewhirst. During his tenure at Duke, Tim presented his research at the 2009 Annual MSTP Symposium. Tim was also the recipient of a Pre-doctoral Department of Defense Breast Cancer Research grant. From 2006-2007 Tim was a voting member of the Duke University Institutional Review Board where he currently remains an alternate member. Tim currently resides in Durham and will be returning to Duke Medical School to finish his MD.

List of Publications:

1. Robinson TJ, Dinan MA, Dewhirst M, Garcia-Blanco MA, and Pearson JL. SplicerAV: A tool for mining microarray expression data for changes in RNA processing. *BMC Bioinformatics*. 2010 Feb 25;11(1)

2. Robinson TJ, Forte, E, Lutig, M, Garcia-Blanco MA. Conventional Affymetrix U133 Arrays Provide Superior Detection of 3' Located Differential mRNA Processing Compared to Human Exon Arrays. *In preparation.*

3. Miller HB, Robinson TJ, Gordan R, Hartemink AJ, Garcia-Blanco MA. Identification of Tat-SF1 cellular targets by exon array analysis reveals widespread roles in alternative exon choice. *Submitted to RNA.*

4. Sessions OM, Barrows NJ, Souza-Neto JA, Robinson TJ, Hershey CL, Rodgers MA, Ramirez JL, Dimopoulos G, Yang PL, Pearson JL, Garcia-Blanco MA. Discovery of insect and human dengue virus host factors. *Nature*. 2009 Apr 23;458(7241):1047-50.

5. Pearson JL, Robinson TJ, Muñoz MJ, Kornblihtt AR, Garcia-Blanco MA. Identification of the cellular targets of the transcription factor TCERG1 reveals a prevalent role in mRNA processing. *J Biol Chem*. 2008 Mar 21;283(12):7949-61.